JPRS-JST-90-004
10 JANUARY 1990

FOREIGN BROADCAST INFORMATION SERVICE

JPRS Report

Science & Technology

Japan

JPRS-JST-90-004
10 JANUARY 1990

SCIENCE & TECHNOLOGY

JAPAN

CONTENTS

Preparation of SiO_2-TiO_2 System by Alkoxide Processes

43067099a Tokyo CERAMICS KISO KAGAKU TORONKAI in Japanese 30-31 Jan 89 p 2

[Article by Shoji Kaneko, Kunitomo Suzuki, Tamotsu Yamada, Yasushi Kubo and Fumio Imoto, Shizuo University]

[Text] 1. Compounds and solutions that combine silica with other metal oxides represent an effective means to improve and utilize its high-temperature properties. With regard to an SiO_2-TiO_2 system, however, its solute relationship cannot be established because of its high melting point and high viscosity, which leave unclear points about its condition. Therefore, we attempted to produce a homogeneous mixed gel by using a metal alkoxide as the starting material and sought to achieve crystallization and a solute state during high-temperature sintering. In addition, we attempted a partial revision of the condition of this system in light of the state of its solid solution, because it is conceivable that this kind of gel is in a state similar to that of a melt.

2. We mixed $Si(OC_2H_5)_4$ and $Ti(O\text{-}i\text{-}C_3H_7)_4$ at a stated ratio and added 3.3 cm of 0.15 $moldm^{-3}$ ammonium water to a 500 cm^3 solution that was diluted with ethanol to give the metal ions a density of 0.5 $moldm^{-3}$, while cooling the mixture with ice water. Next, we slowly hydrolyzed the solution while stirring it at room temperature. After 9 days, we made the mixture into a gel by adding 3 $moldm^{-3}$ of ammonium water, again in ice water. We heated the jelly-like gel to 100°C, evaporated the solvent, and dried the gel at 110°C for 24 hours. After calcinating the dried gel at 800°C for 2 hours, we molded it and further heat-treated it at a high temperature. We used the fluorescent X-ray method to measure the total amount of titania in the gel, and employed the powder X-ray diffraction method to identify the crystal phase and to measure the fixed quantities of anatase and rutile.

3. From the X-ray diffraction pattern, we confirmed that our test sample --produced by heat-treating the mixed gel with a titanium content of 5.5 wt percent at 1,400°C for 48 hours--consisted of cristobalite and very small amounts of anatase and rutile. However, the value of the lattice parameter of this α-cristobalite fell gradually with the lapse of heating time, and became constant after 32 hours. This shows that the dispersion of the fine titania particles in the gel right after its formation was extremely satisfactory, revealing the formation of a composite, atomic-level Si-O-Ti combination. This means that at this temperature the surplus titania was

gradually pushed out of the α-cristobalite crystal lattice during the heating and crystallization. In other words, it can be said that the amount of titania in the α-cristobalite, whose lattice parameter had become constant, reached the limit of solid solution at this temperature.

From the relationship between the titania content and the lattice parameter when the mixed gel--with a titania content accounting for 0~12 percent--was heat-treated at 1,400°C for 48 hours, it looks as if the limit of solid solution at this temperature was 7.4 wt percent. However, since small amounts of anatase and rutile existed at that time, as mentioned above, the actual limit of solid solution was 5.5 wt percent when they are deducted. The limits of a solid titania solution at 1,450°C and 1,500°C, obtained in the same way, were 4.9 wt percent and 3.4 wt percent, respectively. It should be noted that these limits decreased with a rise in heating temperature.

Crystallization of PZT Powder Synthesized by Sol-Gel Process

43067099b Tokyo CERAMICS KISO KAGAKU TORONKAI in Japanese 30-31 Jan 89 p 3

[Article by Eiji Ohnishi and Hiroshi Hirashima, Faculty of Science and Technology, Keio University]

[Text] **Introduction**

PZT is widely used as an electronic material for piezoelectric materials, pyroelectric materials, etc. A sol-gel method that can create a uniform mixture is advantageous for the synthesis of ceramics consisting of such a multicomponent system. In our research we synthesized $PbO-TiO_2-ZrO_2$ powders by a sol-gel method using Pb, Ti and Zr alkoxide as raw materials, and we explored the process of PZT growth from these powders.

Experimental Method

We used $Pb(iso\text{-}OC_3H_7)_2$, $Ti(iso\text{-}OC_3H_7)_4$ and $Zr(n\text{-}OC_4H_9)_4$ as raw materials and employed ethanol as a solvent. While stirring a mixed alkoxide solution with an alkoxide density of 4.1×10^{-2} (mol/l) at a component ratio of Zr:ti=53.47 at room temperature, we dripped distilled water at a rate 10 times that of the theoretical amount for 30 minutes after it was diluted with ethanol, and stirred it for another hour. We dried the precipitation resulting from hydrolysis at 80°C for 24 hours, and analyzed the powders through a DTA/TG measurement, heat treatment and an X-ray diffraction measurement.

Results and Examination

X-ray diffraction of these powders at a stage after they had been dried at 80°C for 24 hours showed them to be morphous. Through the DTA/TG measurement, an exothermic peak conceivably due to crystallization was observed in the vicinity of 500~600°C. Figure 1 shows the X-ray diffraction patterns after heat treatment. The result of heat treatment at 400°C revealed that the powders remained amorphous for 4 hours, that the halo intensity increased with the lengthening of the heating time to 24 hours and then to 48 hours, and that a PZT peak appeared after 72 hours. When the powders were heat-treated at 450°C for 4 hours, the halo peak began to divide in two. Of the two peaks, the one located at the same angle as the halo is shown in the illustration as peak a) and the other as peak b). At

500°C, the intensities of the two peaks reversed with the lapse of heating time from 0.5 hours to 1 hour and then to 4 hours. Peak b) was evidently a (101) peak of PZT. The intensity of peak a) decreased considerably at 500°C after 4 hours, and it became utterly invisible at 650°C. Based on these results, peak a) is thought to represent an intermediate product formed before the PZT crystal is separated out. This intermediate product is thought to be $Pb_2Ti_2O_6$.

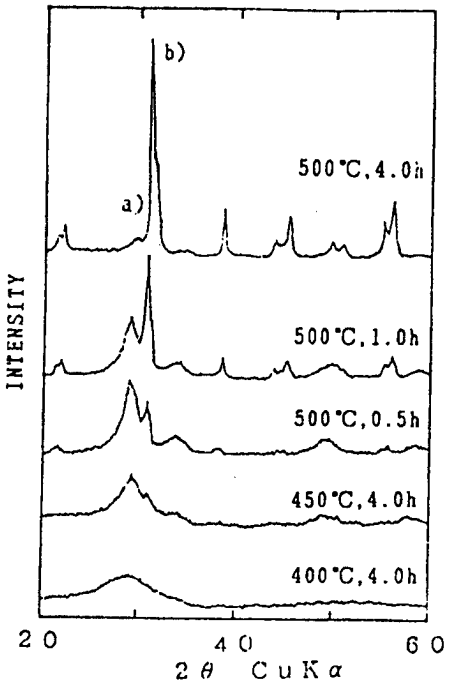

Figure 1. X-Ray Diffraction Patterns of PZT53/47 Powders

Preparation of $BaTiO_3$ Fibers by Sol-Gel Method

43067099c Tokyo CERAMICS KISO KAGAKU TORONKAI in Japanese 30-31 Jan 89 p 11

[Article by Toshinobu Yoko, Institute for Chemical Research, Kyoto University, and Kanichi Kamiya, Katsuhisa Tanaka and Kimiaki Tanaka, Department of Industrial Chemistry, Faculty of Engineering, Mie University]

[Text] **1. Introduction**

The sol-gel method has recently been attracting attention as a process for synthesizing functional ceramics. The major reason for this is that it makes it possible to synthesize high-purity, homogeneous materials at comparatively low temperatures. Glass and ceramic fibers are important as fibers for reinforcing composite materials. Representative fibers among those currently used include E glass, alumina glass and SiC fibers. Alumina fibers and silica glass fibers are currently prepared by the sol-gel method. Under this method, raw materials are mixed in a liquid state, which makes it very suitable for the synthesis of highly homogeneous composite oxides as well. Moreover, the sol-gel method makes it possible for gel fibers to be spun directly without going through a complex process simply by controlling hydrolysis and polycondensation. When these fibers are heated, they can be turned into ceramic fibers. In this research, therefore, we took up $BaTiO_3$, one of the dielectric materials that are very important as composite oxides, and attempted to prepare ceramic fibers from it by using the sol-gel method.

2. Experiments

We used a Ba metal and $Ti(O\text{-}iC_3H_7)_4$ as starting materials, and employed anhydrous ethanol and anhydrous acetic acid as solvents. In addition, we used acetic acid as a catalyst or a deflocculant. We were able to spin fibers even when ethanol was used as a solvent, but they were very short as compared to those produced when using acetic acid. Therefore, in our subsequent experiments we used only anhydrous acetic acid. We conducted sol aging at 30°C and spun the fibers using revolving spinning equipment. To examine the crystallizing behavior of the gel fibers obtained, we used the X-ray diffraction method, IR spectroscopy and TG-DTA. We determined Curie points by means of DTA.

3. Results

It was possible to effect spinning in an area where the mol ratio of H_2O to $[Ba+Ti(O\text{-}iC_3H_7)_4]$ was less than 1 and where the ratio of acetic acid was between 4 and 7. We obtained fibers 5~10 cm long. The yarn pulling property was also recognized even in an area where no water was present. It is conceivable, therefore, that acetic acid not only acts as a solvent and a deflocculant but also directly takes part in manifesting the yarn-pulling property of the sol.

We examined the gel fibers through X-ray diffraction by heat-treating them at given temperatures for 1 hour. As a result, we found that although they were amorphous fibers at 500°C, $BaTiO_3$ began to be separated out at 600°C, that the peak intensity increased with a rise in heating temperature, and that the half width decreased. In addition, we confirmed through IR spectroscopy that both chelate and a crosslinked acetic acid radical existed in the gel. The acetic acid radical was present at temperatures up to 400°C Above this temperature it was resolved and partially turned into a carbonic acid radical. The carbonic acid radical began to resolve about 700°C, and completely disappeared at 800°C. However, the carbonic acid radical was not observed in X-ray diffraction.

The gel fibers spun from a water-free sol, when heated, turned into powder. However, the fibers spun from a hydrolyzed sol, with water added, partially turned into powder after they were heated, retaining a fiber form 5~10 mm long. This difference is conceivably due to the fact that, although Ti is crosslinked by the acetic acid radical when water is not added, the addition of water causes it to be partially hydrolyzed and it becomes a Ti-O-Ti metalloxane radical.

TiC Coating on Metal by Chemical Vapor Deposition

43067099d Tokyo CERAMICS KISO KAGAKU TORONKAI in Japanese 30-31 Jan 89 p 17

[Article by Hajime Takeya, Takashi Goto and Toshio Hirai, Institute for Materials Research, Tohoku University]

[Text] **1. Introduction**

Some reaction processes for the thermochemical resolution of water have been proposed as ways to manufacture hydrogen. Among these processes, "UT-3" is one of the methods on which the greatest expectations are being placed. The UT-3 method includes a process using Br_2 and Hbr at a high temperature, standing about 1,000 K. Thus, the development of materials for equipment that is fit for such severe corrosive conditions is an important task. In this research, therefore, we aimed at improving the corrosion resistance of heatproof steel at high temperatures by coating it with ceramics. In this article we will report the results of coating heatproof steel with TiC by the chemical vapor deposition (CVD) method and will examine the area of its formation, its orientation, the speed of precipitation, its corrosion resistance, etc.

2. Experimental Methods

Using a $TiI_4+Ch_4+H_2$ gas as a raw material, we coated heatproof steel with titanium carbide (TiC) by using a CVD furnace of the indirect heating type. We used SUS304 for the substrate. The deposition temperatures (Tdep) were fixed at 1,173~1,423 K and the intra-furnace pressure at 0.1 MPa. We changed the C/Ti ratio within the limits of 0.17~17 by changing the flows of $TiCl_4$ and CH_4 in the material gas. We examined the structure and tissue of a TiC film obtained by X-ray diffraction and SEM. In addition we investigated its corrosive behavior in a Br_2-O_2-Ar atmosphere through the use of a thermal balance.

3. Results of Experiments

Figure 1 shows the relationship between the synthesis terms and the condition of the TiC film. Below Tdep=1,250 K, the TiC obtained took a soot-like form instead of the shape of a film. Above Tdip=1,250 K we obtained a filmy TiC, but found that it peeled when the Tdep or the C/Ti ratio became higher. The condition most appropriate for coating was found

to lie with the region indicated by oblique lines in Figure 1. The relationship between the speed of precipitation and the C/Ti is given in Figure 2. We discovered that the precipitation speed increased with an increase in the C/Ti ratio and a rise in the Tdep. The crystal orientation of the TiC film varied with the Tdep and the C/Ti ratio, and the (110) plane or the (100) plane was oriented in parallel with the SUS304 substrate. It was confirmed that the SUS304 that was coated with TiC by the CVD method demonstrated a superior resistivity to corrosion in a Br_2-O_2-Ar atmosphere.

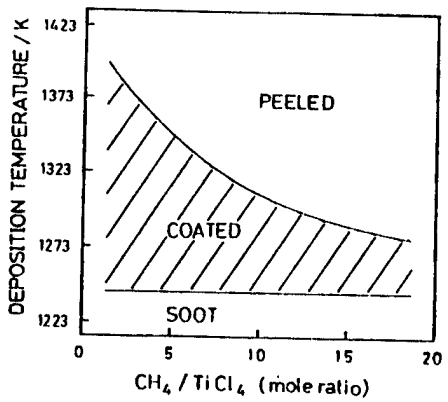

Figure 1. Area of TiC Formation

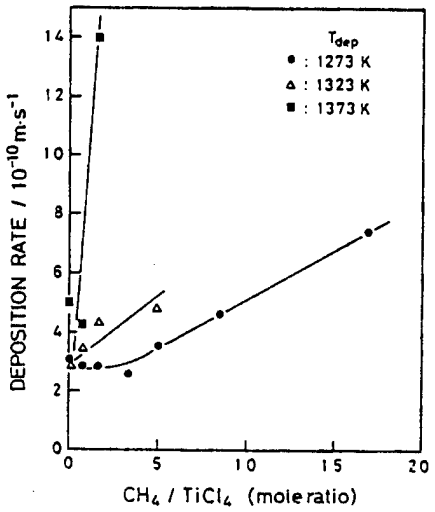

Figure 2. Relationship Between Precipitation Speed and C/Ti7

Preparation of AlN by Chemical Vapor Deposition

43067099e Tokyo CERAMICS KISO KAGAKU TORONKAI in Japanese 30-31 Jan 89 p 18

[Article by Jun Tsuneyoshi, Takashi Goto and Toshio Hirai, Institute for Materials Research, Tohoku University]

[Text] **1. Introduction**

Since AlN (aluminum nitride) is better for heat transfer than it is for electric insulation, it is being expected to serve as a material for semiconductive substrates. It is also promising as a material for surface acoustic wave (SAW) filters, because the acoustic velocity in AlN is extremely high. For any of these uses, it is necessary to produce high-purity, high-density AlN films with a crystal orientation. In this research we synthesized AlN films by the chemical vapor deposition [CVD] method and examined the relationships of synthesizing conditions for this substance with its crystal orientation, its surface morphology, its density, film fabrication velocity, etc.

2. Experimental Methods

Using an $AlCl_3+NH_3+H_2$ gas as a material, we synthesized AlN on a graphite substrate with a cold-wall-type CVD furnace operated by induction heating. We changed $NH_3/AlCl_3$ within the limits of 1.2~12 (mol ratio), holding the $AlCl_3$ supply constant ($0.85x10^{-2}$ mole/h) and changing the flow of NH_3 gas. The total gas flow was fixed at 1,000 cm^3/min, the synthesizing temperature (Tdep) at 600°C, and the total pressure in the furnace (Ptot) at 30~760 Torr. We examined the structure, composition and tissues of the AlN films obtained by such means as X-ray diffraction [XRD], scanning electron microscope [SEM], fluorescent X-rays and chemical analysis.

3. Results of Experiments

Figure 1 depicts characteristic surface tissues of an AlN film obtained in the experiments. At the 1.2 mol ratio of the raw material and below Tdep=800°C, a pebble-like tissue consisting of fine crystals was observed, as shown in Figure 1(a), and a facet-like tissue was observed above Tdep=900°C, as shown in Figure 1(b).

Figure 2 shows the orientation factor (based on a lot gelling formula) in the (001) plane of an AlN film obtained at Tdep=1,000°C. In all the $NH_3/AlCl_3$ samples, the (001) orientation factor became conspicuous with a rise in the Ptot. An AlN film obtained above Tdep=1,000°C had a theoretical density, and its lattice constant also agreed with a bibliographical value at an N/Al=1 component ratio. In the AlN film obtained below Tdep=800°C, however, the Cl was recognized as mixed, and it was confirmed that the value of its lattice constant was higher than a bibliographical value.

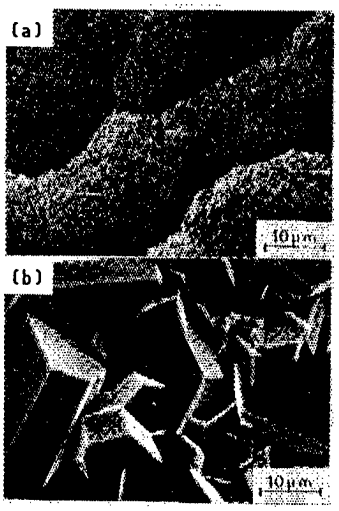

Figure 1. SEM Photo of AlN Film Surface Tissues

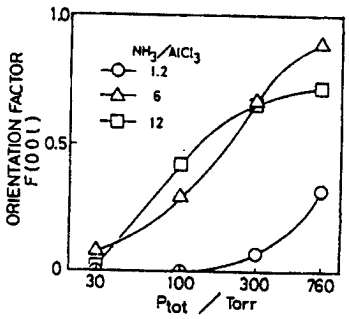

Figure 2. Dependence of (001) Orientation Factor on Infra-Furnace Pressure

Changes on Crystallization of Amorphous Si-N-C Fine Powders

43067099f Tokyo CERAMICS KISO KAGAKU TORONKAI in Japanese 30-31 Jan 89 p 25

[Article by Tadaaki Amano and Toshio Hirai, Institute for Materials Research, Tohoku University, and Kansei Izaki, Mitsubishi Gas Chemical Co., Inc.]

[Text] **1. Introduction**

An Si_3N_4-SiC composite is expected to serve as an engineering ceramic material in view of its strength and tenacity at high temperatures. To date, this composite material has been produced by mixing various powders. Recently, amorphous Si-N-C fine powders have been synthesized by thermally resolving a nitrogen-containing organic silicon compound, and it has become clear that composite materials using these powders as raw material have superior mechanical properties. The improvement in their mechanical properties is thought to be due to a nano compound of Si_3N_4 and SiC formed by the crystallization of amorphous powders. In this research we examined the morphological and microstructural change on the crystallization of Si-N-C fine powders synthesized through the thermal dissolution of hexamethyldisilazane [$(Me_3Si)_2NH$, $Me=CH_3$].

2. Methods

We synthesized four kinds of amorphous Si-N-C fine powders with different Si, N and C contents (C5: Si-35.8 N-4.8 C, C8: Si-32.8 N-8.1 C, C17: Si-29.0 N-17.3 C and C20: Si-24.2 N-19.7 C) through the thermal resolution of hexamethyldisilazane NH_3. After pretreating these amorphous fine powders in N_2, we heat-treated them in Ar at 1,713~1,803 K and 1.8~64.8 KS. From the result of our mass measurements conducted before and after the heat treatment, we calculated the mass decrease (percent) due to the heat treatment. We examined the morphological and microstructural changes in these test samples by means of X-ray diffraction [XRD] equipment (Rigaku RAD-B), an infrared spectrometer (Nippon Bunko IR-G), a transmission electron microscope [TEM] (JEOL-2000EX), an analytical electron microscope [AEM] (JEOL-2000FX) and chemical analysis.

3. Results

The amorphous fine powders before heat treatment were generally globular and 100~500 nm across. Their crystal phases comprised α-Si_3N_4 (including β-Si_3N_4) and β-SiC (including α-SiC), with β-SiC increasing and αSi_3N_4 decreasing with an increase in carbon content. The β-SiC was formed through a solid phase reaction between Si and carbon at the initial stage of heat treatment. During the heat treatment up to 1,803 K and 21.6 KS, the β-SiC was rod-shaped or angular in all kinds of powders, and its size was 20~100 nm. However, β-SiC was recognized to have grown in C17 and C20 powders at 1,803 K and 64.8 KS. The growth of α-Si_3N_4 was later than that of β-SiC, and the rod-shaped or hexagonal α-Si_3N_4 was formed through a gaseous phase reaction. On the other hand, α-Si_3N_4 fine crystals and foil-like single crystals were observed at 1,803 K and 64.8 KS in all kinds of powders. It is thought that this growth of fine, foil-like α-Si_3N_4 causes the formation of a nanostructure of Si_3N_4-SiC composite ceramics and contributes to the improvement of their mechanical properties. The decrease in the mass of the fine powders was expedited with a rise in heating temperature and with the lapse of time. The extent of mass decrease at 1,743 K was greater in the case of test samples involving larger amounts of carbon. The extent of mass decrease at 1,803 K became greater up to 21.6 KS with an increase in carbon content, but it became smaller at 64.8 KS in test samples involving larger amounts of carbon.

Microstructure of TiB_2-Cr-C System Ceramics

43067099g Tokyo CERAMICS KISO KAGAKU TORONKAI in Japanese 30-31 Jan 89 p 29

[Article by Junichi Matsushita, STK Ceramics Laboratory; Hideo Nagashima, Toshiba Ceramics; and Shinsuke Hayashi and Hajime Saito, STK Ceramics Laboratory]

[Text] **1. Introduction**

TiB_2 (titanium boride) ceramics have a number of superior properties such as a high melting point, great strength and high conductivity, and they are regarded as promising ceramics for structural materials. However, they have a shortcoming in that it is difficult to sinter TiB_2 independently. We discovered that dense and very strong ceramics can be obtained by adding small amounts of Cr and C to TiB_2 simultaneously and sintering them at normal pressure.

In this article, we will report on the microstructures of a simple TiB_2 substance and Cr-C-added ceramics.

2. Experimental Methods

As material powders, we used commercially available TiB_2 (purity: 99%; average grain size: 6 μm), Cr and carbon. We combined them at a stated ratio and sintered them at 1,900°C in an Ar gas for 1 hour, after subjecting them to wet blending, metallic mold and CIP processes. We measured the density of the ceramics obtained (by the Archimedes principle), their bending strength (test method: JIS R1601, 4-point bending) and their Vickers hardness. Thereafter we examined their microstructure by means of X-ray diffraction (XRD), scanning electron microscope (SEM), and EMPA.

3. Results and Consideration

Table 1 shows the characteristic values of the simple TiB_2 substance and Cr-C-added ceramics. Ceramics composed of 92.5wt%TiB_2+6.2wt%Cr+1.3wt%C showed a remarkable improvement in mechanical properties compared with simple TiB_2 ceramics. As a result of our X-ray diffraction analysis of the TiB_2-Cr-C test sample given in Table 1, we recognized peaks conceivably representing CrB and TiC, in addition to that for TiB_2, but we detected no diffraction peaks for the added Cr and C. Figure 1 [not reproduced] shows SEM photos

Table 1. Properties of Cr-C-Added TiB_2 Ceramics

Composition	TiB_2	92.5%TiB_2+6.2%Cr+1.3%C
Relative density (percent)	78	99
Bending strength (MPa)	160	405
Vickers hardness (GPa)	3	23

of the fractions of the simple TiB_2 substance and the TiB_2-Cr-C ceramics. In the case of the simple TiB_2 ceramics, destruction of the grain boundary is dominant, showing that they are not made sufficiently dense. As for the ceramics with Cr and C added, an intragrain destruction is found to have been caused for the most part. Figure 2 [not reproduced] shows a SEM photo of the polished and etched surface of TiB_2-Cr-C ceramics. As shown in Figure 2 [not reproduced], the TiB_2 grain is surrounded by a continuous grain boundary phase, indicating that it achieved little growth.

In other words, it can be said that dense, very strong ceramics can be obtained with these microstructures.

Crystal Structures of BaB_2O_4 Nonlinear Optical Material

43067099h Tokyo CERAMICS KISO KAGAKU TORONKAI in Japanese 30-31 Jan 89 p 31

[Article by Katsuhisa Ito, Kiyoaki Tanaka, Hideki Morikawa and Fumiyuki Marumo, Engineering Materials Laboratory, Tokyo Institute of Technology]

[Text] Single crystals consisting of low-temperature-phase BaB_2O_4 (β-BaB_2O_4) are among a number of crystals that have recently attracted attention as inorganic nonlinear optical materials. Our research was carried out for the purpose of examining the relationship between the crystal structure of low-temperature-phase BaB_2O_4 and its physical properties (secondary sensitivity) by making its structure precise. We also gave crystallographic consideration to BaB_2O_4-related substances in general by synthesizing a single crystal in which Ba is partially replaced by Ca, Sr, etc., and determining its structure.

In order to cause the low-temperature BaB_2O_4 to have a precise structure, to begin with, we used, as a test sample, a single crystal synthesized by drawing this substance directly from a melt and growing it. After molding the sample in the shape of a ϕ0.1 mm ball, we confirmed that its crystallinity was satisfactory by means of X-ray diffraction [XRD] photography, and then measured its strength. We measured the strength of diffraction within the limit of $2\theta \leq 100°$ with MoKα rays through the use of a four-axis automatic X-ray diffractometer, and obtained 1,608 points of reflection data meeting the condition of $|F| > 3\sigma$ ($|F|$). After a necessary revision, we carried out analyses using these data. In addition, we applied a YAG laser to the single crystal used as a test sample and confirmed the generation of secondary harmonics.

The lattice constants of the low-temperature BaB_2O_4 obtained in this research are given in Table 1, together with other crystallographical data. With regard to the space groups to which this BaB_2O_4 crystal belongs, there is one report that views them as R3, while another report views them as R3c. In this instance we sought to make the structure precise by hypothesizing them as R3c. As a result, we obtained R=0.0171 (wR=0.0185). However, when we carried out a differential Fourier synthesis, a comparatively high electron density, amounting to 1.9 e/A^3, remained around the Ba. For such reasons, our analysis is not yet sufficient, and therefore we are currently checking into such points.

Table 1. Crystallographical Data for Ba_2O_4

a	12.5316(4)A
c	12.7285(9)A
V	1731.1(1)A

Table 2. Crystallographical Data on $(Ba_{1-x}(Ca_x)B_2O_4$

a	7.2305(6)A
b	5.1807(8)A
c	11.521(2)A
β	92.914(9)°
V	431.0(1) A^3

As a material related to the BaB_2O_4, meanwhile, we synthesized a new material ($(Ba_{1-x}Ca_x)B_2O_4$) in which Ba was partially replaced by Ca. We synthesized this single crystal by gradually cooling a melt, using Na_2O as a flux. The space groups and lattice constants of the $(Ba_{1-x}Ca_x)B_2O_4$ single crystal are given in Table 2. The structure of this crystal differs in both BaB_2O_4 and CaB_2O_4 (Pnca: orthorhombic system), and we are seeking to determine its structure.

Effect of O_2-HIP for Oxide Ceramics

43067099i Tokyo CERAMICS KISO KAGAKU TORONKAI in Japanese 30-31 Jan 89 p 53

[Article by Yasuo Manabe, Takao Fujikawa and Yutaka Narukawa, IP Center, Kobe Steel, Ltd.]

[Text] **1. Introduction**

It is known that oxide ceramics, when treated with HIP in an inactive gas, such as an argon gas, change in quality because the oxygen leaves the oxide. Recently, research (O_2-HIP) has been conducted on the use of oxygen as part of the gas used for hot isostatic pressing (HIP) treatment.

However, there have been few systematic examinations of the atmosphere to be used during HIP treatment and the characteristics of the objects undergoing this treatment. In our research, therefore, we looked into the change in their characteristics when the HIP treatment atmosphere is changed.

2. Experimental Methods

After molding Al_2O_3 (0.25 wt percent MgO added) and TZP (ZrO_3-3 mol percent Y_2O_3) powders under 1 ton/cm^2 of pressure, we preliminarily sintered them at 1,530°C and 1,500°C, respectively. By measuring the densities of these ceramics, we found that they had a relative density above 95 percent, which made it possible to use capsule-free HIP. For the HIP treatment, we adopted the following four combinations of gases and heater materials: 1) Ar gas, Gr (graphite) heater; 2) Ar gas, Mo heater; 3) Ar + 10 percent O_2 gas, Pt-Rh heater; 4) Ar + 20T O_2 gas, Pt-Rh heater. The HIP was conditioned at 1,400°C x 1,500 kgf/cm^2.

After the HIP treatment, we measured the bending strength, densities and X-ray diffractions. In addition, we looked into the change in the characteristics of the HIP-treated materials by subjecting them to an aging process (1,000°C x 1,200 hr) in the atmosphere.

3. Results of Experiments

The relationships of the HIP treatment atmosphere to the densities and bending strength are given in Table 1. As a result of the density

measurements, both Al_2O_3 and TZP showed a (2)>(3)>(4)>(1) pattern. However, the bending strength after the HIP treatment showed no significant difference, exhibiting much the same value. Looking into the change in color before and after the TZP aging process, we found that it changed from black to yellow in case (1) where a Gr heater was used. This is conceivably due to deoxidization and the entry of carbon during the HIP treatment. In case (2) where an Mo heater was used, the color showed little change before or after the aging process, presumably because no carbon entered during the HIP treatment.

The results of our bending test and other experiments after the aging process will be reported subsequently.

Table 1. Relationships of HIP Treatment Atmosphere to Densities and Bending Strength

Heater material		Atmosphere	Al_2O_3-0.25wt%MgO		ZrO_2-3mol%Y_2O_3	
			Density (g/cm^3)	3-point bending strength (kgf/mm^2)	Density (g/cm^3)	3-point bending strength (kgf/mm^2)
(1)	Gr	Ar	3.971	67.0	6.090	146.2
(2)	Mo	Ar	3.984	67.1	6.104	155.0
(3)	Pt-Rh	Ar+10%O_2	3.977	69.6	6.103	156.2
(4)	Pt-Rh	Ar+20%O_2	3.975	65.5	6.100	165.3

Effective Partial Oxygen Pressure in HIP Apparatus

43067099j Tokyo CERAMICS KISO KAGAKU TORONKAI in Japanese 30-31 Jan 89 p 54

[Article by Akio Watanabe, Hajime Haneda, Shun-ichi Hishita, Hiroshi Yamamura, Yusuke Moriyohi and Shin-ichi Shirosaki (NIRIM, TOSOH)]

[Text] **1. Introduction**

It is known that many oxides, including ZrO_2, are deoxidized by a hot isostatic pressing (HIP) apparatus. To avoid damage to deoxidization, it is necessary to measure and control the partial oxygen pressure in a furnace. However, it is technically difficult to measure the partial oxygen pressure in an HIP furnace because the measurement has to be made in a high-pressure gas. In our research, therefore, we carried out indirect examinations of the effective partial oxygen pressure in an HIP apparatus, looking into how a test sample is deoxidized after the HIP process and examining the partial oxygen pressure under which the sample, forcibly deoxidized at 1 atm, is put in the same state of deoxidization.

2. Experiments

As a sample, we used an $SrTiO_3$ transparent ceramic (10 mm across and 1 mm long) obtained by HIP.

We subjected the sample to an HIP process at 1,300°C for 2 hours at pressures from 5~200 MPa in Ar. Then we measured its optical transmittance. Next, we deoxidized the same sample, changing the partial oxygen pressure by applying an Ar-O_2 mixed gas for 2 hours under 1 atm at 1,300°C. Then we measured its optical transmittance at that time.

For the HIP process we used a hot isostatic press manufactured by Kobe Steel, Ltd. (Pt-Rh wire is used for the heater in this equipment).

3. Results and Consideration

Figure 1 shows the representative optical transmittance of the sample. The solid line represents the transmittance before the HIP, and the dotted line shows that measured after the HIP (50 MPa). Deoxidization causes the optical transmittance to drop for all wavelengths, and the loss of

transmittance due to the deoxidization is easily restored to its original value through reoxidation.

Figure 2 shows the change in transmittance (800 nm) due to HIP pressure. The transmittance rises with an increase in HIP pressure, presumably under the influence of impure oxygen in Ar.

On the day of discussions, we will also report the result of our measurement of electric conductivity.

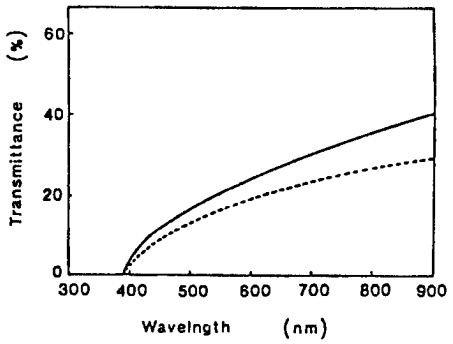

Figure 1. Optical Transmittance

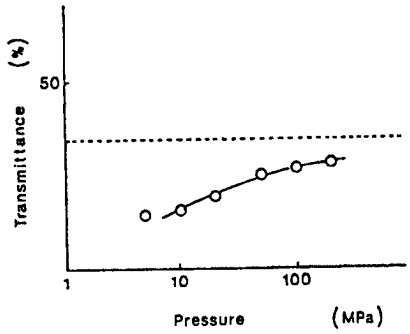

Figure 2. Change in Transmittance Due to HIP Pressure

References

1. Masahiko Shimada, CERAMICS, No 22, 1987, p 479.

2. Akio Watanabe, et al., Preprint for the First Autumn Symposium of the Japan Ceramics Society, 1988, p 499.

Densification of SiC by Hot Isostatic Pressing

43067099k Tokyo CERAMICS KISO KAGAKU TORONKAI in Japanese 30-31 Jan 89 p 55

[Article by Masaharu Kajita, Shinji Kawasaki and Keiji Matsuhiro, NGK Insulators, Ltd.]

[Text] **1. Introduction**

In the case of capsule-free hot isostatic pressing [HIP] upon removing the pores in a molded body through primary sintering, the microstructure of the primary ceramic material is thought to be an important factor for the effective densification of the ceramic. In this study we fabricated primary ceramics with different microstructures by adding MgO to B-C SiC as the third additive, and examined the effects of the microstructure of the primary ceramic material on their densification through HIP.

2. Experimental Methods

We pulverized and mixed 100 g of β-SiC powder, 0.3 g of B_4C powder, 2.0 g of carbon black and 0~2.0 g MgO powder by means of a vibration mill, molded them after dry granulation and sintered them at 2,080°C in a vacuum for 1 hour. This was followed by a HIP process by 2 hours at 2,000°C and 2,000 kf/cm^2.

3. Results and Consideration

With an increase in the amount of the added MgO, the density of the primary ceramic material dropped, but the density of the post-HIP ceramic increased with an increase in the amount of the MgO. Moreover, the addition of the MgO made it possible to densify the primary low-density ceramic through the HIP processes, compared to the case of not adding it (only B-C was added) as shown in Figure 1. In the primary ceramic material to which the MgO was added, there were many sharp pores in the grain boundary (Figure 2).

The effectiveness of adding MgO in the densification through HIP is conceivably due to the difference in the microstructure of the primary ceramic material, particularly in the form of the pores as well as in the distribution of pore size. In our next report, therefore, we will describe the relationship between the microstructure of the primary ceramic material and densification behavior through HIP.

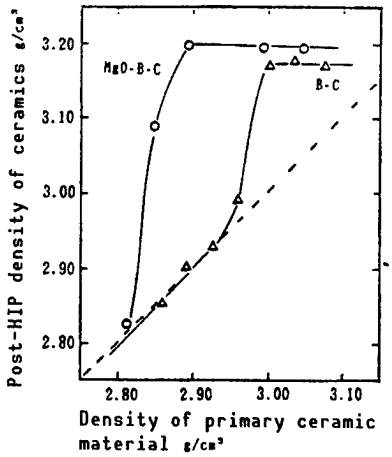

Figure 1. Change in Density Before and After HIP Process

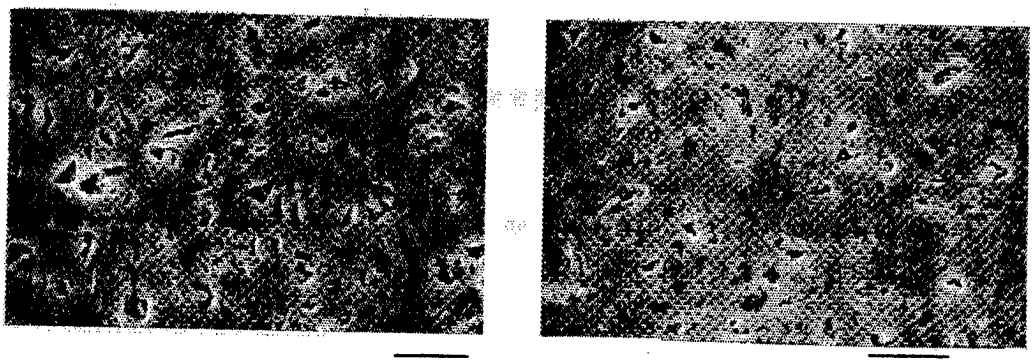

(A) MgO: 2.0%, 2.89 g/cm^3 10 μm

(B) MgO: 0%, 3.02 g/cm^3 10 μm

Figure 2. SEM Photo Representing the Polished Surface of the Primary Ceramic Material

Sintering of β-Si_3N_4

430670991 Tokyo CERAMICS KISO KAGAKU TORONKAI in Japanese 30-31 Jan 89 p 63

[Article by Mamoru Mitomo, NIRIM, and Satoshi Uenosono, Kawasaki Steel Corp.]

[Text] **1. Introduction**

Raw materials with a high α content have been regarded as desirable in terms of their sintering and mechanical properties. To reexamine the sintering property β-Si_3N_4 powder and the microstructure of the ceramics obtained therefrom, we compared them against the results of our examinations of α-Si_3N_4 powder, using a gas pressurized sintering method.

2. Experiments

As material powders, we used β-silicon (average grain size: 1.7 μm; oxygen content: 1.3 percent) produced by heat-treating high-purity α-Si_3N_4, and α-Si_3N_4 (Toso-made TS-7; average grain size: 0.6 μm; oxygen content: 1 percent). As auxiliary sintering agents, we employed 5 wt percent Y_2O_3 and 2 wt percent Al_2O_3. After primary formation at the rate of 0.2 t/cm^2, we performed rubber pressing at a rate of 2 t/cm^2 and turned them into a molded body measuring about 16 mmϕ. We sintered it at 1,800~2,000°C in nitrogen at a pressure of 10 atm. We measured the shrinkage of the sample with the shrinkage measuring equipment fitted to the sintering furnace. After sintering, we examined the decreases in its density and weight. By means of a scanning electron microscope (SEM) we observed the fracture, the ground surface and the etched surface.

3. Results and Consideration

Figure 1 shows the relationship between the sintering temperature and the decreases in density and weight. Below 1,900°C, the ceramics obtained from the β powder had a higher density than those obtained from the α powder. When the temperature exceeded 1,900°C, their densities became almost equal. Under various conditions, the rate of the crop in weight was lower in the case of the β powder. In spite of the fact that the average grain size of the β powder was about three times that of the α powder, they had much the same or a higher sintering property.

Figure 2 shows the microstructure of the ceramics obtained from the β powder. This structure consists of a coaxial grain measuring about 1 μm, a larger coaxial grain measuring about 3 μm and a pillar-shaped grain 1.2 μm across and about 6 μm long. The aspect ratio of the pillar-like grain is about 5, while that of the pillar-like grain of the ceramics obtained from the powder is 7~8. This is the reason why they have a high degree of tenacity. Since the β powder ceramics have a lower aspect ratio than the α-powder ceramics, their tenacity (strength) is presumed to be lower. This difference is thought to derive from the difference in the mechanism of grain growth.

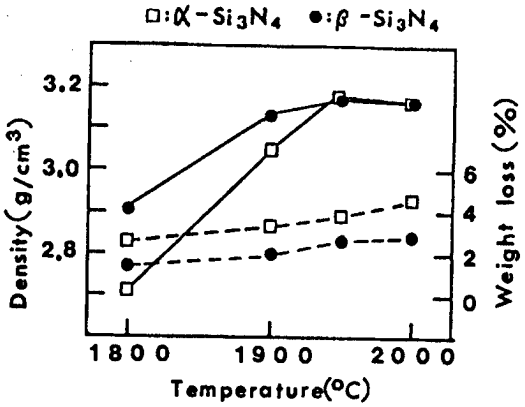

Figure 1. Relationship Between Sintering Temperature and Decreases in Density and Weight

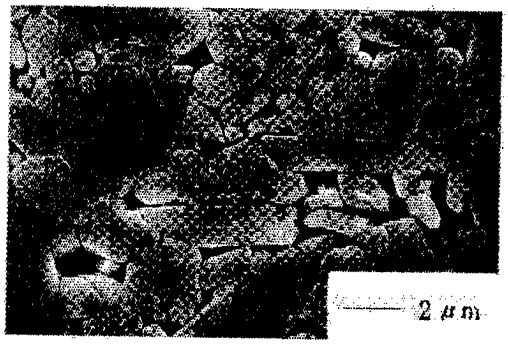

Figure 2. Microstructure of Ceramics Obtained From Powder (Etching surface)

Preparation of High-Tc Oxide Superconductor

43067099m Tokyo CERAMICS KISO KAGAKU TORONKAI in Japanese 30-31 Jan 89 p 105

[Article by Shingo Katayama, Masahiro Sekine and Yoshitaka Nomiya, Colloid Research Institute]

[Text] **1. Introduction**

Since the discovery of a $YBa_2Cu_3O_{7-x}$ superconductor, various preparation methods have been studied with an eye to putting it to practical use. The metal alkoxide method is characterized by its ability to manufacture high-purity, homogeneous ceramics and to provide them with structure and form. Therefore, there are expectations that it can be applied to highly efficient superconducting oxide films, fibers, etc.

In this study we looked for agents to improve the solubility of Y and Cu alkoxides, which are hard to melt in such organic solvents as alcohol. We also explored the synthesis of a $YBa_2Cu_3O_{7-x}$ supercomputer from a uniform Y-Ba-Cu mixed alkoxide solution.

2. Experimental Methods

We studied the solubility-improving effects of various kinds of amino-ethanols and chose 2-dimethylaminoethanol as an agent for improving the solubility of both Y and Cu alkoxides. We melted $Y(O\text{-}iC_3H_5)_3$, $Cu(OCH_3)_2$ and metallic barium at a $YBa_2Cu_3O_{7-x}$ component mol ratio, respectively, in ethanol that contained 2-dimethylaminoethyl with the same mol as the alkoxide radical of Y and Cu alkoxides, thereby obtaining uniform solutions of various alkoxides. As for the product resulting from the reaction between a metallic alkoxide and the solubility improving agent, we examined its structure by means of EXAFS, IR, NMR, etc. We hydrolyzed this solution by adding water with the same mol as the alkoxide radical, removed the solvent, and obtained a $YBa_2Cu_3O_{7-x}$ precursor. We examined the heating behavior of the precursor by means of TG-DTA and identified the formation phase through X-ray diffraction [XRD]. We calcined and sintered the $YBa_2Cu_3O_{7-x}$ precursor and measured the resistance of the ceramics thus produced by using a DC four-terminal method.

3. Results and Consideration

In the TG-DTA analyses of the precursor, we observed an exothermic DTA peak and a decrease in TG weight due to the dissolution and combustion of the residual organism, followed by an endothermic DTA peak at 800°C due to the formation of a $YBa_2Cu_3O_{7-x}$. Figure 1 shows the powder X-ray diffraction patterns at various calcination temperatures in air. The $YBa_2Cu_3O_{7-x}$ precursor was noncrystalline. The formation of Y_2O_3, $BaCO_3$ and CuO was recognized at 700°C, but the $YBa_2Cu_3O_{7-x}$ phase was formed above 800°C and a $YBa_2Cu_3O_{7-x}$ single phase between 800°C and 850°C. The formation of a medium phase was recognized in the course of sintering, but the $YBa_2Cu_3O_{7-x}$ single phase was formed at a lower temperature than in the case of the solid phase method. This hints at the effect of the uniformity of the precursor. The powder calcined at 900°C was molded at a rate of 900 kg/cm^2, sintered at 930°C for 2 hours in an oxygen current, and annealed at 400°C for 10 hours in the same current. The ceramics thus produced showed a Tc onset=88 K and a Tc zero=85 K.

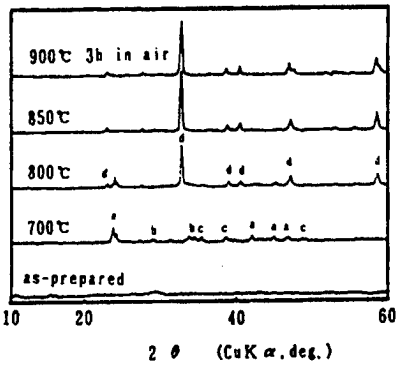

Figure 1. Powder X-Ray Diffraction Patterns at Various Temperatures

Synthesis of TiB_2TiNi Composite Materials

43067099n Tokyo CERAMICS KISO KAGAKU TORONKAI in Japanese 30-31 Jan 89 p 168

[Article by Norio Yanagisawa, Osamu Asano and Nobuhiro Sata, Government Industrial Research Institute, Tohoku]

[Text] **1. Introduction**

The self-propagating high-temperature synthesize (SHS) process is attracting attention as a new method for manufacturing ceramics and intermetallic compounds, and a number of studies have been conducted on the technique's applications. The purpose of our research was to exploit the SHS process in the synthesize of ceramic-intermetallic compound systems of composite materials. We tried to synthesize TiB_2-TiNi ($NiTi_2$) system composites using a powder--a mixture of Ti, B and Ni--as the raw material.

2. Experiment

Our hypothesis was that all three elements--Ti, B and Ni--would react to form TiB_2 and TiNi or TiB_2 and $NiTi_2$. The raw material powders were mixed at a ratio based on the above assumption. For synthesize, we employed a single spindle pressure device that used a spring compression method. The raw materials weighed a total of 2 grams. The raw material powder underwent a preliminary compression at normal temperature and 50 MPa in a vacuum vessel, while its synthesis was initiated by igniting a fire at a pressure of 25 MPa. The synthesized samples thus obtained were measured with respect to tissue observation, identification of the compounds by X-ray diffraction [XRD], and relative density.

3. Results

For the TiB_2-TiNi system, the reaction progressed within a range in which the composition of the TiNi varied from 0~95 percent of the total mass. As the TiNi content increased, the relative density went up, surpassing 90 percent when the TiNi was above 70 percent. As for compounds, the generation of TiB_2 and TiNi was confirmed, but the TiNi contained both monoclinic and cubic crystals (Figure 1). Meanwhile, the composite containing 50 percent TiNi, TiB_2 and TiNi showed microscopic structures on the submicron order (Photo 1).

As for the TiB_2-$NiTi_2$ system, the reaction progressed within a range in which $NiTi_2$ accounted from 0~80 percent of the total. The relative density went over 90 percent when the $NiTi_2$ constituted 60 percent and above. As for compounds, the generation of TiB_2 and $NiTi_2$ was confirmed, and TiB and TiNi were also detected when $NiTi_2$ was 70 percent and above (Figure 1).

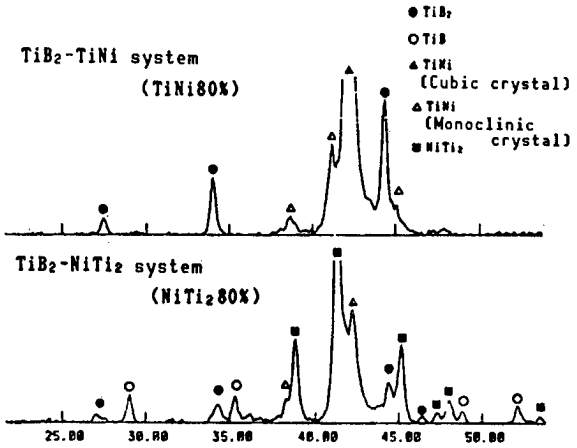

Figure 1. X-Ray Diffraction Patterns of Synthesized Products

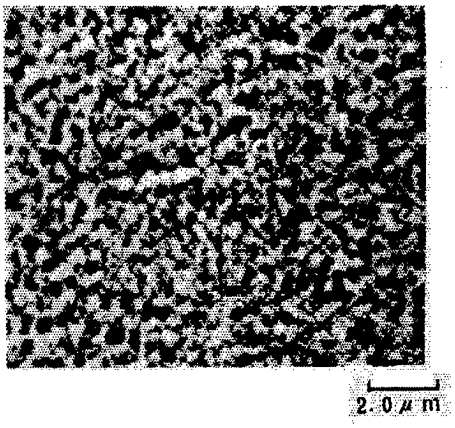

Photo 1. Microscopic Tissue of Synthesized Product

Self-Propagating Reaction Process for Simultaneous Synthesis

43067099o Tokyo CERAMICS KISO KAGAKU TORONKAI in Japanese 30-31 Jan 89 p 169

[Article by Nobuhiro Sata, Osamu Asano, Norio Yanagisawa, Government Industrial Research Institute, Tohoku]

[Text] **1. Introduction**

Studies are being conducted on methods for applying self-propagating high-temperature synthesis [SHS] reaction processes in material synthesis. The authors have been engaged in research on simultaneous synthesis and formation technology. This is based on the concept of conducting synthesis and formation simultaneously by exploiting the large amount of reaction heat produced during synthesis. In this paper we will report on the results of our research into the synthesis and formation process under hydrostatic pressure--a process in which water is used as the medium to exert pressure. We believe this process will not only make it possible to apply a coating over a large area as well as to manufacture compact items with complex shapes, but will also prove to be economical.

2. Experiment

Figure 1 is a schematic diagram of the apparatus for synthesis and formation under hydrostatic pressure that we used. the pressure vessel was a flow-type autoclave with the following capacities: 1.5 liter internal capacity, a maximum of 30 MPa of pressure, and a water-feeding rate of 6 liters per minute. The pressure vessel has a gas-filled accumulator connected to it that works as a pressure buffer. The forming jig that contains the sample powder is lowered into the water as if suspended. Initially we used a copper device for the forming jig but then switched to a simpler silicon rubber device with graphite sheet shielding. The forming jig was enclosed in a vacuum with a sample powder that had earlier been dust formed using a CIP under a pressure of 2 ton/cm^2. As for the synthesis method, we adopted an indirect process in which an electric current was led to the ignition agent (Ti + 2B powder) and the sample was ignited indirectly via an 0.2-mm thick graphite sheet extending from the ignition agent.

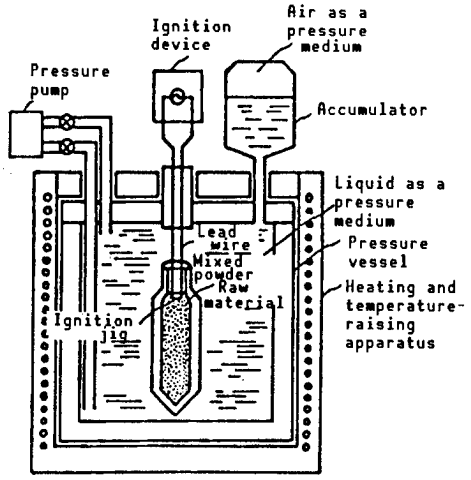

Figure 1. Schematic Diagram of Apparatus for Synthesis and Formation Under Hydrostatic Pressure

3. Results

Our SHS process succeeded in the synthesis of a TiB_2-Cu system material from a mixed powder of Ti, B and Cu, and the material was fabricated into a disk-type synthetic compact 50 mm in diameter and 5 mm thick. Since the pressure vessel's content volume is 90 mmϕ by 230 mm, a sheet material with a maximum size of 70 mm by 200 mm can be manufactured. By installing partitions as shown in Figure 2(b) and 2(c), several samples can be synthesized and formed simultaneously. Based on these results, we are exploring ways to apply this technology to the fabrication of products with more complex shapes.

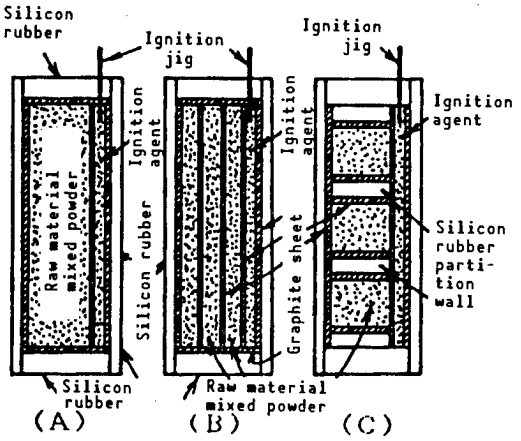

Figure 2. Various Forming Jigs Used in Synthesis and Formation

TiN-Mo, TiN-Ta Metallization of AlN Substrates

43067099p Tokyo CERAMICS KISO KAGAKU TORONKAI in Japanese 30-31 Jan 89 p 196

[Article by Hironori Asai, Hideki Sato, Nobuyuki Mizunoya, Yasuyuki Sugiura and Fumino Ueno, Toshiba Corp.]

[Text] **1. Introduction**

We have metallized AlN substrates with refractory metals and TiN. This report describes the results of our experiments and the boding mechanisms involved.

2. Experimental Method

AlN single-phase substrates having a thermal conductivity of 270 W/m•K were used in our tests. Two types of mixed pastes, Ta/TiN and Mo/TiN, were used as metallizing pastes. As for the composition of the pastes, the contents of the refractory metals were 100, 80, 67, 50, 33 and 0 in volume percentage. Pads measuring 2 mm^2 were formed on the substrates by a printing method and burned at 1,740, 1,800 and 1,850°C. The metallized sections were coated with a Ni/Au plating. The bonding strength of each metallization was obtained by the following method: A soft copper wire, 1 mm in diameter including soldering, was connected to the metallization using a 63 Sn-Pb solder and it was pulled vertically at a speed of 3 mm/min. The substrates metallized with the mixed powders--whose refractory metal content varied from 100 to 67 to 50 to 33 to 0 in volume percentage--were press formed and burned at 1,400, 1,575, 1,710 and 1,850°C to measure the rate of contraction of the compacts made of the mixed powders. The density of the compacts were calculated by measuring their external dimensions.

3. Results and Consideration

Figures 1 and 2 give the bonding strength of Mo (burned at 1,800°C) and the ratio of the density of the sintered body of the mixed powder to its theoretical density, respectively. Similarly, Figures 3 and 4 give the corresponding values for Ta. Mo contracted as it burned, but Ta showed very little contraction. When TiN was added separately to the Mo and Ta, their rates of contraction at 1,850°C neared that of TiN (about 80 percent).

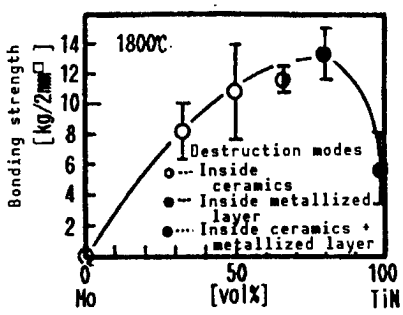

Figure 1. Bonding Strength of Mo/TiN Metallization

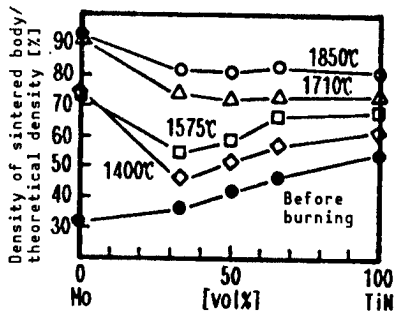

Figure 2. Ratio of Mo to TiN in Density in Mo/TiN Mixed Powder

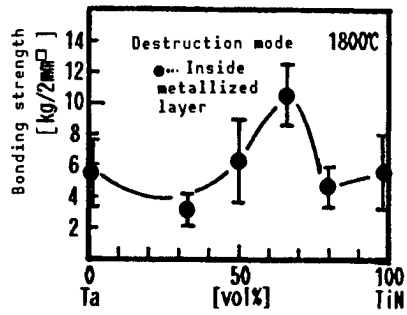

Figure 3. Bonding Strength of Ta/TiN Metallization

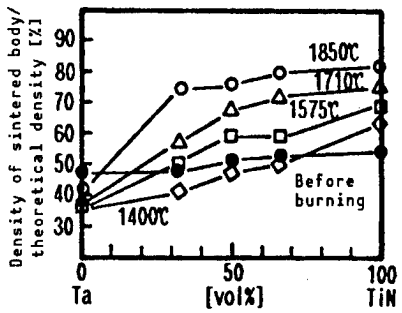

Figure 4. Ratio of Ta to TiN in Density in Ta/TiN Mixed Powder

Used alone, TiN bonded to the AlN. However, Mo, when used alone, failed to make such a bond and it peeled off at the AlN/metallized layer interface. When Tin was added, Mo increased its bonding strength, attaining a maximum value of 80 in volume percentage. This represents about a two-fold improvement in bonding strength over the bonding strength achievable with TiN alone. Ta when used alone displayed a bonding strength about the same as that available through the use of TiN alone, but no significant improvement was observed in its bonding strength even when TiN was added. Cracks accompanying strength measurements were observed in the metallized layer in the case of TiN, in the interior of the ceramics in the case of Mo when the Mo content was high (except for the case in which Mo accounted for 100 percent of the volume), while Ta showed ruptures throughout the metallized layer.

From the foregoing results, one can see that TiN can be bonded with AlN, but since the TiN fails to become compacted, the resulting metallized layer has a weak bonding strength. By contrast, the strong bonding strength of Mo-TiN comes from the fact that, due to the compaction of the Mo, the metallized layer gains in strength, which gives rise to the occurrence of a mechanical bonding effect between it and the substrate, while TiN suppresses the compaction of the Mo on the lower temperature side, thereby preventing the Mo from peeling off the substrate. When using Ta/TiN, both the Ta and TiN fail to compact, which is the cause for the weak strength of the metallized layer formed by a mixed powder comprising the two metals.

Studies are being conducted on other refractory metals.

Metallization of Ceramics by Ion Beam, Vapor Deposition

43067099q Tokyo CERAMICS KISO KAGAKU TORONKAI in Japanese 30-31 Jan 89 p 197

[Article by Yoshinao Kato, Norio Sugiyama and Eiji Kamijo, Nissin Electric Co., Ltd.]

[Text] The metallization of ceramic surfaces is a critical surface treatment technique for etching interconnections on a ceramic substrate as well as for bonding ceramics with other materials. For ceramics of the oxide system, such as Al_2O_3, use of the high melting point metallization method has made it possible to attain sufficient adhesive strength. But in the case of nonoxide ceramics, such as AlN, no metallization technology has been established that can impart to the metallization the degree of adhesive strength necessary for practical application. We introduce here metallization of ceramics by IVD (ion beam and vapor deposition)--a process that makes it possible to bond metal thin films to ceramic surfaces with good adhesion. This is done by exploiting the mixing effect of the ion beam which we have developed. The use of this technique has made it possible for a monolayer of thin metal film, deposited at room temperature, to have a high level of bonding strength to ceramics of both the oxide and nonoxide systems.

1. Experiment

After being subjected to ultrasonic cleaning, the ceramic sample was placed inside the IVD equipment for processing. While a thin metal film (Cu, Ti, Ni, etc.) was being deposited in a vacuum, the surfaces of the sample were exposed simultaneously to irradiation by ion beams (Ar and N_2; 5~25 keV). When the metal film thickness reached the ion's range (~10 nm) inside the metal, ion irradiation was stopped but deposition of the metals continued until the coating was about 50 nm thick. The processed sample was subjected to tensile strength tests to measure the adhesive strength of the thin metal film.

2. Results

Figure 1 shows the results of a metallization in which an AlN sample has been metallized with Cu. It shows that when the amount of Ar ions (dose) being injected simultaneously reached a certain level, the Cu film adhered to the AlN surfaces with an extremely high degree of adhesive strength

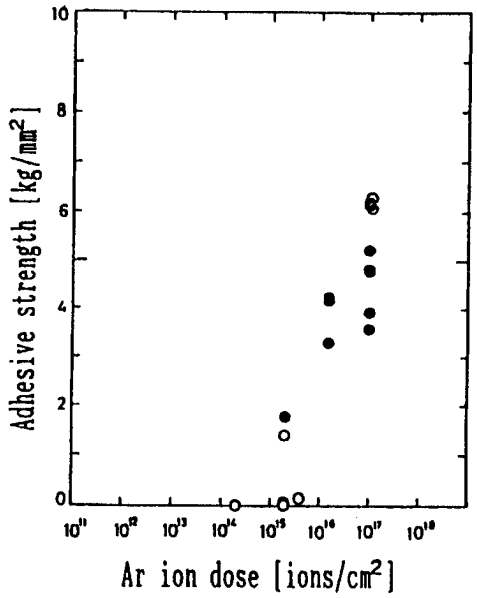

Figure 1. Relationship of Adhesive Strength of Cu Thin Film Deposited on AlN and Ar Ion Beam Dose
The accelerating voltage of the ion beam was set at 5 kV (o) and 25 kV (•).

($\geq$6 kg/mm^2). We intend to present our research on the effect of heat treatment on adhesive strength.

References

1. Kato, Sugiyama and Moriyama, INDUSTRIAL MATERIALS, Nikkan Kogyo Shimbunsha, Vol 36 No 15, 1988 p 61.

2. Ibid., NISSIN ELECTRIC CO. JOURNAL OF TECHNOLOGY, Vol 33 No 2, 1988 p 18.

Shape Effect of SiC Whiskers on Al_2O_3-SiC Whisker Composites

43067099r Tokyo CERAMICS KISO KAGAKU TORONKAI in Japanese 30-31 Jan 89 p 198

[Article by Hidemi Watanabe, Ashikaga Institute of Technology, and Atsushi Nakahira, Takashi Hirano and Koichi Niihara, National Defense Academy]

[Text] **1. Introduction**

A technique involving the reinforcement of ceramics with fibers has been proposed in recent years as a method for overcoming the brittleness of ceramics. As part of this trend, active studies have been conducted on Al_2O_3-SiC whisker-reinforced composite materials. However, much is still not known about the conditions that make it possible to obtain high-strength and high toughness composites. Further, the characteristics that the whiskers need to be provided with have yet to be fully explained. In order to examine the effects of whiskers on Al_2O_3, in our research we mixed differently shaped SiC whiskers with two types of Al_2O_3 in various combinations to produce composites. These composites were fabricated by hot pressing, and the sintering temperature and the ambient atmosphere were used as the parameters for the conditions of hot pressing.

2. Experimental Method

Two kinds of Al_2O_3 (α and γ) were used as the starting raw materials. For whiskers, we used two types of products manufactured by the Tateho Kagaku (Chemicals) Co.--SCW No 1S (fine) and SCW No 1-S-105-0.7 (coarse). These materials were mixed in an alcohol dispersion medium at a ratio of 80 percent Al_2O_3 and 20 percent SiC whiskers by volume. The mixture was subjected to hot pressing in an environment of inert gases (Ar and N_2) and also in a vacuum (30 MPa/60 min). The sintering temperatures were set at 1,700, 1,800 and 1,900°C. In accordance with JIS 1601, specimens were cut out from the composites obtained in a way so that their plane vertical to the axis of the hot press formed the tension plane. The samples were then ground. The specimens were measured with respect to density (Archimedes' method), three-point bending strength, fracture toughness and Vickers hardness. The fractures were observed using a scanning electron microscope (SEM).

3. Results and Consideration

Figure 1 shows the bending strength and the relative density of the specimens obtained by hot pressing in an N_2 atmosphere. Using the results, we studied the effect of whisker diameter. A comparison of the two types of specimens--one using coarse γ-Al_2O_3 whiskers and the other using fine γAl_2O_3 whiskers--shows a conspicuous difference between the two, with the spread in strength between the two showing more than 300 MPa, especially at 1,800°C. Similarly, a combination of α-Al_2O_3 and the coarse whiskers shows a value larger than that for the amorphous-Al_2O_3 and fine whisker combination. As for the influence of the difference in the types of Al_2O_3, γ shows a value about 150 MPa higher than that for α at 1,800°C. As for density, specimens mixed with fine whiskers failed to gain in compaction. This fact alone suggests the reason why improvements in strength have not been realized. As indicated above, it has become apparent that coarse whiskers can improve composite properties much more than fine whiskers. The best result was obtained under the following conditions: a combination of γ-Al_2O_3 + coarse whiskers and a sintering temperature of 1,800°C. The fracture toughness K_{IC} showed its highest value at 1,800°C but decreased at 1,900°C.

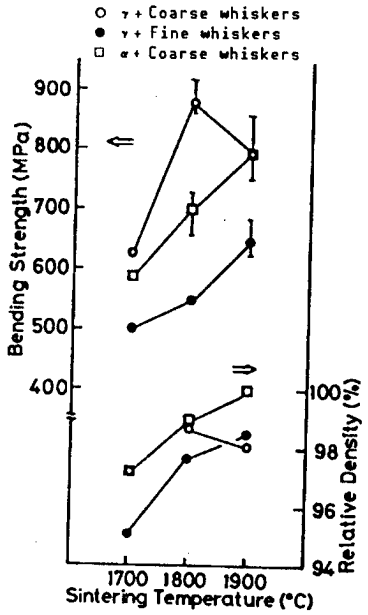

Figure 1. Changes in Bending Strength and Relative Density With Changes in Sintering Temperature

Effect of Heat Treatment on Al_2O_3/SiC Nanocomposites

43067099s Tokyo CERAMICS KISO KAGAKU TORONKAI in Japanese 30-31 Jan 89 p 199

[Article by Atsushi Nakahira and Koichi Niihara, National Defense Academy

[Text] 1. **Introduction**

Our research to date has revealed that Al_2O_3/nonoxide ceramic composites are highly effective in improving the properties of Al_2O_3. It has been learned, in particular, that Al_2O_3/SiC nanocomposites--a material obtainable by dispersing extremely fine SiC grains among Al_2O_3 grains--have a greatly improved breaking strength and that heat-treating these high-strength Al_2O_3 nanocomposites can increase their strength still further. This report describes the effects of heat-treating these Al_2O_3 nanocomposites on their mechanical properties.

2. **Experiment**

The starting materials used to produce the Al_2O_3 composites were Al_2O_3 manufactured by the Asahi Chemical Industry Co. and SiC (2 μm and <0.3 μm) manufactured by the Ibiden Co. These raw materials were mixed in a ball mill and then sintered by hot pressing to prepare the composites. The hot pressing took place in a nitrogen atmosphere at 28 MPa and at temperatures that ranged from 1,600~1,800°C. The fracture toughness values were measured by the IM method and the breaking strengths were evaluated using three-point bending tests. The heat treatments were conducted both in the air and in an Ar atmosphere at temperatures ranging from 1,000~1,400°C. This was done to assess the effects of heat treatment temperature and heat treatment duration on fracture toughness and strength as well as on the composition phase.

3. **Results**

Figure 1 shows the effects of heat treating on the breaking strength of Al_2O_3/5-volume percent SiC (2 μm) and Al_2O_3/5-volume percent SiC (0.3 μm) composites. In the case of Al_2O_3/SiC (2 μm) composite, the increase in breaking strength after heat treating was slight, but the Al_2O_3/SiC (0.3 μm) composite greatly improved in breaking strength when heat treated at temperatures from 1,200~1,300°C. This improvement was from about 1,000 MN/m^2 before heat treatment to about 1,500 MN/m^2 after heat treatment in both air and Ar atmospheres.

Since X-ray diffraction analyses of the composites after heat treatment did not reveal any change in their composition phase, we believe the increased breaking strength accompanying the heat treatment came about for the following reason: The heat treatment blunted the damage that occurred during the processing of the specimens.

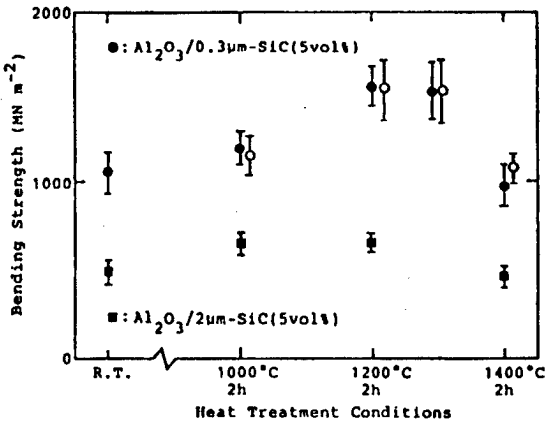

Figure 1. Effects of Heat Treating on the Breaking Strength of Al_2O_3/SiC Composites
■●: in air
o: in Ar

Improved Mechanical Properties of Si_3N_4 Nanocomposites

43067099t Tokyo CERAMICS KISO KAGAKU TORONKAI in Japanese 30-31 Jan 89 p 206

[Article by Koichi Niihara and Takeshi Hirano, National Defense Academy, and Kansei Izaki and Takamasa Kawakami, Mitsubishi Gas Chemical Co., Ltd.]

[Text] **1. Introduction**

There have been a number of efforts to utilize Si_3N_4, along with SiC, as a high-temperature structural material in various applications. In its single phase, however, the material has limited properties. Thus, attempts have been made to utilize it in the form of composites with whiskers or particles. In conventional methods for forming composites, however, the size of the dispersion phase has been at the micron level. In our research we tried to produce Si_3N_4 nanocomposites by hot pressing a composite Si-C-N powder obtained by chemical vapor deposition (CVD) and letting the SiC grains, several tens of nanometers in diameter, disperse among the Si_3N_4 grains. Our goal was to improve the composites' construction and properties.

2. Experimental Method

The Si-C-N composite powder was synthesized by letting hexamethyldisilazane react with ammonium in a gaseous phase, which was then subjected to a heat treatment in an N_2 atmosphere for stabilization. To this powder were added 6 wt% Y_2O_3 and 2 wt% Al_2O_3 as sintering-assisting agents, and everything was mixed in a ball mill. The mixture was hot pressed in an N_2 atmosphere for 2 hours at 1,800°C at a pressure of 34 MPa to obtain a sintered body. With regard to the mechanical properties of the sintered body, we measured the hardness value with a micro-Vickers test and a high-temperature hardness tester at temperatures that ranged from room temperature to 1,150°C. We measured its strength with a three-point bending method at temperatures that ranged from room temperature to 1,500°C, while we obtained the rupture toughness value by the IM method. The modulus of elasticity was measured by the resonance method. With regard to thermal characteristics, heat conductivity was measured by a laser flash method at temperatures that ranged from room temperature to 1,000°C. The coefficient of linear expansion was measured with a push bar thermal expansion meter at temperatures that ranged from room temperature to 1,400°C. Antithermal shock properties were evaluated by means of rapid quenching in water. The

microscopic structure was observed by using an X-ray diffraction machine, an optical microscope, a scanning electron microscope (SEM), a transmission electron microscope (TEM) and a high-resolution electron microscope (HREM).

3. Results of Experiment

TEM and HREM observations have revealed the presence of fine SiC grains, several tens of nanometers in diameter, dispersed not only in the grain boundaries but also inside the grains of Si_3N_4. This attests to the fact that the material was formed as a result of Si_3N_4 and SiC having complexed at the nanometer level to form a nanocomposite. SEM observation revealed that the Si_3N_4 nanocomposite had a structure finer than that of the single-phase product of Si_3N_4 that was used for comparison, and that no abnormal growth of grains had taken place. The average value of the aspect ratios was the greatest when the SiC content was 10 percent in volume, at about 6. The strength of the nanocomposite was about 20 percent larger than that of the single-phase product, and it also featured reduced drops in strength in the high temperature region. The fracture toughness value varied with changes in the aspect ratio and attained its maximum value--which represented an increase of about 40 percent--when the SiC content was 10 percent by volume. Based on the rule of complexing, the Si_3N_4-SiC composite was expected to have increased thermal conductivity, but this value was from one-half to one-third that of the single-phase product due to increased scattering of photons as a result of the complexing at the nano level, showing the composite's excellent heat-shielding properties.

Combustion Synthesis of Si_3N_4-SiC Composite Powders

43067099u Tokyo CERAMICS KISO KAGAKU TORONKAI in Japanese 30-31 Jan 89 p 207

[Article by J. Zeng and Yoshio Miyamoto, ISIR, Osaka University; Mitsue Koizumi, Ryukoku University; and Osama Yamada, Osaka Industrial University]

[Text] **1. Introduction**

We have synthesized simple Si_3N_4 and SiC powders in combustion reactions under high nitrogen pressures and have reported the results. In this experiment we attempted combustion synthesis of Si_3N_4-SiC composite powders and have sintered the synthesized composite powders by HIP. The following describes the properties of the composite powders and their sintered bodies that we have found.

2. Experimental Method

Following the reaction formula (1-Y) $[3(1-x)Si + xSi_3N_4 + 2(1-x)N_2]$ + Y $[Si+C] \rightarrow (1-Y)Si_3N_4$ + YSiC, we mixed the raw materials consisting of Si (average grain diameter 1 μm) and C (average grain diameter 0.02 μm) in a wet ball mill at the mixing ratios shown in Table 1 and dried them in a vacuum for use as starting raw materials. The Si_3N_4 was mixed with the starting raw materials in advance so that the various compositions of the raw materials could be burned at a fixed temperature (2,700°C). Each mixed powder was poured into a porous refractory vessel and sealed. Next, part of the upper section of the powder was ignited by intense heat in a nitrogen environment of 100 atmospheres in order to synthesize Si_3N_4-SiC composite powders. The powder thus obtained was pulverized in a ball mill and sintered, without the help of any sintering-promoting agents, at 1,950°C and 1,700 atm for 1 hour.

Table 1. Mixing Solar Ratio X, Y of the Reactant

Y	X	Nominal composition
1/4	0.37	$3Si_3N_4$ + SiC
1/3	0.35	$2Si_3N_4$ + SiC
1/2	0.30	Si_3N_4 + SiC
2/3	0.21	Si_3N_4 + 2SiC
3/4	0.11	Si_3N_4 + 3SiC

3. Results and Consideration

(Composite Powders) Si_3N_4-SiC composite powders featuring agglomerates of fine grains that contained 33 percent to 75 percent SiC in molar ratio were obtained, thereby demonstrating the applicability of the combustion synthesis method for directly synthesizing Si_3N_4-SiC composite powders in a short time. The BET relative surface area was about 3 m^2/g but doubled in size to 6 m^2/g, and uniform powders were obtained. X-ray diffraction analyses revealed that the composite powders were made up of crystal phases of β-Si_3N_4 and α-Si_3N_4 and β-SiC. Although we detected small amounts of Si_2N_2O, the powders contained virtually no unreacted Si and C.

(Sintered Bodies) In all compositions, the relative density of the HIP sintered bodies exceeded 97.6 percent. The presence of β-Si_3N_4, β-SiC and Si_2N_2O was identified. Since the amount of Si_2N_2O increased in proportion to the Si content in the raw material, these substances are thought to have been caused by oxygen impurities on the surfaces of the raw Si. The Vickers hardness of the sintered bodies increased as the amount of Si increased, but the rupture toughness values were almost the same. Figure 1 shows the JSI-four point bending strength. The bending strength reached more than 600 MPa at room temperature. Although there was little correlation between strength and composition, the strength tended to increase with increasing SiC content at 1,400°C. We will report on the microscopic structures of the sintered bodies later.

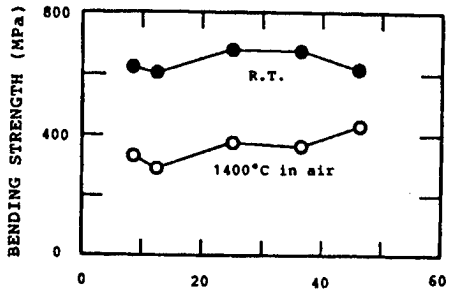

Figure 1. Composition Dependence of Four-Point Bending Strength

Self-Propagating High-Temperature Synthesis of TiB_2-Cu FGM

43067099v Tokyo CERAMICS KISO KAGAKU TORONKAI in Japanese 30-31 Jan 89 p 213

[Article by Yuji Matsuzaki and Haruki Hino, Kawasaki Heavy Industries; and Nobuhiro Sata and Norio Sanada, Government Industrial Research Institute, Tohoku]

[Text] **1. Introduction**

In the synthesis of inclined functional materials of the TiB_2-Cu system using the self-propagating high-temperature synthesis (SHS) process, the heat of formation of TiB_2, especially on the lower Cu side, induces the temperature of the reaction systems to rise, thereby causing the Cu to vaporize. The portions from which Cu has vaporized remain as blow holes, and these holes prevent the density of the material from increasing. This in turn has an adverse effect on its mechanical properties. We have tried to constrain this reaction-caused heat generation by adding small amounts of TiB_2 compound powder to the raw material powders (Ti, B, Cu) in advance, in an attempt to improve the material properties. The following describes the results of our trial.

2. Method

The synthesis was conducted using a spring compression method where the spring had an elastic coefficient of 2.4×10^4 N/m at room temperature and in a vacuum. The raw material powders were Ti, B, and Cu powders mixed with varying amounts of TiB_2--from 0~40 wt%--and the amount of each raw material powder weighed 2.0 grams. After preliminary compression at a pressure of 50 MPa, these raw material powders were each ignited under a pressure of 25 MPa for synthesis. The specimens thus obtained were observed to identify their structure and were measured to determine their relative density.

3. Results

Figure 1 shows the effect of TiB_2 addition on relative density in TiB_2-Cu system uniform materials. In uniform materials of the TiB_2-Cu system containing Cu 0~50 wt%, the relative density continued to increase with increases in the TiB_2 content in the raw material powder, but it dropped sharply when the TiB_2 content went beyond a certain level. In the FGM's synthesized under the most favorable conditions for compaction for each of

the weight percentage levels in Cu content, those that contained TiB_2 compound powders as the raw material had fewer blow holes and cracks than those synthesized with no added TiB_2. Based on these results, we studied the process of the compaction brought about by TiB_2 addition and the feasibility of controlling the growth of blow holes.

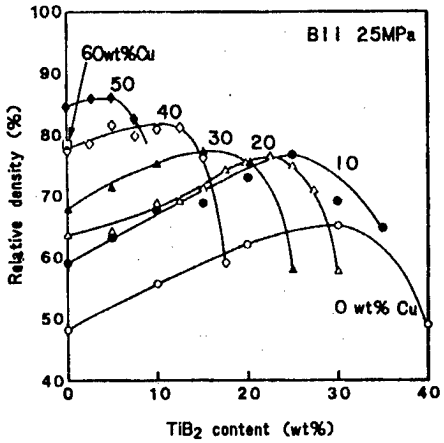

Figure 1. TiB_2 Addition and Relative Density

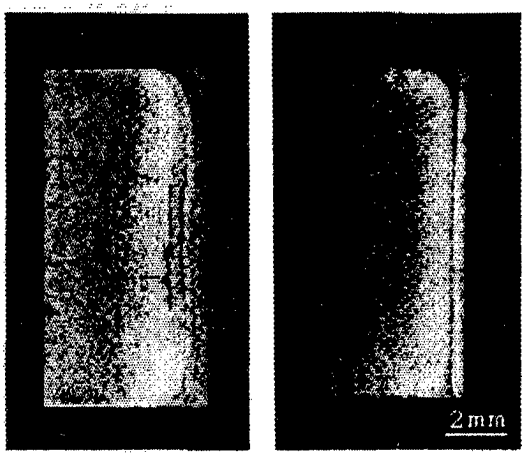

Photo 1. Effects of TiB_2 Addition on Structure of FGM (Left: no addition; right: with addition)

References

1. Sata and Ikeuchi, JOURNAL OF THE JAPAN CERAMIC INDUSTRY ASSOCIATION, Vol 95 No 2, 1987, pp 243-47.

Study on the Measurement of Radar Cross-Section

43062520 Tokyo TRDI Japan Defense Agency Technical Report 5465 in Japanese issued Feb 89, pp 1-8

[Article by Osamu Hashimoto, Masanobu Shinriki and Osamu Mizoguchi, Technical Researchers of the 2d Laboratory, Japan Defense Agency]

[Text] Abstract:

This study is a description of our experiment on a method of measuring the backscattering volume of each part of the measuring target in connection with measurement of a cross-section reflected on radar.

In this study, we rotated a measuring target, picked up its Doppler frequency deviation and processed it with FFT (Fast Fourier Transform) for the basic data of the backscattering volume of each part of the target in a comparatively simple measurement system. That is, we mounted two corner reflectors (as measuring targets) with different reflecting cross-sections) on a 1.2 m rod-like mounting base on the rotating stand and rotated the stand with a frequency of 25.0 sec.

In this way, we detected a Doppler frequency deviation from the target and measured the backscattering volume from the corner reflectors and distance from the rotation center by processing the reflected waves with FFT and then compared the results with theoretical values for discussion.

For this experiment, we set the FFT sampling frequency at 1 ms for an example with 800 point samples for the FFT processing. As a result, we could pinpoint the distance from the rotation center within an error of about 2 cm and measure the reflection level with a good accuracy of the maximum error of 4 $dBcm^2$, which would be very helpful for studies on the forthcoming backscattering radar cross-section.

Key Words: Radar Cross-Section

1. Introduction

This study was conducted in the "Research on ECM" and refers to measurement of the backscattering radar cross-section (hereafter to be called RCS "Radar Cross-Section").

Up until now, various measurement methods such as the Pulse Method and Phase Interference Method[1-3] have been established in the RCS measurement.

However, these methods were used to measure RCS by measuring the reflection volume from the entire target with the drawback that no reflection volume from a certain part of the target could be measured. Therefore, in a study on reducing RCS of a target effectively, we could not evaluate in a study stage which part of the target should be improved in terms of a surface-shape effect or a mounting effect of the wave-absorbing material, etc.

For these problems in the above Pulse Method, for example, it was once proposed to narrow the pulse width considerably and vary the range pin for measuring reflection of a part of the target.[4] However, this method could not decrease the distance resolution as its usable pulse width was limited.

Therefore, in this study, we experimented with a method of measuring backscattering volume from each part of a target in a comparatively simple measurement system by rotating the target and processing its Doppler frequency deviation with FFT. That is, we mounted a 1.2-m rod-like mounting base (to be called mounting base hereinafter) on the center of a rotating stand and placed corner reflectors with different RCS as the targets on the mounting base, and rotated the stand at a cycle of 25.0 sec. The Doppler frequency deviation was detected and the reflected wave was converted to a frequency domain with FFT for measuring the distance from the rotation center of each corner reflector and its reflection level. In the FFT processing, we used the sampling frequency of 1 ms and 800 points for the number of samples.

As a result of this experiment, this method proved that a target position was measured within an error of about 2 cm and RCS up to about 0 $dBcm^2$ was measured with an error of about 4 $dBcm^2$, offering significantly helpful data for the backscattering radar cross-section study in the future.

In this study, the distance resolution was about 2 cm in view of a relation of the FFT sampling frequency but it is expected a higher accuracy distance resolution will be possible by using a higher speed FFT.

2. Theory

Here, we are going to explain that it is theoretically possible to observe part of a measuring target reflection by detecting the Doppler frequency deviation from the target and processing it with FET.

First, as shown in Figure 1, suppose a wave of exp (j ωt + jkx) is transmitted at a time of T from a wave source placed at a distance of D on the x coordinate axis to a rod-like L-long target rotating at an angular speed of Ω on the x coordinate axis. Then, the time t required for the wave to reach the target is:

$$t = T + \frac{D - x \sin \Omega t}{C}$$

Therefore, the total wave V (T) to reach the rod-like target is expressed in the following:

$$V(T) = K \int_{-\infty}^{\infty} \int_{-L/2}^{L/2} \exp(j\omega t + jkx \sin \Omega t) \delta (T + \frac{D - x \sin \Omega t}{C}) \, dx \, dt$$

Here, δ is the delta function and K is an optional proportion constant. Then, the reference time T in the formula is converted to a time at the original point.

$$V(T + \frac{D}{C}) = K \int_{-\infty}^{\infty} \int_{-L/2}^{L/2} \exp(j\omega t + jkx \sin \Omega t) \delta (T - t + \frac{x \sin \Omega t}{C}) \, dx \, dt$$

$$\fallingdotseq K \int_{-L/2}^{L/2} \exp[j\omega (T + \frac{\sin \Omega}{C}) + jkx \sin \Omega T] / (1 - \frac{x \cos \Omega T}{C}) \, dx$$

$$\fallingdotseq K \int_{-L/2}^{L/2} \exp(j\omega T + j 2 kx \sin \Omega) \, dx$$

Here, an approximation $T \fallingdotseq t$ is used as $|\Omega T| \ll C$ or the target rotation is very slow in comparison with the light speed C. Further, the above formula is rewritten using t as a time at the original point as in the following.

$$V(t) = U(t)\exp(j\omega t) \qquad (1)$$

ここで Here,

$$U(t) = K\int_{-L/2}^{L/2} \exp(j2kx\sin\Omega t)\,dx$$

As a result, the reflection volume can be obtained by processing this V(t) with FFT but, if it is as it is, an averaged reflection volume of all data only obtained for FFT processing is measured. For example, if everything in one whole cycle of a target is sampled, only its averaged level is observed and each part of the reflection volume cannot be known.

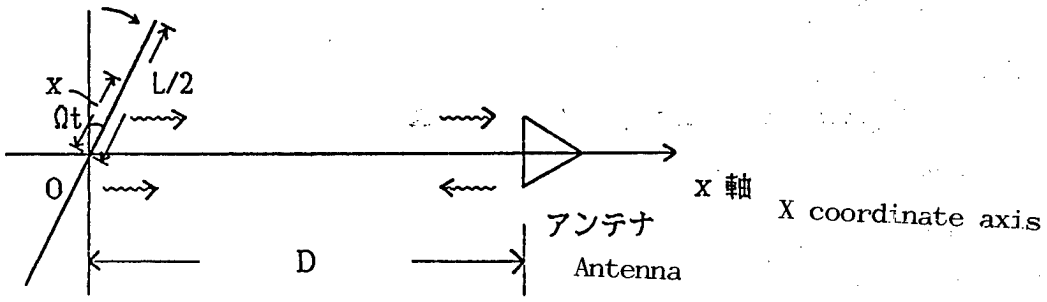

Fig. 1 Analysis Model and Coordinate System

Therefore, in our measurement method here, we made it possible to measure each part of the reflection volume of a target. That is, though we handled a uniform rod-like target in the above analysis, a general target has different reflection volumes for each part and U (t) can be expressed in the following if the weight function showing its reflection volume is W (x).

$$U(t) = K\int_{-L/2}^{L/2} W(x)\exp(j2kx\sin\Omega t)\,dx$$

The U (t) in this case is observed on the time axis, it will be roughly as shown in Fig. 2.

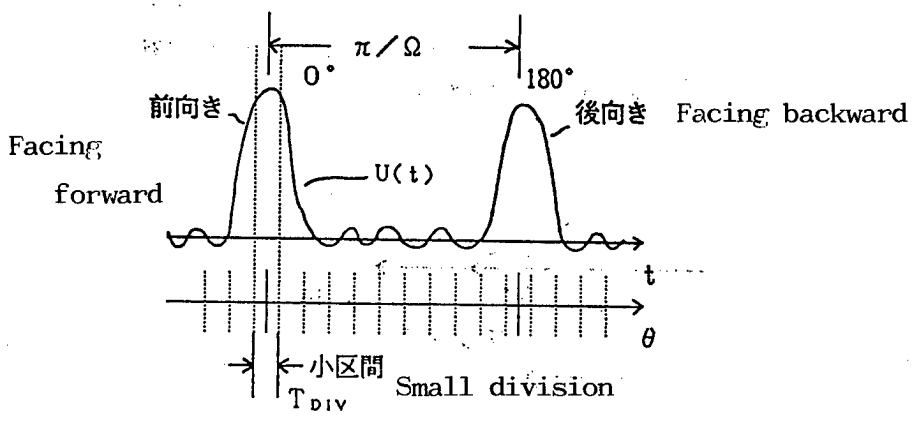

Fig. 2 Schematic Diagram of Function U (x)

Then, when the reflection wave U (t) is segmented with small divisions T_{DIV} and Fourier-converted, it is possible to know the reflection volume of each part by observing on the frequency axis.

In the Fourier conversion, the observed frequency f has the following relationship with the rotation angular speed Ω.

$$|f| \leqq L\Omega/\lambda = f_{max} \qquad (2)$$

And, the sample interval Δt to cover this bandwidth must be

$$\Delta t \leqq 1/2 \quad f_{max} = \lambda/(2L\Omega) \qquad (3)$$

Therefore, the relationship between the time divided with small divisions T_{DIV} and the number of samplings N is as follows:

$$N \geqq T_{DIV}/\Delta t = 2T_{DIV} \quad L_c\Omega/\lambda \qquad (4)$$

The distance resolution Δt of the target at this time is as follows when the FFT frequency range is F and the number of above samplings is N:

$$\Delta x = L \ \Delta F/(2f_{max}) \qquad (5)$$

Here, it can be expressed in the following:

$$\Delta F = 2F/N$$

3. Measurement Method

A block diagram of this measurement method will be shown in Fig. 3 and the target mounting base appearance in Fig. 4, and the measurement method will be described one by one in the following:

The 1 MHz CW wave generated in the oscillator is converted up to a frequency f_1 of the X band or Ku band with the first mixer, amplified to about 0.5 W with the amplifier and transmitted to a target from the antenna. Here, as shown in Fig. 4, the target is placed on the 1.2 m rod-like base on the horizontal stand rotating at a cycle of 25.0 sec. As a result, the reflection wave from the target includes the Doppler frequency deviation Δf in its transmission frequency f_1 and is received at the reception antenna.

As it is necessary to measure the Δf accurately in this measurement method, the local oscillator used in the up-conversion is used again for the down-conversion as a local oscillator of the second mixer and the frequency 1 MHz + Δf is picked up. Using a local oscillator for both purposes in this manner has the merit that a local frequency fluctuation does not affect the Δf.

Then, from the MHz + Δf, unnecessary frequency components such as the high harmonic component generated in the frequency conversion are removed using a filter and only Δf is picked up with the third mixer. Here again, as in the foregoing case, the oscillator is used as a local oscillator and the Δf is picked up accurately. At the end, this Δf is converted to a frequency domain by processing it with FFT to obtain the reflection volume from each part. As shown in Fig. 4, to minimize reflection from the measuring base itself, a wave-absorbing material is used in the front.

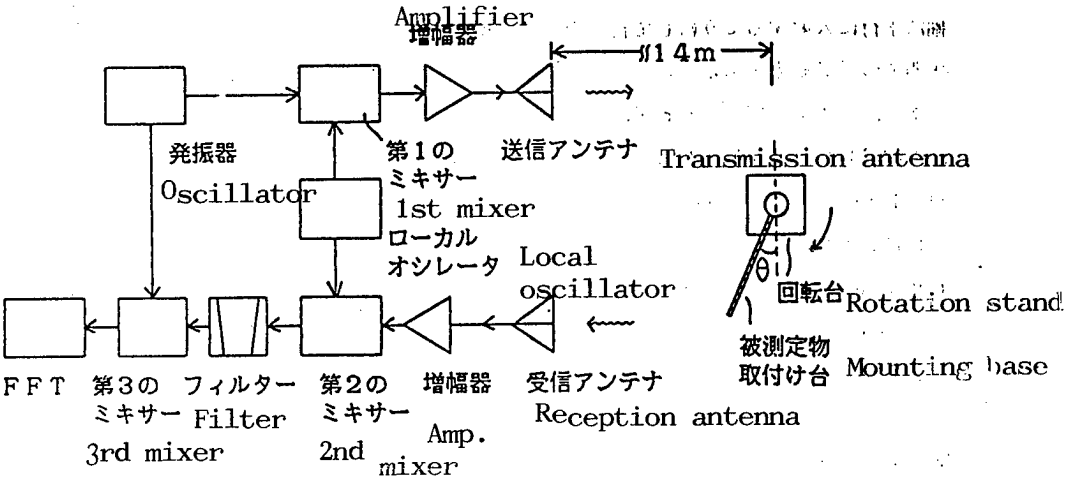

Fig. 3 Block Diagram of the Measurement System

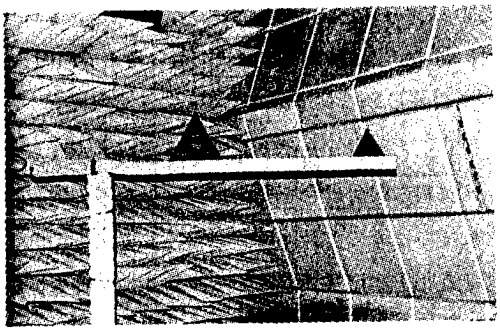

Fig. 4 Appearance of the Targets (Corner Reflectors) and the Mounting Stand

4. Measuring Samples

In this measuring, two different corner reflectors (the smaller one is referred to as reflector A and the larger one as reflector B hereinafter) are placed on the above-mentioned 1.2 m rod-like mounting base (wooden, with a cross-section of 4 cm x 4 cm) apart, respectively, from the rotation center and, after measuring their positions and reflecting levels quantatively, they were compared with the theoretical values. Here, we used 15 GHz for the frequency. The dimensions and the radar reflecting area of the two corner reflectors are shown in Table 1.

The calculation values of RCS here are measured results when the corner reflectors are placed so that the incident wave is parallel with their symmetry axis.[5]

Table 1. Dimensions and RCS Calculation Values of Two Corner Reflectors (f = GHz)

Type	Dimensions (cm)	RCS ($dBcm^2$)
A	8.4	37.18
B	15.5	47.82

The FFT used here has the frequency range of 500 Hz as described above and its sampling cycle is 1 ms and the 800 points are sampled for the FFT processing. Therefore, the FFT processing requires 0.8 seconds and the rotation angle requires 11.52° in the rotation angle conversion for the FFT processing as the target rotation cycle is 25.0 seconds. This means that, while the reflecting volume of each part is measured when the target is

abreast of the transmission/reception antenna in this measuring, to be strict, an averaged reflecting volume of $\pm 5.76°$ is measured actually if the abreast angle is supposed to be 0°. However, as the corner reflectors are used here in this measuring, its RCS can be almost disregarded for an incident angle change as little as 5.76°.

5. Measurement Results and Evaluation

Before showing the measurement results, we calculated the distance resolution Δx and frequency resolution ΔF theoretically in this measurement method. That is, in this measuring method, the Δx is calculated to be 4.98 cm as the N = 800, F = 500 Hz and L/2 = 1.2 m, and as the maximum Doppler frequency f_{max} is 30.16 Hz, the ΔF is 1.25 Hz. Furthermore, the relationship between the Doppler frequency f after the FFT processing and the distance R from the rotation center is as follows:

$$R\ (\text{cm}) = 3.979 \cdot f\ (\text{Hz}) \qquad (6)$$

From this, the distance from the center can be calculated. Considering these basic items, we fixed R for the larger reflector B at 40 cm and varied R (hereinafter R_1) for the smaller reflector between 70 cm and 110 cm with an interval of 10 cm and measured the reflecting volume and R_1 in each case. Further, to know the measurement limit of RCS in this measuring method, we measured the reflecting volume only from the mounting base without the reflectors A and B. These results are shown in Fig. 5(a) and (f).

The frequencies shown from the reflector A from these graphs and the measured Distance R_1 converted from the frequencies using the formula (6) are shown in Table 2 together with the measured results of the level difference with the reflector B.

Table 2. Measured Results of Distance (R_1) From the Rotation Center of Reflector A and the Reflection Level Difference With Reflector B

Position R_1(cm) of Reflector A	Doppler Frequency Deviation (Hz)	Measured R_1 (cm)	Level Difference with Reflector B(dB)
70	17.500	69.6	10.6
80	20.000	79.6	11.0
90	22.500	89.5	12.0
100	25.000	99.5	12.5
110	28.125	111.9	14.3

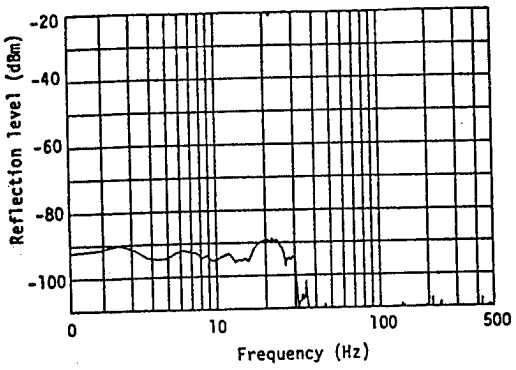

(a) 取付け台の反射レベル

(a) Reflection Level of the Mounting Base

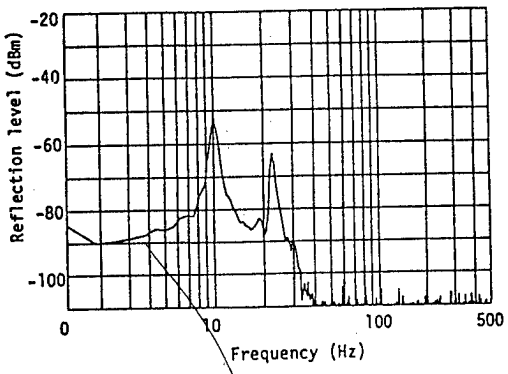

(d) R_1 = 90 cmの場合

(d) When R1 is 90 cm

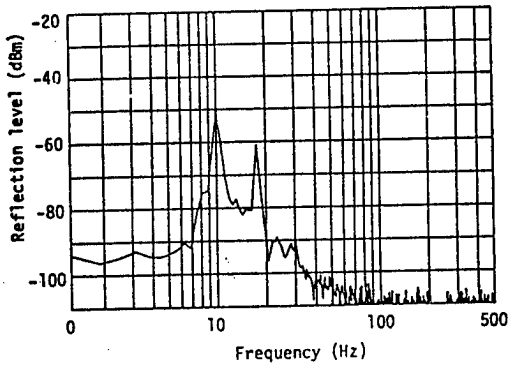

(b) R_1 = 70 cmの場合

When R1 is 70 cm

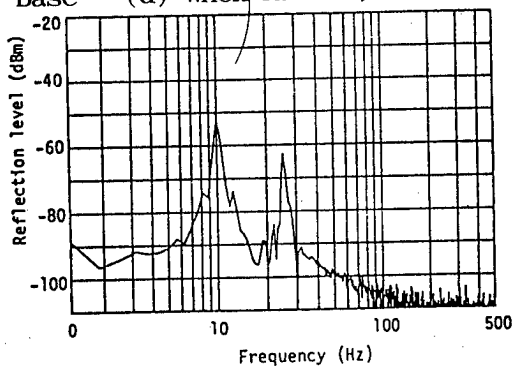

(e) R_1 = 100 cmの場合

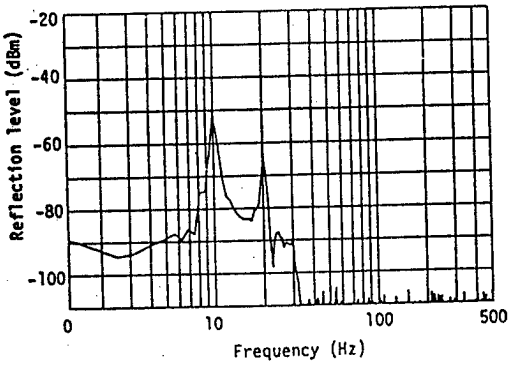

(c) R_1 = 80 cmの場合

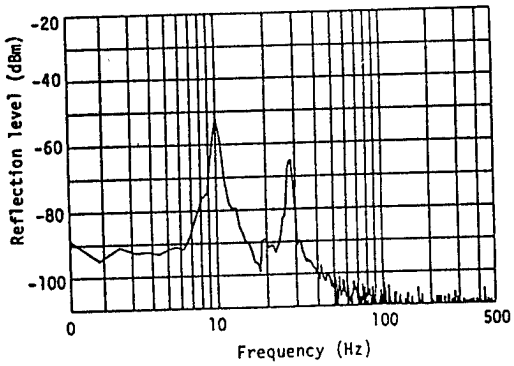

(f) R_1 = 110 cmの場合

Fig. 5 Measurement Results Against a Change of R_1 and Their Noise Levels [(a) - (f)]

From these results, Figure 5 (a) shows the reflection volume only from the mounting base and this level is the background RCS level in this measurement method and at the same time the level to determine the minimum RCS measurable in this measurement method. When this pattern is observed well, it is assumed RCS of about 0 $dBcm^2$ is measurable in this measurement method considering the reflection level of reflectors A and B.

However, this background RCS level may be further lowered by manufacturing the mounting base from a non-reflecting electromagnetic material such as foaming styrole and, if it is lowered, it may be possible to measure even smaller RCS. When this pattern is observed, it is known the reflecting level from 0 to about 30 Hz is almost even and drops drastically at about 30 Hz showing the rod-like mounting base shape is accurately observed.

Figure 5 (b) - (f) show measurement results when the reflectors A and B are mounted. From these results, it is known the measured patterns show accurately in each graph an even section of the mounting base, high reflection level when reflectors A and B are mounted and very low reflection level beyond the 1.2 m mounting base, respectively. When these patterns are checked in detail, it is confirmed that the maximum measurement distance error is about 2 cm as shown in Table 2 and the reflection level error is about 4 $dBcm^2$ when compared with the theoretical value (10.6 $dBcm^2$) regarding the relative level difference of the two reflectors. It is also noted that the measurement distance and reflection level errors increase as R_1 gets larger, possibly because the antenna beam width used in the measurement is comparatively narrow and the plane wave has not reached the reflectors uniformly, more so apart from the rotation center.

6. Conclusion

In the foregoing study, we described a comparatively simple measurement method of the reflection volume of each part of a target by rotating the target and processing its Doppler frequency deviation with FFT.

That is, we mounted two reflectors of different RCS as the targets on a 1.2 m rod-like mounting base circulating on a rotating stand. The stand was rotated at a cycle of 25.0 seconds and the Doppler frequency deviation at that time was detected, its reflection wave was processed with FFT and converted into a frequency domain for measuring the reflection level of each corner reflector.

As a result, it was confirmed that we could measure accurately a target within an error of about 2 cm and, as to the reflection level, we could measure RCS up to about 0 $dBcm^2$ within an error of about 4 $dBcm^2$, assuring a great significance in the radar reflection cross-section study in the future.

In this study, the distance resolution is limited due to an FFT sampling cycle relation but we believe that in the future we can measure distance resolution with higher accuracy using a higher speed FET.

References

1. S. H. Dike and D. D. King: "The Absorption Gain and Backscattering Cross-Section of Cylindrical Antennas," Proc. I.R.E., Vol 40, July 1952, p 853.

2. C.C.H. Tang: "Electromagnetic Backscattering Measurements by a Time-Separation Method," I.R.E., Trans. MTT-7, Apr, 1959, p 209.

3. Matsuyuki et al.: "Indoor Measurement of a Target's Radar Cross-Section With Phase Interference Method," Electrocommunications Society, Navigation Electronics Study Group reference, Mar, 1964.

4. Hashimoto et al.: "Measurement Method of Radio Wave Using Short Pulses," Signal Society Technical Report, EMCJ-82-52, 1982.

5. R.B.S. Krichbaum: "Radar Cross-Section Hand Book," Vol 2, 1970, p 593.

NASDA Revises Space Development Policy

Basic Direction, Key Points

906C0007 Tokyo PUROMETEUSU in Japanese Aug 89 pp 11-18

[Article: "Prospects for Space Development--Revision of the Outline Policy for Japanese Space Development--Feature Article: To Start Japan's Own Manned Space Activities Headed for the 21st Century"]

[Text] The Japanese technology in space development has improved in recent years and the nation's private space development activities have also intensified. With mounting expectations for the space station and space environments, ambitious plans for the future have been determined in Europe and America. Thus, a new international current in space development has emerged. The new Outline Policy for Japanese Space Development is aimed at beginning new manned space activities with a view, mainly, to international cooperation and contribution.

The Space Activities Commission, whose Outline Policy for Japanese Space Development was reviewed by its Long-Standing Policy Section (chairman: Isamu Yamashita) which was established in December 1987--with the participation of experts from industrial and other circles including men of learning and experience--set a new Outline Policy for Japanese Space Development on 28 June 1989.

In Japan, space development is carried out according to the Outline Policy for Japanese Space Development, the "constitution" of Japanese space development, laid down by the Space Activities Commission headed by the director general of the Science and Technology Agency.

This recent revision was made to clarify the basic direction of the nation's space development in the next 10 years or so to cope with the change in five domestic and foreign situations:

1. Progress of Japanese space development activities and improvement of Japanese technical capabilities

2. Expansion of private sector space development activities

3. Growing expectations regarding the use of space environments and manned space activities

4. Changes in the international environment

5. Ambitious future plans in Europe and America

The new Outline Policy, while following the basic line of the old Outline Policy, contains items that have been revised almost completely. Its three key points are:

1. space development activities which will befit Japan's international position;

2. first step toward the start of manned space activities; and

3. a shared role between government and private circles.

The history of Japanese space development began with the successful launching of a Pencil rocket in 1955 by the Tokyo University Institute of Production Technology. Then, Japan continued efforts to overtake Western countries advanced in space development. In March 1978, the Space Activities Commission set the Outline Policy for Japanese Space Development as the nation's long-term basic guideline for space development. It was revised in February 1984.

A New Current in Space Development Behind Revision; Ambitious Long-Range Vision for the 21st Century

Progress in the nation's space development activities and improvement of its technical capabilities are the first situational changes that were the background for the recent revision of the Outline Policy for Japanese Space Development, the use of satellites is steadily progressing in many areas including communications, broadcasting and meteorological observation. Technically, there are good prospects for satellite and rocket technologies at the international level. Japan is steadily making achievements in the field of scientific research, and such achievements are highly respected internationally. Thus, Japan is building a foundation to begin more diverse space development activities than ever.

Second, the expansion of private space development activities. So far, Japanese space development has been carried out mainly under the leadership of the government but, now, private circles have begun to develop techniques and their activities related to space development are being intensified.

Third, there is the growing expectation for space environments and manned space activities. With the progress of the space station project through the international cooperation of Japan, the United States, Europe and Canada, there is growing expectation for space environments, including the creation of new materials due to the special environments of outer space. Japan is increasingly interested in manned space activities.

Fourth, the change of international environments around Japan. International society strongly demands Japan's international contribution and in the area of space development, Japan is now expected to actively participate in international joint projects and play a leading role in international cooperation.

Fifth, ambitious future plans in Europe and America. President Reagan announced a new national space policy in February 1988. Also, the European Space Agency (ESA) set a new long-term plan in November 1987. Thus, the Western countries are about to push space development vigorously with ambitious long-term visions for the 21st century.

Establish the Necessary Technical Foundation and Realize Give-and-Take in Advanced Technologies

The new Outline Policy contains three basics. One is the newly added "conduct of space development activities which will befit Japan's international position." The new Outline Policy propounds more strongly than the old that Japan should make contributions befitting its capabilities in international society.

The new Outline Policy requires the nation to actively carry out space development activities befitting its international position, especially on the following three points:

The first point is to establish a technical foundation necessary for the free conduct of space development activities. For example, when engaged in an international joint project, Japan must not only pay some of the development cost but, to make its participation substantially useful to the progress of the project, it must have certain capabilities. And it is important for Japan to be able to participate in these international joint projects on equal footing with the other participants through the give-and-take of advanced technologies.

Of course, establishing a technical foundation does not mean doing everything using Japanese techniques. Parts and materials whose quality is satisfactory, are cheap and can be commercially bought must be bought from a wide range of sources, Japanese or foreign. The important thing is to insure "design authority," namely, insuring the technique to design, manufacture, maintain and operate artificial satellites and rockets independently as a basic technique supporting space activities.

The second point is pushing international cooperation positively and independently. Space development activities include meteorological observation, scientific research and other activities that should be conducted on a global scale. Regarding these activities, Japan must, as a member of the group of advanced nations, offer its technical capabilities willingly for the benefit of international society.

Regarding meteorological observation which is included in the above activities, a meteorological satellite observation network is being internationally operated under a world weather watching (WWW) plan agreed upon by the World Meteorological Organization (WMO). As part of this work, observation data gained by the Japanese meteorological satellite "Himawari" is presently being received not only in Japan itself but a total of 21 other countries and areas including Australia, China, Brunei and the Republic of Korea.

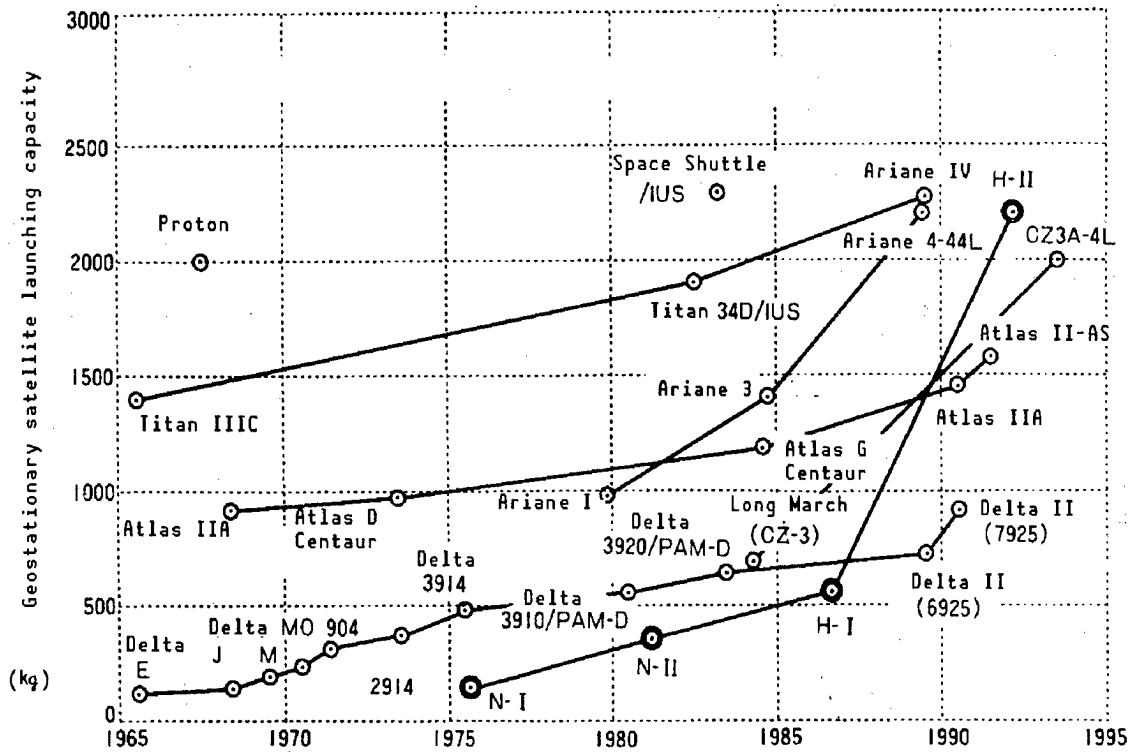

Trends in Launching Capacities of World's Rockets Used To Launch Geostationary Satellites

In the category of scientific research, Japan actively participates in international cooperative activities and its efforts are highly respected internationally. Recently (1985), Japan, the United States and Europe, with Soviet cooperation, conducted observation, each launching a Halley's Comet probe spacecraft, etc. In 1987, the Japanese X-ray astronomical observation satellite "Ginga" (ASTRO-C) was launched, carrying observational equipment developed jointly with the United States and Great Britain. It is still fresh in our memory that this satellite was noted worldwide for observing the birth of a supernova in the Large Magellanic Cloud contributing greatly to the study of black holes.

Meanwhile, at present there are areas in which Japan financially and technically cannot act independently. In these areas, it will be necessary for Japan to participate in international activities and conduct its advanced space activities in concert with them.

For example, the First Material Processing Test (FMPT) Program is now being prepared in which Japanese nationals riding in a U.S. Space Shuttle will conduct material, life sciences and other space experiments in 1991. Also, a space station program is being prepared so that it may start during the second half of the 1990s as an international joint project by Japan, the United States, Europe and Canada. Japan will participate in this with its own test module (JEM). Each country pushed its preliminary design stage from 1985 and an intergovernmental agreement on cooperation from the development stage was signed on 29 September 1988. The space station will not only make prolonged manned space activities possible but also be effectively used as a base for space environments, the study of space science or earth observation. It is expected to be a major contribution toward the remarkable expansion and development of future space activities. Japan will positively participate in the space station program to play a role befitting its international position as an advanced nation.

Thus, Japan, which has so far assiduously sought to acquire space capabilities befitting its national strength, must henceforth step up this effort with a view to international contribution and cooperation.

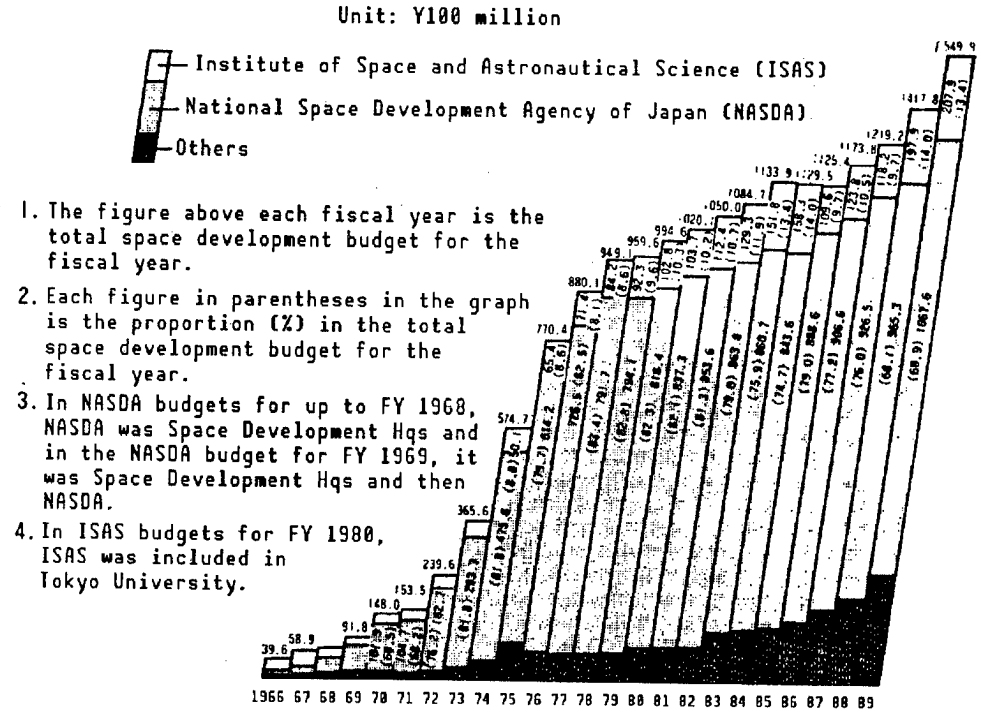

Trends in Japanese Space Development Budget

Participating in Spaceplane and Other International Joint Projects and Taking the First Step Toward Manned Space Activities

The new Outline Policy seeks to create "manned space activity series" as one of the "space development series"--a major part of the Outline Policy--and to conduct manned space activities as a long-range effort. Thus, it clearly reflects the desire to conduct manned space activities.

The advisability of conducting manned space activities is deeply concerned with the fundamental problems of 1) what space development means to Japan, and 2) what space development should aim at and how far it should go.

The meaning of conducting manned space activities can be found in effectively using space environments and advancing science and technology but man's very march into space, a new sphere of his activities, is most important in pointing to hitherto unknown possibilities and bringing new information.

Here, the problem concerns the pace and steps with which Japan should conduct its manned space activities. Needless to say, the conduct of manned space activities requires the accumulation of research and development over a very long period of time and the investment of large sums of money. Therefore it is necessary to maintain harmony between the Japanese national strength and technical capabilities.

So, the Space Activities Commission will 1) take an active part in the space station and other international joint projects and 2) conduct basic, preliminary studies on the manned spaceplane to transport personnel between space and Earth as an immediate task for Japan in consideration of the importance of manned space activities and harmony between the national strength and technical capabilities. The Commission considers it realistic to prepare for regular future manned space activities and steadily acquire necessary basic technology and concludes that, in the long run, Japan should seek to conduct activities independently.

The new Outline Policy has clearly expressed Japan's intent to begin regular manned space activities.

Government Must Be Central to Development of Preliminary Technology While Private Industries Must Tackle Cost Reduction and Improved Reliability

Among the three basics of the new Outline Policy is expediting private space development activities. In view of the part to be played by private industries, progress in accumulating technologies by private industries and the intensification of related activities, the new Outline Policy requires that private space development activities be positively stepped up so that the energies of private circles may be effectively used in the appropriate government/private shared role.

So far, space development in Japan has been conducted mainly under government leadership. But in the future, the part to be played by private industries in space development will become increasingly important as technical

development progresses. It is high time to review how the role should be shared between the government and private circles.

Normally, the government is central to the development of more preliminary technologies, which are technically and economically risky. Meanwhile, such things as the establishment of technologies, including cost reduction and improved reliability, should probably be gradually taken over by private circles when technical development has progressed to a certain extent. Space development should be carried out according to this role sharing.

Under these circumstance, those space development activities requiring the development of risky, preliminary technologies which are important from the national point of view must be actively carried out hereafter with the understanding that they represent basic investment vital to the socioeconomic growth of Japan and an international obligation to be taken on by this country as an advanced nation. Thus, the government will exert utmost efforts to this end. But at the same time, private circles are expected to make further efforts to establish technologies by various means including financing.

The improvement of Japan's technical foundation will finally lead to the stabilized utilization of space by rocket and satellite users. Therefore it is important that private industries actively participate and cooperate in government development projects or help with technical development from a long-term point of view.

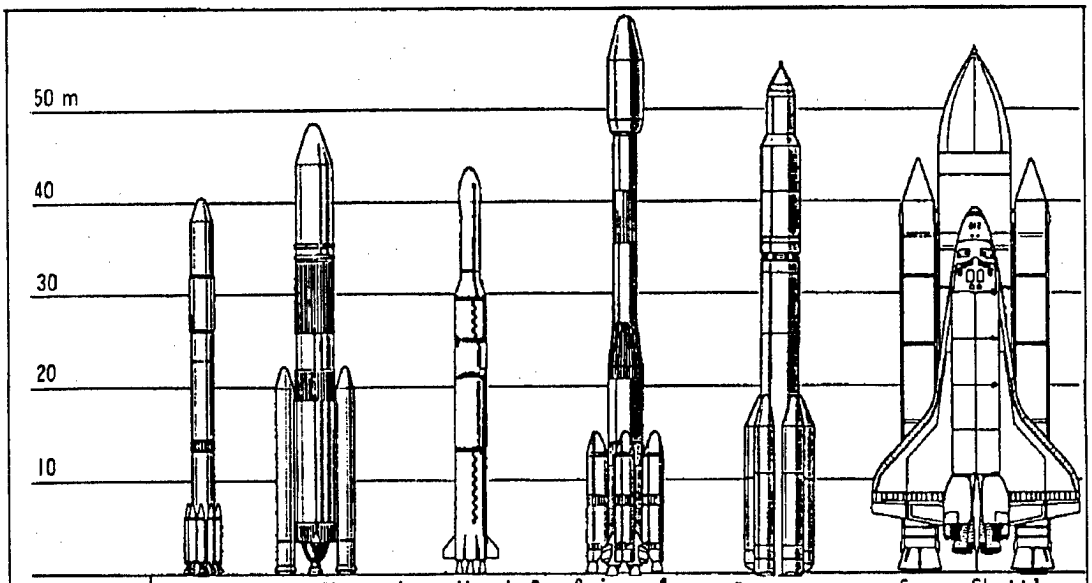

Name of rocket	H-I	H-II	Long March 3	Ariane 4	Proton	Space Shuttle
	Japan		China	Europe	USSR	United States
Total weight	140 t	260 t	202 t	460 t	680 t	2,041 t
Capacity to launch into geostationary orbit	550kg	2,000kg	650kg	2,200kg	2,000kg	2,270kg

Comparison of Main Rockets in the World

Space Development Which Is Now Familiar...Regular Use of Space

With the progress of space development, use of space by various artificial satellites has become so familiar to us and the benefits from this use are such that we can no longer do without it in our daily life.

1. Communications

Communication satellites play an active part in international communications, etc., as space relay bases for telephone service and television programs. They enable us to immediately see television-relayed Olympic Games and scenes from the Showa Base in the Antarctic. Japan launched Sakura No 3 in February and September 1988. In addition, four more communications satellites are scheduled to be launched by two satellite communication companies by the end of 1989.

So far, Japanese communication satellites have been used for such purposes as ensuring communication in an emergency or communicating with isolated islands. But from now on, their utilization will develop from this role as a supplement to terrestrial communication to a new form making more effective use of the features of satellite communication, such as communicating the same message simultaneously to many recipients. In the future, communications satellites are expected to play an important part as a key infrastructure of an intelligent society as informationization of society progresses.

2. Broadcasting

A broadcasting satellite transmits television broadcasts and other electric waves from space directly to the home receiver. It not only solves the problems of radio disturbance, such as the difficulty in getting electric waves to reach mountainous areas and poor reception in urban areas due to such features as high rise buildings, but can also present high-vision broadcasting with fine images and sounds. Japan now leads the world in two-channel nationwide hookup satellite broadcasting, using Yuri No 2. Moreover, Broadcasting Satellites No 3 are scheduled to be launched in FY 1990 and 1991 as successors to Yuri No 2.

3. Meteorology

The meteorological satellite takes cloud distribution photographs and measures temperature for daily weather forecasts, typhoon warnings, etc., to help meteorological observation in areas with only a few observation points, such as the Pacific Ocean. Japan has launched the Himawari, a meteorological satellite, since 1977 and is scheduled to launch Himawari No 4 in the summer of 1989. Meteorological data from the Himawari satellites are now received not only by Japanese organs concerned but also in 21 foreign countries and areas.

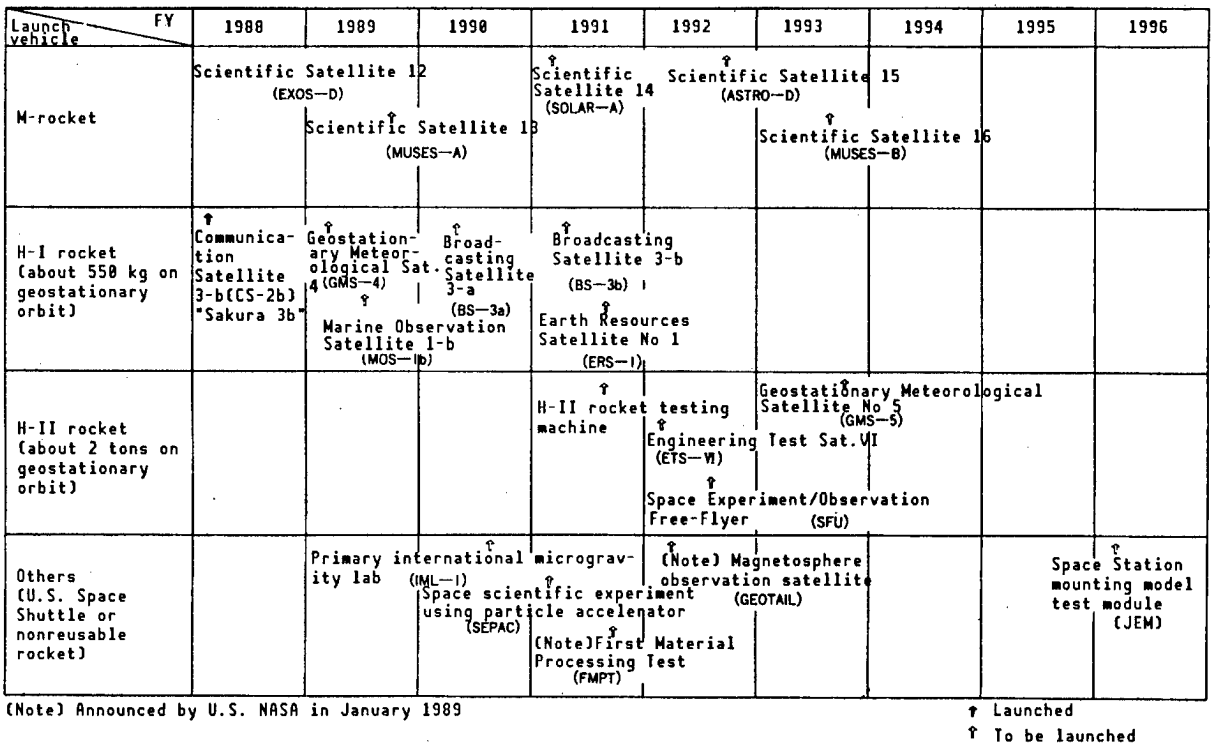

4. Earth Observation

The earth observation satellite is an artificial satellite carrying an observation sensor and transmits data gained by observing the earth's surface from space.

Such data is used for many purposes including agriculture/forestry/fisheries, land use, prospecting for natural resources and protecting the environment. Japan began to receive data from the U.S. earth observation satellite Landsat in 1979. Moreover, in 1986 it launched Momo No 1, its first earth observation satellite, to observe marine phenomena, etc. It is scheduled to launch a successor to Momo No 1 in FY 1989 and launch its first earth resources satellite to prospect for resources.

5. Scientific Research

Scientific satellites can be divided into those which observe the environs of Earth, those which explore the moon and planets and those which observe astronomical systems.

Artificial satellites were instrumental to the discovery of radiation belts (Van Allen belts) which surround Earth. We can understand the conditions of the planet on which we live all the better by observing: radiation belts, ionosphere, magnetosphere, solar winds, etc., occurring in the vicinity of Earth.

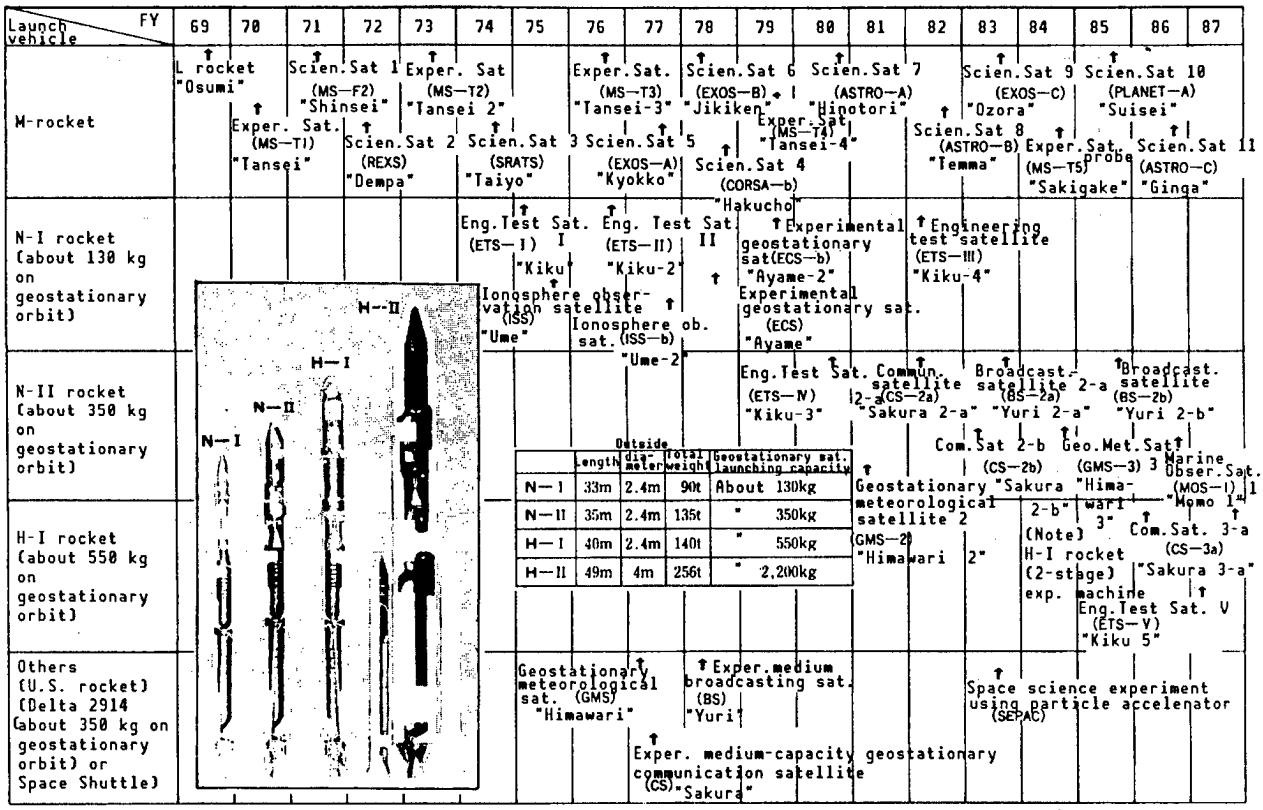

(Note) This was used to launch engineering geodetic satellite (EGS) "Ajisai," amateur satellite (JAS-1) "Fuji," etc.

Furthermore, seeking details on planets, interplanetary spaces and comets and learning the realities of special heavenly bodies, such as the X-ray nova, by observing them will promote our understanding of the universe and serve as a clue in classifying the origin of the solar system and the origin of the universe.

6. Space Experiments

Outer space is a world of weightlessness, almost complete vacuum, high temperature and low temperature, large quantities of cosmic rays and infinite solar energy. Composite alloys, semiconductors, pharmaceuticals, etc., better than those produced on earth can be manufactured by making effective use of these special environments.

Japan is planning various space experiments. Of these, the First Material Processing Test (FMPT) will consist of material and life sciences experiments to be conducted for 7 days by Japanese astronauts manning a space shuttle with experimental equipment. The experiments will be carried out for a total of 34 subjects, namely, 32 for materials and 12 for life sciences, selected from among applications from scientific societies and industries.

7. Participation in the Space Station Program

President Reagan in 1984 announced his plan to build a space station with international cooperation and asked Japan, Europe and Canada to participate. Responding, Japan has participated since 1985 with Europe and Canada in the preliminary design activities prior to the development of the space station.

The space station is an ambitious multipurpose manned facility to be constructed on a low-altitude earth-circling orbit. Japan will participate in this plan with its own experimental module (JEM).

Keidanren Position

906C0007 Tokyo PUROMETEUSU in Japanese Aug 89 pp 20-21

[Article by Tadahiro Sekimoto, chairman, Keidanren Space Development Promotion Council: "On the New Outline Policy for Japanese Space Development"]

[Text] **Introduction**

I participated as chairman of the Space Development Promotion Council of the Keidanren (Federation of Economic Organizations) in the work started in January 1988 by the Long-Term Policy Section of the Space Activities Commission to revise the Outline Policy for Japanese Space Development. In October last year, the Keidanren summarized the wishes of industries concerning the future conduct of space development and presented them to concerned circles as recommendations so that these wishes might be reflected in the revised Outline Policy.

Keidanren's Wishes Concerning New Outline Policy for Japanese Space Development

The basic position of the Keidanren is that space development, the nucleus of development of advanced technologies, is the motive force of future socioeconomic development and must be a mainstay of the nation's survival strategy for the 21st century. From this position, the Keidanren made the following proposals:

First of all, technical capabilities must be strengthened and international cooperation must be promoted. Properly, space development is an area requiring international cooperation since it deals with vast outer space without national borders. For effective international cooperation, it is imperative that each country have excellent technical power of its own. And our recommendations stressed that the government should exercise leadership in strengthening these technical capabilities. The second point is the conduct of important projects. We recommended that the government be central to active manned space activities, in which we are inexperienced and the development of space infrastructures, such as the space station and the spaceplane, must be tackled positively as something basic to manned space activities. The third is preparing conditions for commercializing space.

The main problem in commercializing space is establishing Japan's international competitiveness in the areas of technology and cost. So, we pointed out first that the implementation of an appropriate industrial policy by the government is imperative. The fourth is realizing a fine system of space development and utilization and we contended that the Space Activities Commission should be made a true policy forming organization that can ensure that a comprehensive development/utilization strategy be studied according to the progress of actual utilization. The fifth is securing an appropriate budget and deciding a middle-term executive plan. Here, we required an immediate increase in the space development budget from the present level of ¥100 billion or so to hundreds of billions of yen to be able to handle the many vital projects waiting to be carried out and also demanded that the cabinet decide on a middle-term executive plan with the financial support to connect the Outline Policy and the annual plan. We finally mentioned the necessity of relaxing regulations concerning the rocket launch schedule (in conjunction with fishery measures), train and secure talented personnel, properly protect the knowledge acquired through space activities and intensify broad activities to ensure understanding and cooperation from the general public.

On the New Outline Policy

One can appreciate the fact that, whereas the old Outline Policy highlighted the development of large satellites and rockets, the new Outline Policy looks in the direction of broader, diverse activities including the development of manned space activities and space environment utilization. Yet, the new Outline Policy is partially unsatisfactory in light of the aforementioned Keidanren requests. For, it was a compromise of opinions presented from different points of view. It is, therefore, vague in some respects and cannot be adequate as a guiding principle for industries eager to engage in space development. I may be criticized as being prejudiced but I must state the following main problems from the viewpoint of the industrial world.

First, the relation between the new Outline Policy and the report of the Long-Term Policy Ad-Hoc Committee of the Space Activities Commission (referred to hereafter simply as Long-Term Ad-Hoc Report) is not quite clear. As you may know, the Long-Term Ad-Hoc Report was prepared in May 1987 as preliminary work before the revision of the Outline Policy. It envisions how Japan should play a central role in the world's space development in the 21st century by inviting a total of ¥6 trillion during the 15 years ending in the year 2000 (or a fiscal year average of ¥400 billion) in space development to discharge its responsibility appropriate to its international position. How to realize this ¥6 trillion concept should have been a main point in the recent revision of the Outline Policy and it interested industrial circles most. In its preamble, the new Outline Policy generally referred to its relation with the Long-Term Ad-Hoc Report by the expression, "reflection of the Long-Term Ad-Hoc Report on the real policy." I regret that I cannot say yes if I am asked whether the new Outline Policy completely follows the ¥6 trillion concept of the Long-Term Ad-Hoc Report. Specifically, the government, overly concerned with the difficulty of securing the necessary

budget, postpones the preparation of the spaceplane and the spaceplane-centered space transport system. It also falls behind the Long-Term Ad-Hoc Report on the development of such items as the on-orbit work vehicle, the interorbital transport plane and the platform. The problem of coordinating the new Outline Policy and the Long-Term Ad-Hoc Report has not been solved though a compromise was attempted by finally cutting the period of the new Outline Policy from 15 years, as first proposed, to 10 years and concentrating for the present on projects that are certainly feasible.

Second, the necessity of conducting manned space activities and preparing space infrastructures were not studied sufficiently. In the view of the industrial world, space infrastructures will be social capital in the 21st century as roads, waterworks and sewers on the earth's surface now are. So, it was our desire that the government would consider using the public works budget to prepare space infrastructures and initiate other positive measures and, moreover, incorporate a Japanese space station plan into the new outline policy.

Third, the new Outline Policy gave no adequate explanation of how to secure funds necessary to finance projects. It merely stated that the government "will diversify fund sources by methods including the use of private and various other funds." But we had expected it to state its resolve to drastically expand the national budget first of all and, if possible, even estimate the necessary funds.

Fourth, the new Outline Policy made no specific mention of preparation of a space development and utilization system. It is true that the present Space Activities Commission works too much at coordination on technical development matters. To meet the needs of the new era, it is imperative that the Space Activities Commission be drastically reorganized for renewed functioning with a view to setting policies on both development and utilization.

Conclusion

There is no denying that, as seen above, the new Outline Policy does not reflect all wishes of the Keidanren but it is scheduled to be revised hereafter, if necessary. Anyway, the new Outline Policy is a step forward since it envisages related, more diverse activities than in the Outline Policy of the past. However, a setup for the cabinet decision on a fund-supported middle-term executive plan must be established as soon as possible in order not to let the Outline Policy end in a castle in the air. At the same time, one must remember that FY 1990 is, indeed, most important as the first fiscal year to be covered by a budget under the new Outline Policy.

Gas-Phase Epitaxial Technology for Mass Production

43064044A Tokyo SEMICON NEWS in Japanese May 89 pp 34-40

[Article by Yoshiya Suzuki and Yosuke Inoue, Hitachi Laboratory, Hitachi, Ltd.]

[Text] 1. Preface

Almost 10 years have passed since 1980 to 1981 when American magazines[1,2] reported the effectiveness of using an epitaxial wafer as a measure to meet latchup and α-ray soft errors of MOS LSI elements. During this period, some crystal manufacturers began the commercial production of epitaxial wafers for MOS and some device manufacturers announced the commercialization of and R&D results on epitaxial MOS elements, but the commercialization of epitaxial MOS is neither in the full-fledged state nor in the main current yet on the enterprise level. One of the largest obstructions standing in the way of the advancement of epitaxial MOS is said to be the high cost of the epitaxial wafer, i.e., the epitaxial growth devices currently in use are large-scale and expensive, but their wafer production processing capability is small. Therefore, great enhancement of the growth device is desired to increase the wafer production processing ability.

Since the epitaxial growth technique was introduced into the semiconductor element production process, the growth device has also developed, and this development can be grasped, in a sense, as the history of the improvement of the wafer production processing ability by making the device larger and automatic. However, the basic device concept has not changed very much. The trend of growth device development based on this new concept has become actively only recently for purposes of mass production.

This article, therefore, briefly describes the various factors that determine the cost of epitaxial wafers, then mentions the status of and problems with the mass growth device, which become the key point. This article then introduces a new, high-frequency heating, vertical hot wall growth device[3,4] which the authors recently investigated.

2. Cost Factors of Epitaxial Wafer

As shown in Table 1, the cost of the epitaxial wafer is based on many factors. Not only the number of wafers processed per batch, but also the power consumption, quantity of H_2 gas used, maintenance cost, and floor area occupied by the device are important factors. If the processing ability as a growth device alone is taken into consideration, it can be represented by the following expression.

$$P_t = P_f \cdot P_{max} \quad \cdots\cdots (1)$$

where, P_t = processing ability per device [wafer area/(hr·device)], P_f = processing ability coefficient, and P_{max} = maximum processing ability. P_t and P_{max} are further shown as follows:

$$P_f = (\text{growth yield}) \cdot (\text{working rate of device}) \times (\text{use rate of device}) \quad \cdots\cdots (2)$$

$$P_{max} = \frac{(\text{number of charged wafers})}{(\text{total growth process time})} \quad \cdots\cdots (3)$$

The total growth process time differs to some degree depending on the thickness of the growth layer and growth conditions, but is usually about 45 to 75 min, i.e., roughly about 1 hour. Since 20 to 30 percent of this time is used solely for silicon deposition, a slightly faster growth rate does not lead to a large reduction of the total growth time. The maximum processing ability of the device is determined by the number of charged wafers per batch. On the other hand, the growth yield and the use rate of the device depend on the device user's circumstances. Therefore, important factors that greatly influence the original processing ability of the device have been determined to be the number of charged wafers per batch and the working rate of the device.

From the above, the most important conditions for a mass production growth device are that 1) the number of charged wafers is large, 2) the shape is not indiscriminately large and complex, but instead simple and compact to improve the working rate, and 3) the method is one that does not make the total growth process time, including the temperature rise and fall time of the furnace, too long. Of course, the automation of some operations is required.

Table 1. Various Factors Influencing Cost of Epitaxial Wafer

Factor	Main contents
(1) Process conditions	1)Total growth process time 2) Growth process contents 3)Growth film thickness
(2) Power·raw material gas	1)N_2 2)H_2 3) HCl 4)Si, raw material 5) dopant 6)Power 7) Cooling water
(3) Life and cost of replacement parts	1)Infrared lamp 2) RF coil 3)Bell jar 4)Susceptor 5)Various quartz parts
(4) Maintenance parts, cost	1)Vacuum pump oil 2)Filter 3) Rolling 4)Cleaning of various parts 5) Maintenance of vacuum tube 6) Time and interval of various maintenance tasks
(5) Operating time, working time, indirect expense	1)Operating time of device 2) Work efficiency 3)Production time 4) Worker cost 5)Indirect expenses
(6) Wafer processing ability of device	1)Number of chargeable wafers/batch 2)Operating efficiency 3)Yield
(7) Floor area of device	
(8) Price of device	

3. Circumstances and Present Status of Mass Production Growth Device

Figure 1 shows the methods involved in various typical epitaxial growth devices which have been used so far. The epitaxial growth devices most used as mass production devices are the pancake-type (also called vertical-type or disk-type) and barrel-type (or cylinder-type) devices.

Table 2 summarizes numbers of chargeable wafers, furnace types, heating methods, and flow rates of the H_2 gas used, for various growth devices currently on the market, in descending order of processible quantities. Most of the devices are pancake-type or barrel-type as shown in Nos 2 and 3. In both cases, the wafer charge ability per batch for the largest device at present is 27 to 28 sheets of 5-inch wafers, and the conventional-type furnace for which these wafers are laid out on a plane seems to have already reached a limit in respect to size. Incidentally, quite recently, Gemini Research Inc. announced a new type of device[6] entirely different from the conventional ones, as shown in No 1 [Table 2] (Figure 2). With this device, wafers are laid out like standing circular set blades and are grown by passing reaction gas among them (the circular cluster method or set blade layout method). This device is said to be capable of throughput of 40 to 50 sheets/hr, but detailed technical data has not yet been reported. However, in attempting to significantly increase the chargeable wafers in the future, the conventional method of laying out the wafers on a planar heating susceptor cannot but be replaced by the method of laying out wafers standing three-dimensionally.

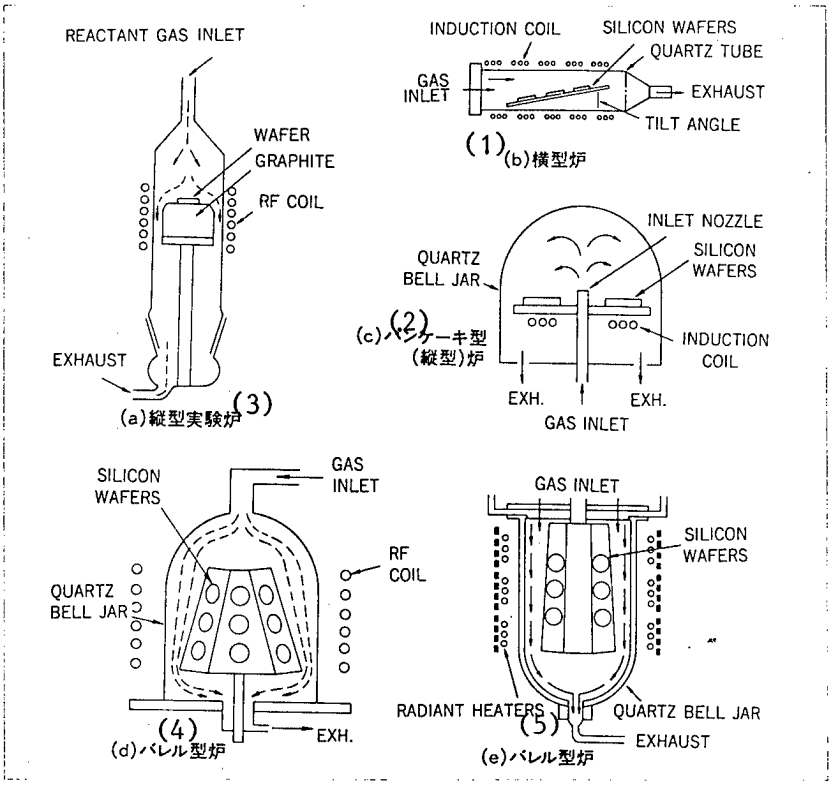

Figure 1. Structures of Various Typical Epitaxial Growth Furnace

Key:

1. Horizontal furnace
2. Pancake (vertical) furnace
3. Vertical experiment furnace
4. Barrel furnace
5. Barrel furnace

The attempt to increase the number of processible sheets of wafers by three-dimensionally standing wafers has existed for a long time. Ban (1978)[7] reported the method referred to as the rotary disk-type shown in Figure 3(a). The growth furnace reported in this paper was a small one which could charge 14 sheets of waters with diameters of 2.25 inches, but it represented a new attempt in that the standing wafers were laid out. Probably because uniform growth is difficult to secure, however, no report on a large-scale practical machine appeared after that. On the other hand, Ogirima, et al., (1981)[8] and Bloem, et al., (1985)9 have been investigating the so-called hot wall growth furnace, shown in Figure 3(b) that resembles the ordinary diffusion furnace or decompressing CVD furnace. This method is clearly the best for charging a large quantity of wafers, but no practical device has yet been made because of the following two problems: The first problem is that a large quantity of silicon deposits on the wall and other parts of the reaction furnace. The second problem is that the uniform growth of silicon is difficult to secure for all the wafers since the concentration of silicon raw material decreases in the direction of the gas flow.

Table 2. Large-Scale Epitaxial Growth Devices Currently on the Market

#	Vendors	Types	Wafer Load Sizes			Reactor Structure	Method of Heat Input	H_2 Gas Flow Rate
			4"	5"	6"			
1	Gemini Res.	TETRON ONE	50	50	50	Circular Cluster	Resist. + Lamp	~1000 ℓ /min
2	Kokusai Elec.	DC-9000	49	28	22	Pancake (Vertical)	RF	~600
	Applied Mat'ls	PE-7010		27	21	Barrel (Cylinder)	RF	~800
3	Kokusai Elec.	DC-7000	27	19	10	Pancake (Vertical)	RF	~400
	Toshiba Kikai	EVG-28F	27	19	10	Pancake (Vertical)	RF	
	Applied Mat'ls	AMC-7800	24	12	10	Barrel (Cylinder)	Lamp	~150
	Gemini Res.	Gemini-3	22	12	8	Pancake (Vertical)	RF	150—200
	Toshiba Kikai	EVG-23F	21	12	8	Pancake (Vertical)	RF	
	Shimada Rika	AEC-2500	25	12	8	Pancake (Vertical)	RF	

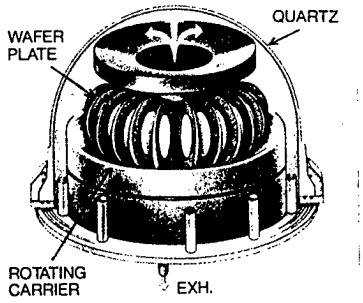

Figure 2. Wafer Layout Method of Gemini Research's TETRON ONE Epitaxial Growth Device[6]

Recently, the authors developed a new growth furnace method (high-frequency heating vertical hot wall method) which overcomes the above-mentioned problems, and is comparatively compact and occupies a small floor area.

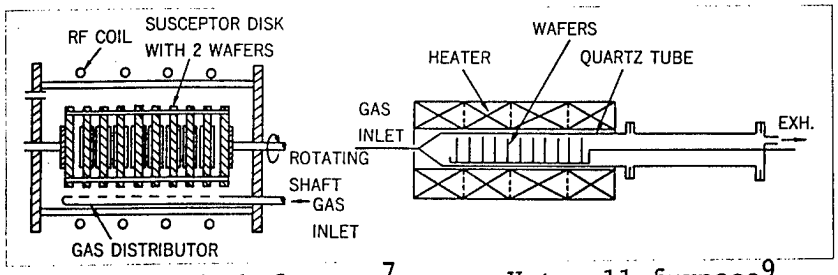

(a) Rotary disk furnace[7] (b) Hot wall furnace[9]

Figure 3. Epitaxial Growth Furnaces Involving the Laying Out of Three-Dimensionally Standing Wafers

4. High-Frequency Heating Vertical Hot Wall Growth Furnace[3,4]

(1) Outline and characteristics of the growth furnace

Figure 4 shows the configuration of the growth furnace of the prototype device which the authors trial manufactured. In this furnace, the wafers are laid out by piling them in parallel in the longitudinal direction. The reaction gas is uniformly supplied from one direction and is discharged from another direction (multi-gas-flow method). The maximum diameter of a chargeable wafer is 5 inches. The main characteristics are as follows:

(i) Wafers are loaded in parallel and at an interval of 10 mm.

The rotation of the wafer holder enables the operator to easily control the uniformity of the film thickness on the wafer's surface.

(ii) Wafer heating is performed by the hot wall method which performs high-frequency heating on the SiC-coat graphite susceptor which surrounds the wafers. The characteristics of this method are that the uniform heating of a large quantity of wafers is facilitated and that the temperature rise and fall time is short.

(iii) Raw material gas is blown out to the gaps between the wafers from ejection holes drilled on multiple quartz gas supply pipes and is exhausted from the exhaust pipes on the opposite side. The uniformity of growth can be adjusted by the optimum design of the gas supply pipes, the optimization of the flow rate conditions, and the rotation of the wafers.

(iv) The raw material gas pipe is of a double structure, and the exterior pipe permits the hydrogen gas flow to cool the raw material gas that flows in the interior pipe, as well as the interior pipe itself. This makes the deposit of silicon in the gas supply pipe easy to prevent and the uniformity of film thickness in the height direction simple to obtain.

(v) The gas density conditions for selective growth are established by mixing an appropriate quantity of HCl gas in the raw material gas to prevent the deposition of silicon in the quartz parts of the growth furnace.

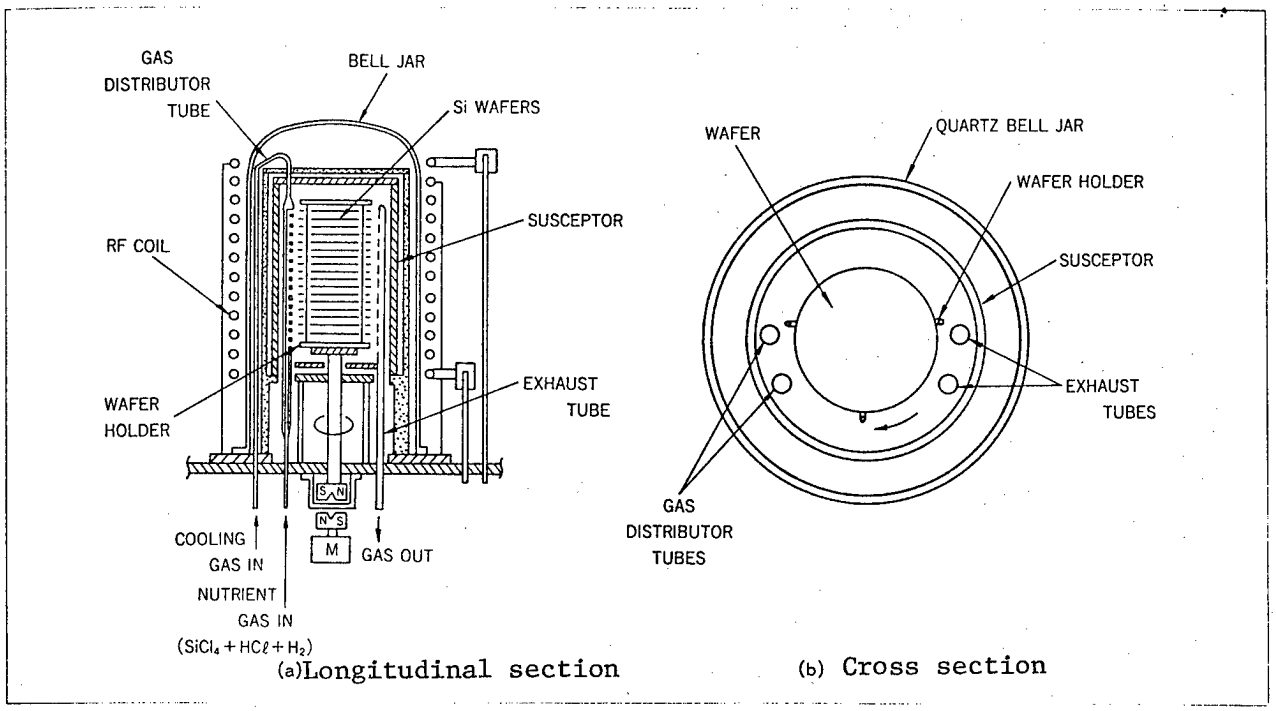

Figure 4. Epitaxial Growth Device of High-Frequency Heating Vertical Hot Wall Method

(2) Prevention of silicon deposition in quartz parts of the furnace

Figure 5 shows an example of the results obtained by investigating the growth conditions which allow only selective growth to occur on a silicon wafer. If performed with a mixed quantity of HCl gas other than that represented by the hatched area in the figure, epitaxial growth can be deposited on a wafer with almost no silicon deposited on the quartz parts of the furnace, such as the gas supply pipe.

(3) Uniform growth

The uniformity of the film thickness on a wafer surface is influenced by the gas supply quantity from the ejection holes and the status of the gas spread. Figure 6 shows the influence of the entire gas flow quantity, i.e., the ejection gas supply flow quantity from the ejection hole, on the film thickness distribution (growth rate) on a wafer when one gas supply pipe is used and gas is blown out toward the center of the wafer from the gas ejection hole. This figure shows that the film thickness distribution in the center of the wafer is particularly sensitive to the influence of the entire gas flow quantity, and one gas supply pipe alone cannot control the uniformity of the film thickness distribution. The reasons for this are that the density of the silicon raw material decreases comparatively quickly in the gas ejection direction and the spread of gas flow from the ejection hole is small. It was found that use of at least two gas supply pipes and the optimization of the supply gas flow rate make the film thickness disperson in a wafer less than ± 5 percent.

Figure 7 shows examples of film thickness distribution in wafer surfaces (a) when the wafer is not rotated and (b) when the wafer is rotated when two gas supply pipes are used for the growth. Figure 7(a) shows clearly how silicon raw material gas density spreads. It is understood that a uniformity of ± 3 percent can be obtained, as shown in Figure (b), if the maximum density spread remains at this level.

To make the film thickness distribution uniform for wafers loaded in the height direction, the raw material must be uniformly supplied for all the wafer gaps from the ejection holes. The flow rate distribution status of the raw material gas coming from ejection holes is determined by the balance between the pressure loss in the flow direction and static pressure recovery when the gas in a temperature state flows in a supply pipe. Actually, the shape of the supply pipe was determined by collating both simulated and experimental results.

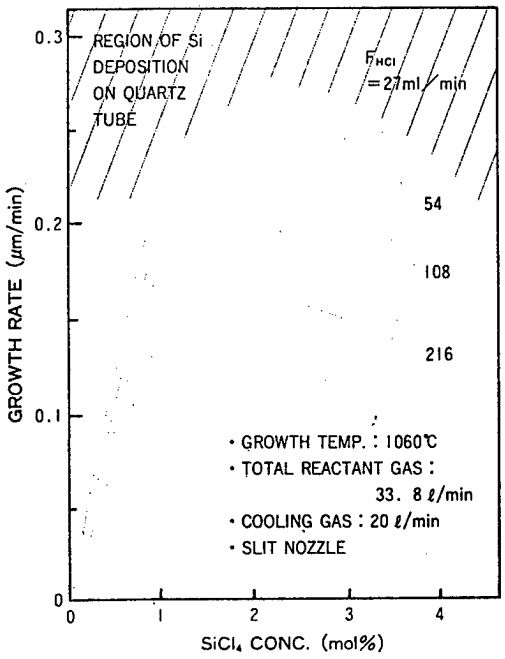

Figure 5. Example of the Conditions for Selective Epitaxial Growth on Silicon Wafer Only

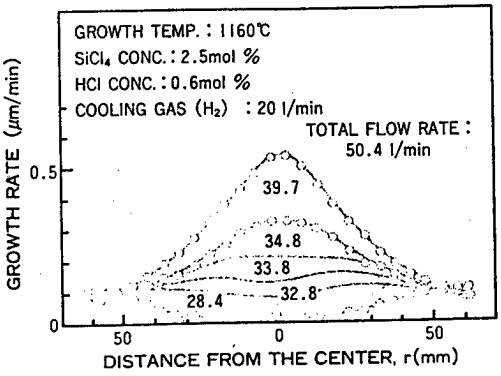

Figure 6. Influence of the Total Gas Flow Quantity on the Distribution of the Film Thickness in Wafer (Growth Rate) When One Gas Supply Pipe Is Used

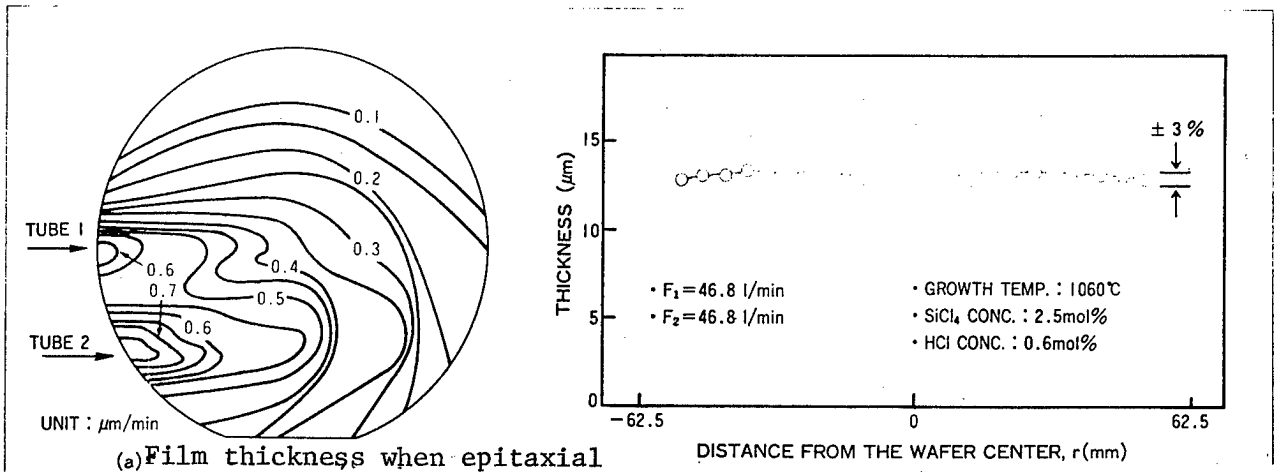

(a) Film thickness when epitaxial growth is made to grow without rotating the wafer (distribution of growth rate)

(b) Distribution of film thickness in wafer when epitaxial growth is made to grow while the wafer is being rotated

Figure 7. Example of the Distribution of the Film Thickness in Wafer (Growth Rate) When Epitaxial Growth Is Made to Grow Using Two Gas Supply Pipes

Figure 8 shows the growth rate (film thickness) distribution in the wafer loading direction obtained when two raw material gas supply pipes, the size of which was determined in this way, were used. Film thickness uniformity within ± 5 percent was confirmed between wafers and within a wafer. Nearly satisfactory results have also been obtained with regard to crystallinity and the basic electric characteristics of the epitaxial layer.[3]

The above-mentioned demonstrate that the use of this type of growth furnace permits epitaxial growth with uniformity within ± 5 percent in a wafer or between wafers if approximately 10 sheets (or about 20 sheets if 2 wafers are charged back to back) of wafers are charged for a loading length of 100 mm. If the loading length is 500 mm, for example, it is possible for a mass production furnace that can process about 50 sheets (100 sheets if 2 wafers are charged back to back) of wafers to be realized by a small device which is comparatively compact and occupies a small floor area. The gas flow rate used is thought to be sharply lower than those of other methods.

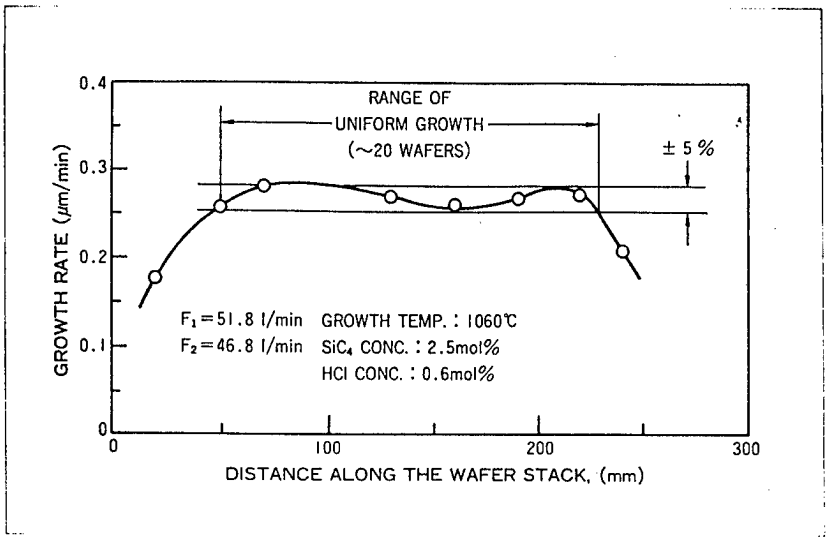

Figure 8. Example of the Distribution of Film Thickness (Growth Rate) in Wafer Loading Direction

5. Technical Subjects of Next-Generation Growth Device and Mass Production Growth

Finally, descriptions of technical subjects for study are given on the future (next-generation) epitaxial growth furnace and the growth of mass processing.

Figure 9 shows how the development of epitaxial growth furnaces has progressed so far. One of the development currents has been the one slice processing method, or the continuous one slice processing method. Recently (1988), ASM Epitaxy Inc. announced a one slice processing growth furnace whose main characteristics included fully automatic cassette handling and high-speed growth.[10] However, the wafer processing ability of this method is five to six sheets/hr at the most, and the method is not suitable for mass processing growth. To obtain a processing ability of 50 sheets/hr or more, 10 units or more must be arranged side by side. The one slice continuous processing method was also attempted in the past (1983),[11] but, in order for a processing ability of 50 sheets/hr or more to be attained, this method requires that the furnace be configured so that one wafer can be extracted within 1.2 min. Therefore, a very large and complex device, occupying a large floor area, becomes necessary. In addition, many technically difficult problems must be solved. The second current is the pancake- and barrel-type devices which have developed from the horizontal multiple slice processing method. Both methods lay out wafers on a plane. These methods are currently being used most extensively, but, as mentioned earlier, their wafer processing abilities have already reached their limits. The third current is the method referred to as the parallel loading method in which wafers are laid out side by side, in parallel, in an almost overlapping manner. This method is subdivided into the following three methods: parallel layout method in which wafers are arranged in the horizontal direction, piled layout method in which

wafers are stacked in the longitudinal direction, and set blade layout method in which wafers are arranged in a circle. In principle, the last method is most suitable for mass growth, and in the next generation, a device of this type is expected to be put to practical use in the manufacturing of epitaxial wafers which requires low-cost mass production. As mentioned earlier, however, many technical subjects remain to be studied.

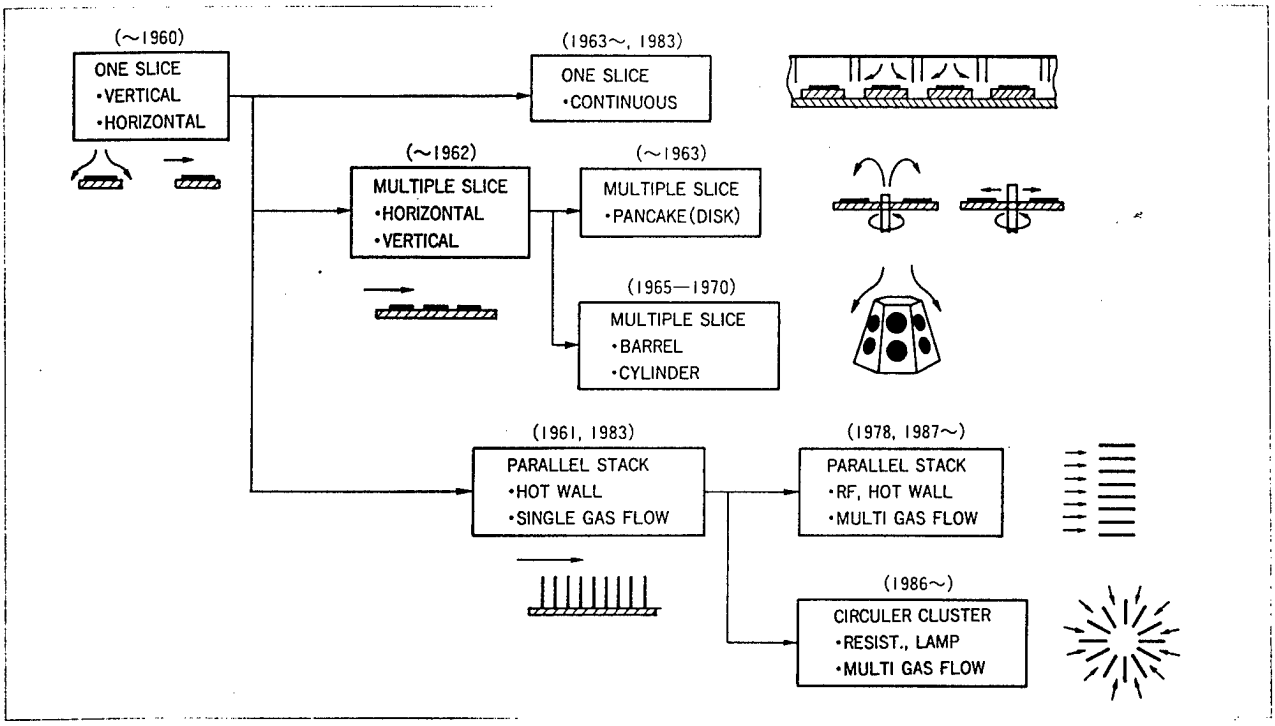

Figure 9. Progress in the Development of the Epitaxial Growth Furnace Method

Table 3 summarizes the technical subjects to be studied if a mass processing device based on such a parallel loading method is to be fully utilized as a practical mass production device. Three kinds of wafer loading methods are available, but an appropriate one needs to be selected. If the floor area is taken into consideration, the piled-layer layout is recommended. The hot wall method is thought to be the most powerful for the uniform heating of a large quantity of wafers. In that case, however, the wall deposition prevention method becomes a new technical subject for study. The high-frequency heating vertical hot wall method, which the authors developed, mixes HCl gas in the reaction gas, brings the silicon density in the gas practically to the equilibrium density, and facilitates selective growth. Also, using the raw material gas supply method to secure uniform growth of a large quantity of wafers is an important technique. The adoption of the multi-gas flow method seems to be indispensable for supplying individual wafers with fresh gas. Furthermore, an important subject whose far-reaching effects will be the most significant in the future is the realization of a

lower growth temperature. As the growth temperature drops and the growth mechanism approaches the surface reaction rule speed from the substance transportation rule speed, securing the uniformity of a large quantity of wafers is thought to be facilitated and growth devices are expected to become simpler. The full automation of the operation is more than reasonable.

Table 3. Main Techniques Necessary for Mass Processing Using the Wafer Parallel Loading Method

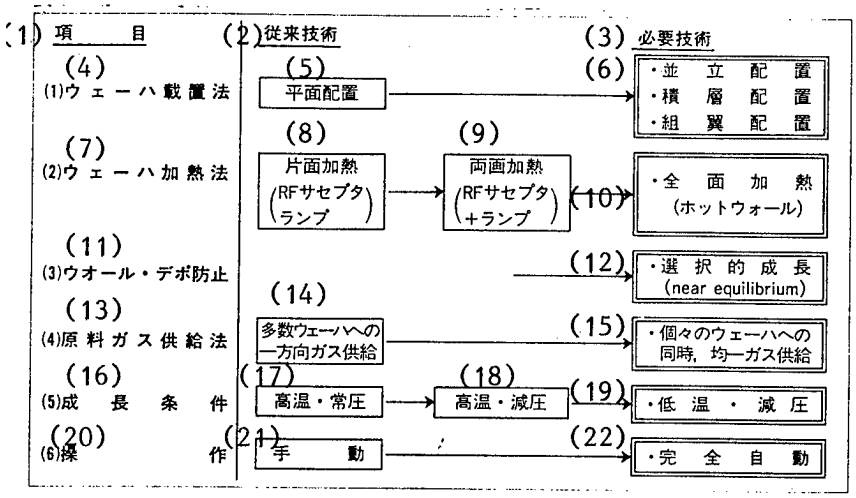

Key:

1. Item
2. Conventional techniques
3. Necessary techniques
4. Wafer layout method
5. Planar layout
6. .Parallel standing layout
   .Layer layout
   .Set blade layout
7. Water heating method
8. Single surface heating (RF susceptor lamp)
9. Double surface heating (RF susceptor + lamp)
10. Entire surface heating (hot wall)
11. Wall deposit prevention
12. Selective growth (near equilibrium)
13. Raw material gas supply method
14. Uni-directional gas supply to multiple wafers
15. Simultaneous and uniform gas supply to individual wafers
16. Growth conditions
17. High temperature and normal pressure
18. High temperature and reduced pressure
19. .Low temperature .Reduced pressure
20. Operation
21. Manual
22. Completely automatic

6. Conclusion

Here, the cost factors of wafers, the techniques currently used, the high-frequency heating vertical hot wall growth furnace proposed by the authors, and future prospects have been described with respect to mass processing epitaxial growth techniques. Mass Processing epitaxial growth techniques are currently thought to be at the stage where the possibility of the next-generation growth device, which will be capable of implementing wafer processing of about 50 sheets/hr or more, has become visible, although the evaluation of its ease of use based on actual results derived from long use on a mass production machine, the evaluation of electric characteristics based on the operation of the actual device, and further improvements in uniformity and crystal quality require continued investigation.

In the future, as the degree of LSI usage is promoted, its fine structure developed further, and very small quantities of pollution become a serious problem in manufacturing elements, the epitaxial wafer is expected to become indispensable for LSI use. It is at that time that the next-generation low-cost mass processing epitaxial growth technique described in this article will be fully utilized.

References

1. SI Staff: SEMICONDUCTOR INT'L., Vol 3, April 1980, p 71.

2. Electronicn Editors: ELECTRONICS, Vol 10, Feb 1981, p 93.

3. Y. Inoue and T. Suzuki: Ext. Abst. 19th Conf. SSDM, Tokyo, 1987, p 243.

4. T. Suzuki, Y. Inoue, H. Onose and J. Kobayashi: Proc. 10th Int. Conf. CVD(ECS Fall Meeting), Honolulu, 1987, p 286.

5. M. L. Hamond: SEMICONDUCTOR INT'L,, Vol 6, 1983, p 58.

6. Tetron Inc.: SEMICONDUCTOR INT'L., Vol 9, 1986, p 250.

7. V. S. Ban: J. CRYST. GROWTH, Vol 45, 1978, p 97.

8. M. Ogirima and R. Takahashi: Ext. Abst. ECS Fall Meeting, (1981) Abst. No. 404, 981.

9. J. Bloem, Y. Oei, H. de Moor, J. Hanssen and L. Giling: J. ELECTROCHEM. SOC., Vol 132, 1985, p 1973.

10. SOLID STATE TECH, Japanese edition, June 1988, p 24.

11. D. Bellavance and R. N. Anderson: Ext. Abst. ECS Spring Meeting (1983) Abst. No. 417, 653.

Low-Temperature Epitaxial for Silicon

43064044B Tokyo SEMICON NEWS in Japanese May 89 pp 42-48

[Article by Shinya Yamazaki, Semiconductor Research Department, Fujitsu Laboratory, Ltd.: "Techniques Centered Around Optical Epitaxial Growth"]

[Text] 1. Preface

At the beginning of the 1960s, epitaxial growth (epi) techniques were applied to the Si bipolar integrated circuit (IC) and sharply enhanced its degree of integration and operation speed. Since then, epi techniques have developed as a bipolar IC process. However, with the MOSIC density becoming higher recently, epi techniques have also come to be applied to MOSIC to solve such problems as latchup and software program errors.

The epi of the chemical vapor deposition method (CVD), which is extensively used in industry at present, is a very inefficient process, and the increase in throughput and a fall of epi cost are necessary if epi techniques are to be fully utilized for MOSIC. The other subject required by the current epi techniques is a lowering of the epi process temperature. This article explains low-temperature epi techniques, with importance attached to the low-temperature epitaxy using optical excitation developed by the author.

2. Necessity for Low-Temperature Epi

First of all, the necessity for low-temperature epi is explained. Usually, a process temperature equal to or higher than 1000°C is thought to be necessary for the CVD epi of Si. Therefore, epitaxial growth is allowed only during the initial stages of an IC process, that is, only as manufacturing techniques of crystalline substrates. This is because the high epi process temperature destroys the impurity distribution which determines the device performance. If the epi process temperature can be lowered, the advantages listed below will be obtained.

1) Epi will be applicable to the element formation process.

2) Steep impurity distribution will be able to be created arbitrarily and with good precision.

3) Control of the film thickness is easy and a very thin epi film can be deposited.

4) Film quality deterioration due to the mixing of a heavy metal can be suppressed.

5) The device will become simple and convenient, and cost reduction will become possible.

As mentioned above, a lowering of the epi temperature can produce high value added epi techniques. The use of low-temperature epi, for example, will enable a company to create an element with a new structure and a new function which cannot be attained using the current process.

3. Requirements of Low-Temperature Epi

This section discussed the conditions necessary for lowering the Si epi temperature.

Figure 1 shows a schematic diagram of the epitaxial growth process of Si. The raw material gas in the vapor phase is thermally decomposed and is supplied to the crystal surface. Adsorbed reaction seeds pass the dehydrogenation or reduction reaction, becoming Si atoms. These Si atoms migrate to the crystal surface and match kinks, which are growth points of the crystal. The repetition of this process makes epi films grow rapidly two-dimensionally. If the growth temperature is lowered, the following problems occur in the growth process.

1) The speed of the thermal decomposition reaction in the vapor phase and that of the dehydrogenation or reduction reaction on the surface drop, and the supply quantity of Si atoms is reduced.

2) The surface mobility of the Si atoms drops and its migration becomes difficult.

Item 1) lowers the growth rate of the crystal and 2) deteriorates the film quality, ultimately leading to the generation of polycrystalline substances. Furthermore, although not shown in Figure 1, the obstruction of crystal growth caused by the surface adsorption of oxygen or moisture becomes remarkable. Therefore, if the epitaxial growth temperature is to be lowered and a significant growth rate attained, the following conditions must be satisfied.

1) Increase in quantity of Si atom supply.

2) Enhancement of Si atom surface mobility.

3) Removal of influence of oxygen and moisture.

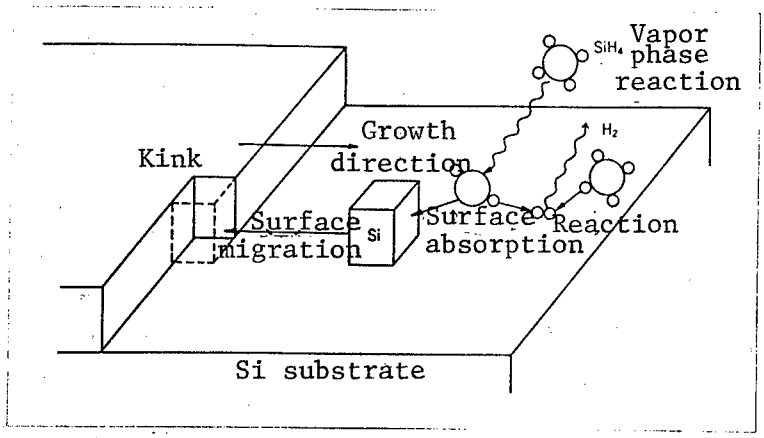

Figure 1. Rough Illustration of Si Epitaxial Growth Process

Since these three items are not independent events originally, and the direction of the crystal surface, the cleanliness of the surface, the density of active seeds during the vapor phase, and the frequency of two-dimensional nuclear growth must be taken into consideration, the mechanism of low-temperature growth becomes very complex. To attain low-temperature growth, however, at least the three requirements mentioned above must be satisfied.

4. History of Low-Temperature Epi

This section surveys the low-temperature epi studied in the past.

Because of its significant impact, low-temperature epi has been studied by many people for a long time. During the initial stages of Si epi invention, a growth temperature of as high as 1200°C was necessary. This high growth temperature was lowered to 1000°C by changing the raw material gas from silicon tetrachloride ($SiCl_4$) to silane (SiH_4) and reducing the ambient pressure to below the ordinary value. This is the CVD epi technique which is currently being extensively used in industry. With this epi, however, further temperature lowering cannot be expected, and it is not the low-temperature epi in the original sense.

The low-temperature epi, as studied in the past, can be roughly classified into two categories according to type. One is the physical method represented by molecular beam epitaxy (MBE), which uses a superhigh vacuum mainly to satisfy 3). The other is the CVD, for which energy assist is performed with plasma and light. Also, the spatter method, which is positioned between these two, is being studied. Table 1 summarizes representative examples.

5. Optically Excited Low-Temperature Epitaxy

This chapter introduces the low-temperature epi using the optically excited process which the author developed, and discusses the low-temperature epi.

5.1 Concept of Optical Epi

The low-temperature epi (optical epi) using optical excitation, which the author developed, takes matching with the conventional epi into consideration and has adopted the CVD method. Furthermore, the following technical characteristics have been added to satisfy the aforementioned low-temperature epi requirements.

1) The ultraviolent rays of a mercury lamp are irradiated onto the reactor and substrate surfaces.

2) Disilane (Si_2H_6) is used as the raw material gas.

3) The influences of oxygen and moisture are minimized as much as possible by raising the degree of attainable vacuum and the gas purity.

Table 1. Low-Temperature Techniques Studied in the Past

Item	Method		Epitaxial growth temperature	Literature
Physical methods	Molecular beam epitaxy (MBE)		300-800	(1)
	Ion beam epitaxy (ICB)		400	(2)-(3)
	Spattering		350	(4)
Chemical methods	Thermal CVD (UHV/CVD)		550	(5)
	Plasma-CVD		700	(6)-(7)
	Optical CVD	Mercury sensitizing method	250	(8)
		Direct reaction	500-800	(9)-(11)

Table 2. Light Absorbing Properties[12] of Silane and Disilane in Ultraviolet Band

Item	Ultraviolet-ray absorption edge (nm)	Light absorption sectional area (at 185 nm) (cm^{-2})
Silane (SiH_4)	160	10^{-21}
Disilane (Si_2H_6)	210	10^{-17}

Table 2 shows the absorption characteristics of the rays in the ultraviolet band for silane, which is the raw material of the ordinary CVD epi, and disilane used for the optical epi. Since silane's absorption edge of rays is 160 nm, it is not sensitive to the ultraviolet rays (wavelength $\geq$ 185 nm) radiated by a mercury lamp. On the other hand, disilane's absorption edge is at 210 nm, and its ray absorption sectional area at 185 nm is larger by four positions than that of silane. Therefore, disilane optically decomposes with the irradiation of mercury lamp light. Furthermore, ultra-violet rays irradiated to a substrate surface are absorbed in a very shallow range of the substrate surface, generate many electron-positive hole pairs, reduce the hydrogen coverage rate of the surface, and activate the substrate surface. In other words, optical epi is the low-temperature epi which complements the decrease in the growth rate due to a lowering of the growth temperature by the opto-chemical reaction of disilane caused by ultraviolet rays and the lowering of surface mobility by the activation of the surface caused by the ultraviolet rays.

5.2 Growth Device

Figure 2 shows an outline of the growth device. The reactor is made of synthetic quartz with high transmittivity of ultraviolet rays. The attainable vacuum has been raised to 10^{-4}Pa by an oil-free vacuum exhaust system which combines a dry pump and a turbo pump. Si wafers with surface direction (100) are washed by a chemical solution and are put into the reactor. Wafers on the susceptor coated by SiC are heated from the back by infrared lamps and are irradiated from the front by the ultraviolet rays from high-pressure mercury lamps. The intensity is 1.2 W/cm^2. To remove natural oxide films before the start of growth, heat treatment was performed for 10 min at 900°C in hydrogen, and the temperature was lowered to the target growth temperature. The growth pressure was fixed at 27 kPa.

5.3 Low-Temperature Characteristics

Figure 3 shows the dependence of the growth rate on the growth temperature in optical epi. At temperatures equal to or higher than 650°C, the growth rate increases monotonously with the increase in the growth temperature, independently of the presence or absence of ultraviolet ray irradiation. At temperatures below 650°C, however, the dependence of the growth rate on

the temperature suddenly changes, i.e., while Si films deposit very little with thermal growth, a growth rate with a small growth temperature dependence is obtained under ultraviolet ray irradiation. These results show that Si film deposition occurs via a thermal process at 650°C or higher, while below 650°C it is controlled by the reaction caused by ultraviolet rays.

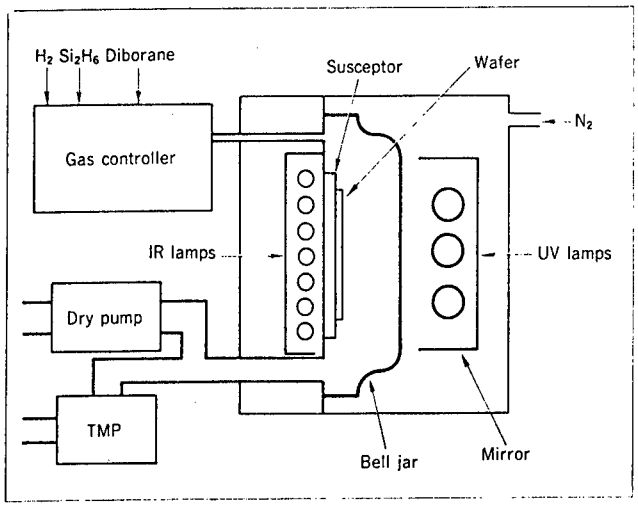

Figure 2. Rough Illustration of Optical Epi Device

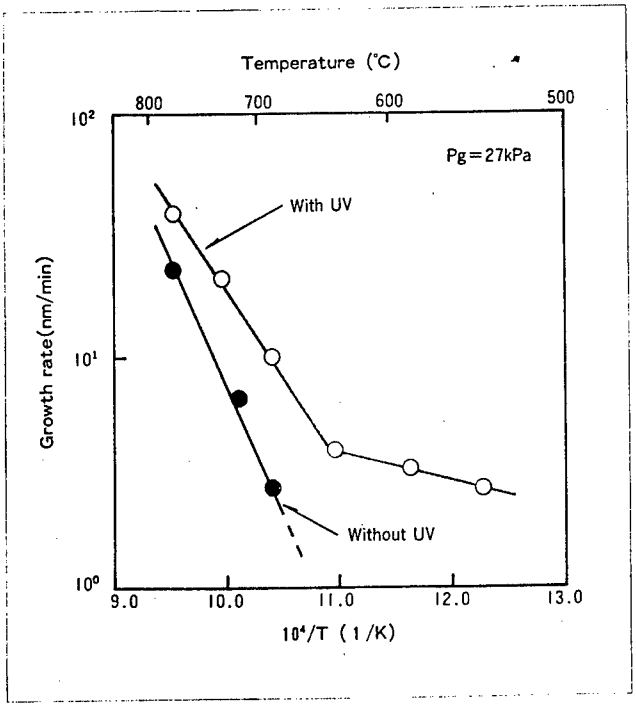

Figure 3. Dependence of Optical Epi Rate on Temperature

To investigate the effect of ultraviolet rays in this low-temperature area, the growth rate was measured by inserting a filter in front of the ultraviolet ray source in order to cut the 185 nm bright line. Figure 4 shows the results of the measurement. At 650°C or higher, the growth rate shows the same value, independently of the presence or absence of the 185 nm line. At temperatures below 650°C, however, the cutting of the 185 nm line lowers the growth rate. The same graph also shows the ratio of the growth rate under total irradiation by the 185 nm line (broken line). As the temperature drops, the proportion of the growth rate caused by the 185 nm line increases, reaching 70 percent at 550°C. In other words, the growth rate in the low-temperature area during optical epi is found to be ruled by the opto-chemical reaction of disilane caused by the 185 nm ultraviolet rays.

The difference between the thermal growth rate and the growth rate upon the cutting of the 185 nm line is thought to be caused by the temperature rise of the substrate surface resulting from ultraviolet ray irradiation and the activation of the surface by the generation of electron-positive hole pairs, but the mechanism is not yet clear.

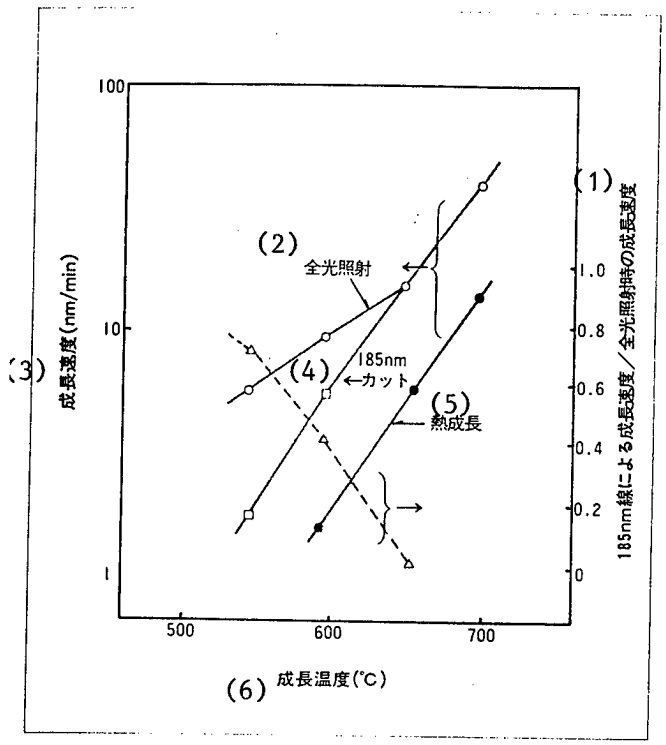

Figure 4. Effective Wavelengths of Ultraviolet Rays for Growth Rate

Key:

1. Growth rate with 185 nm ray/that with total light irradiation
2. Total light irradiation
3. Growth rate(nm/min)
4. Growth rate when 185 nm ray is cut
5. Thermal growth
6. Growth temperature (°C)

Then, in-situ analysis was performed on the opto-chemical reaction of disilane by ultraviolet rays in the low-temperature area by using the infrared absorption spectroscopic method (FT-IR). The reaction gas was directed into an analysis cell from a capillary fixed at a height of 1 mm above the Si substrate, and the infrared absorption spectra were observed. Figure 5 shows the change in the infrared absorption spectra caused by ultraviolet ray irradiation. Before the ultraviolet ray irradiation, only the absorption of disilane was observed. With ultraviolet ray irradiation, however, the absorption caused by the silane stretch mode appears at 2210 cm^{-1}. This shows that disilane optically decomposes according to the following reaction formula, generating silane:

$$Si_2H_6 \xrightarrow{h\nu\ (185\ nm)} SiH_3 + SiH_2 + H$$

The silane (SiH_2) generated by this opto-chemical decomposition rules the growth rate of the optical epitaxy at low temperatures. Therefore, the growth rate of optical epitaxy at temperatures below 650°C demonstrates low temperature dependence.

Then, the optical epi film quality was observed by using reflecting high-energy electron beam diffraction (RHEED) and a high-resolution penetrating electron microscope (HR-TEM). As shown in Figure 6(b) [not reproduced] by the Debye rings, the Si film grown thermally is polycrystalline. If ultraviolet rays are irradiated, however, the RHEED image becomes streak-like, and the growth of a good single crystal is observed (Figure 6(a)) [not reproduced].

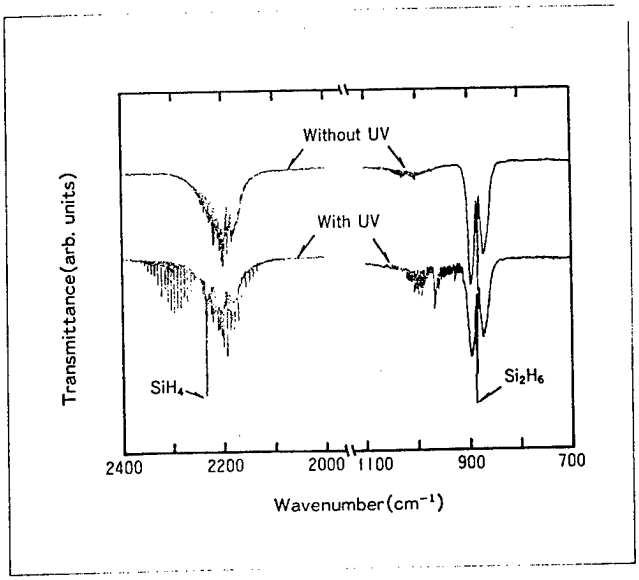

Figure 5. Infrared Absorption Spectra

Figure 7 [not reproduced] shows an HR-TEM image of an optical epi film generated at 600°C. A single crystal grows from the boundary surface of the Si substrate without discontinuity of the crystal lattice. No crystal defects are observed in the optical epi film either, and the optical epi film grown at 600°C has very good film quality. This shows that the crystal surface is activated by ultraviolet ray irradiation, and the surface mobility of the Si atom has been enhanced.

As demonstrated by the above results, optical epi makes low-temperature epi possible by using the opto-chemical reaction of disilane caused by ultraviolet rays and the activation of the substrate surface.

5.4 Doping and Impurity Distribution

To apply the Si epi film to a device, impurity doping is necessary. Specifically, if the epi film is to be applied to the base layer of a bipolar transistor, boron doping of 10^{19} cm^{-3} or more is necessary. Therefore, the author attempted the high-density doping of boron in optical epi. Diborane gas (B_2H_6) was used as the raw material of boron.

Since, with the ordinary CVD epi, deterioration of film quality is caused by boron segregation, boron doping of $1x10^{18}$ cm^{-3} or more is difficult. Figure 8 shows the relationship between the film quality and carrier density when high-density boron was doped at 600°C. The quality of the Si film was evaluated by using Raman scattering. (Crystallinity can be evaluated with the half-value width of the Raman spectrum. It is 3.4 cm^{-1} for bulk Si and about 7.5 cm^{-1} for poly-Si deposited by LPCVD.) In the case of thermal growth, boron doping of $1x10^{18}$ cm^{-3} or more sharply reduces the film quality, with that of $1x10^{19}$ cm^{-3} or more resulting in poly-crystalline growth. Under ultraviolet ray irradiation, however, a good single crystal can grow up to the boron density of $1x10^{20}$ cm^{-3}. Figure 9 shows the activation ratio of the boron taken into the film at this time. In the case of thermal growth, boron doping of $1x10^{18}$ cm^{-3} or more initiates a sharp decrease in the activation ratio. On the other hand, optical epi maintains a 100 percent activation ratio up to a boron density of 1.5×10^{20} cm^{-3}. In this way, strong correlation exists between crystallinity and the activation ratio in high-density boron doping. This is because ultraviolet rays give rise to the opto-chemical reaction of disilane, and the substrate surface is activated to match boron atoms to all the Si lattice points. In this way, optical epi permits not only low-temperature growth, but also very high-density boron doping of 1.5×10^{20} cm^{-3}.

Figure 10 shows the impurity distribution in an optical epi film which grew at 600°C and had a boron density of 2×10^{19} cm^{-3}. Since the growth temperature is low, very steep impurity distribution has been attained.

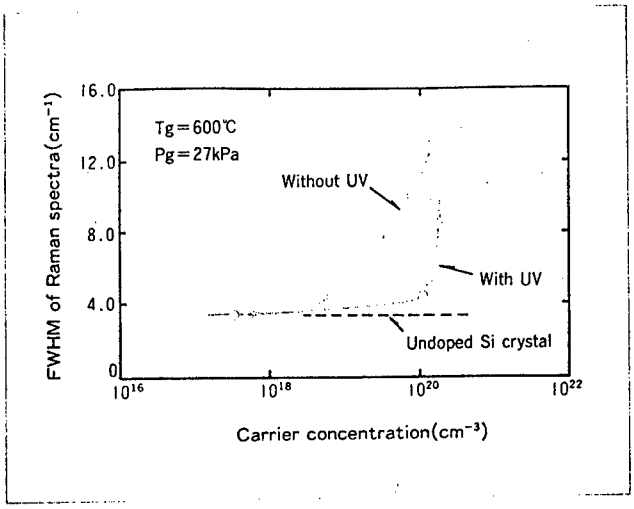

Figure 8. Relationship Between Film Quality and Carrier Density in High-Density Boron Doping

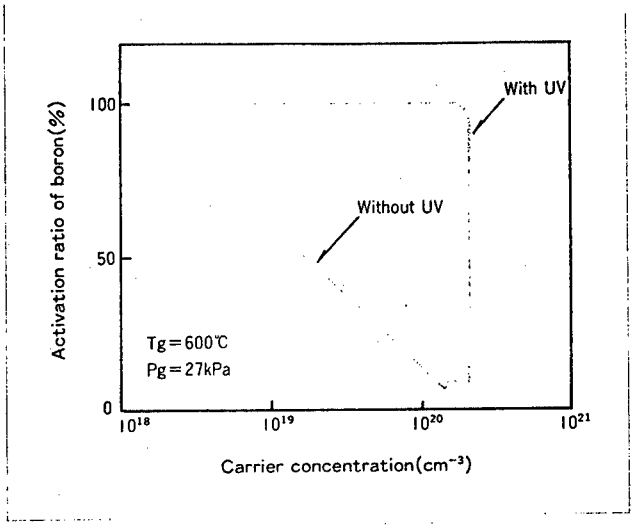

Figure 9. Activation Ratio of the Boron Taken Into Si Film

5.5 Application to Bipolar Transistor

To attain the high speed demanded for the currently-used bipolar device, reduction of the base width and lowering of the base resistance are indispensable. However, with ion implantation and thermal diffusion, the conventional impurity introduction techniques, major channeling of the boron atoms and the realisation of 100 nm or less are difficult to attain. Therefore, an epi film with high boron density and steep impurity distribution, obtainable with optical epi, was applied to the base layer.

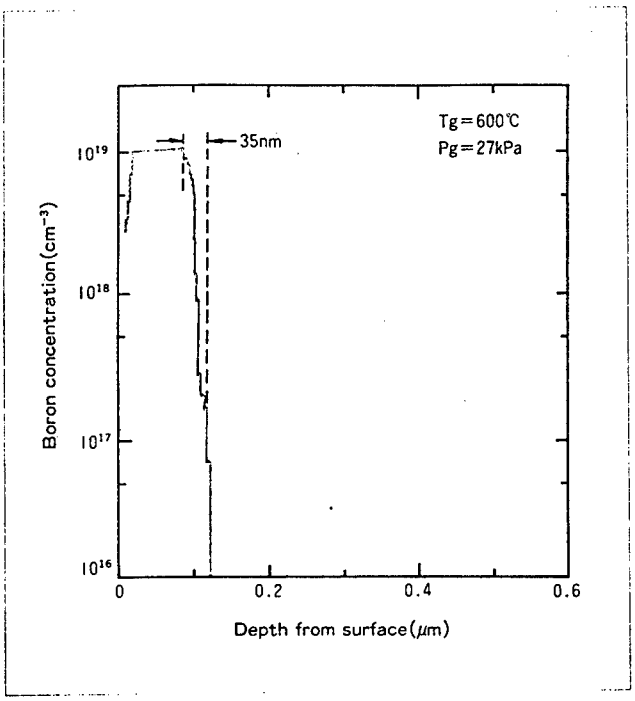

Figure 10. Distribution of Impurities in an Optical Epi Film Subjected to High-Density Boron Doping

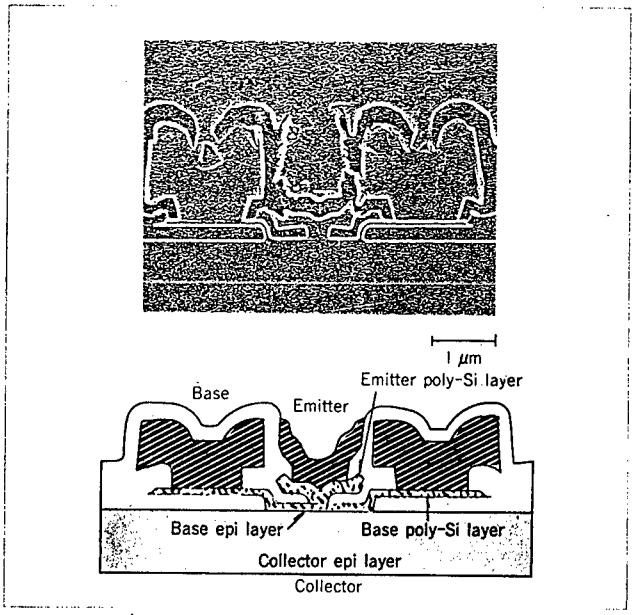

Figure 11. Cross Section of EBT (Epitaxial Base Transistor)

Figure 11 shows a cross section of the epitaxial base transistor (EBT) employing optical epi as the base. This transistor uses an optical epi film for the active base and poly-Si, which is simultaneously formed on the oxide film together with optical epi, as the lead electrode of the base. The emitter was formed by arsenic diffusion from poly-Si.

Figure 12 shows the EBT impurity distribution. An emitter depth of 30 nm, base width of 50 nm, and base peak density of 1 x 10^{19} cm^{-3} have been attained. This impurity distribution cannot be attained with any other technique. Figure 13 shows the I_C-V_{CE} characteristics of EBT. This transistor demonstrates good transistor operation and has a current amplification of about 45. Furthermore, although the base width is as thin as 50 nm, the base density is high. Therefore, early voltage is 100 V or more. In addition, no punch-through or short circuiting between the emitter and collector has been observed. Therefore, the film quality of optical epi is proven to be excellent. The maximum cut-off frequency of EBT is 17.5 GH_z, and the overall run time of the carrier becomes 9 ps. Of the run time, the base run time is 0.9 ps, accounting for only 10 percent. In other words, an EBT with a base width of 50 nm is found to be satisfactory as far as base width is concerned. In this way, optical epi serves as a powerful technique for forming a thin base for superhigh-speed bipolar transistors.

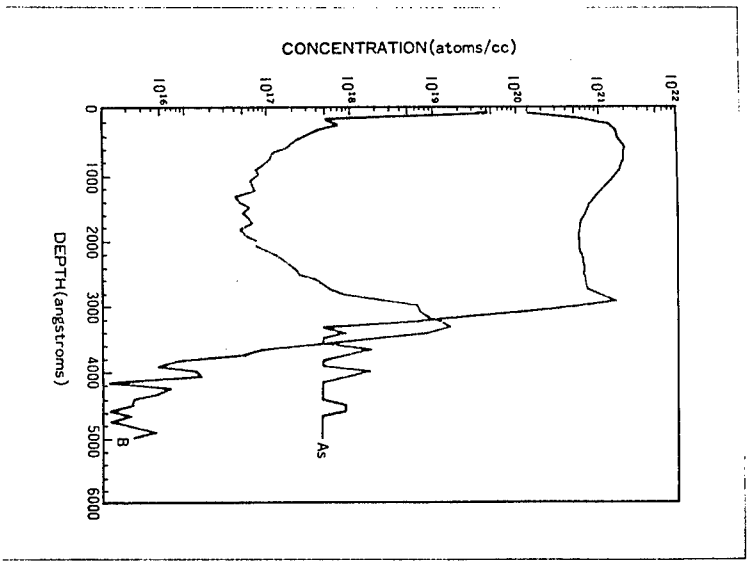

Figure 12. Distribution of Impurities in EBT

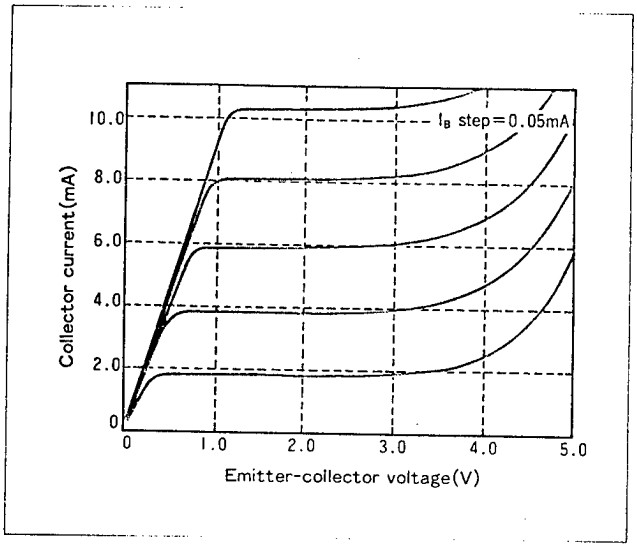

Figure 13. I_C-V_{CE} Characteristics of EBT

6. Future of Low-Temperature Epitaxial Growth Technique

So far, low-temperature epitaxial growth techniques have been studied by attaching importance to optical epi, and it is regrettable that, of those shown in Table 1, no low-temperature epi, including optical epi, has been put to practical use by industry. One of the reasons for this is that low-temperature epi has been positioned as a process in competition with the CVD epi, a technique already established industrially. If low-temperature epi is to be put to practical use, a device with a new structure and new functions which would fully utilize such low-temperature epi characteristics as steep and arbitrary impurity distribution and crystalline superthin films must be attained with the low-temperature epi, as shown in the section relating to optical epi applications.

One more obstacle obstructing the practical use of low-temperature epi is the poor film quality of the low-temperature epitaxial growth film. The crystallinity required by current ICs from the epitaxial growth film is very high and the defect density is very small. As mentioned earlier, however, lowering the growth temperature increases the influence of oxygen and moisture, causing the film quality to deteriorate. Therefore, future epitaxial growth techniques are required not only to adopt an appropriate growth method, but also to attain sharp reduction and very precise management of moisture and oxygen, as well as to control the contamination caused by dust and heavy metals.

The other requirement demanded of low-temperature epi is the lowering of the preprocessing temperature. Before initiating the epitaxial growth of Si, it is always necessary to conduct preprocessing to remove the natural oxide films on the Si surface. If the temperature of this preprocessing is not lowered, the application scope of the low-temperature epi dies not spread. Several low-temperature preprocessing methods have been proposed, but no practical film has been obtained yet.

The future of low-temperature epi has already been surveyed, but many problems exist that must be solved. However, the technical impact of low-temperature epi is large and retains the possibility of totally changing the device structure and functions. It will not be too long before research will put parts of the low-temperature epitaxial growth technique to practical use.

7. Conclusion

The low-temperature epitaxial growth technique has been explained, from its necessity to its future image, with importance attached to the optical low-temperature epitaxial growth technique. The author hopes that this article will help users understand the low-temperature epitaxial growth technology.

References

1. Y. Ota, J. APPL. PHYS., 1980, p 1102.
2. T. Takagi et al., J. VAC. SCI. TECHNOL., Vol 12, 1975, p 1128.
3. P. C. Zalm et al., APPL. PHYS. LETT., Vol 15, 1982, p 167.
4. T. Ohmi et al., "Extended Abstracts of 20th Conference on Solid State Devices and Materials," Tokyo, 1988, pp 49-52.
5. B. S. Meyerson, APPL. PHYS. LETT., Vol 48, 1986, p 797.
6. T. J. Donahue et al., J. APPL. PHYS. Vol 57, 1985, p 2757.
7. S. Suzuki et al., J. APPL. PHYS., Vol 54, 1983, p 1466.
8. S. Hishida et al., APPL. PHYS. LETT., Vol 49, 1986, p 79.
9. M. Kumagawa et al., JPN. J. APPL. PHYS., Vol 7, 1968, p 1332.
10. R. G. Frieser, J. ELECTROCHEM. SOC., Vol 115, 1968, p 401.
11. T. Yamazaki et al., "Extended Abstracts of the 18th Conference on Solid State Devices and Materials," Tokyo, 1986, pp 213-216.
12. V. Itoh. et al., J. CHEM. PHYS., Vol 85, 1986, p 4867.

Low Vacuum Oil-Free Pump for Semiconductor Mass Production

43064044C Tokyo SEMICON NEWS in Japanese May 89 pp 76-77

[Article by Yasuhiko Takeno, Market Research Division, Elecmate Japan, Ltd.]

[Text] 1. Background of Putting Low Vacuum Oil-Free Pump to Practical Use

Beginning with the 256K DRAM mass production process, semiconductor manufacturing tended toward dry processing, and in the current mega age, the trend of almost all processes has been toward dry processing. As shown in Table 1, therefore, the processes in vacuums have increased in number. Especially, since the semiconductor process is unfavorably influenced by dust, the request for a clean vacuum is strong, and various technical innovations have been performed on vacuum pumps. In the high-vacuum area, the Crio pump, turbo molecular pump, and spatter ion pump have been developed and put to practical use as oil-free pumps.

However, the demand for the development of oil-free pumps in the low-vacuum area, such as the oil rotary pump, has strengthened.

The reasons for this are as follows:

1) Since chlorine-based gas is used in Al etching, oil deteriorates. Therefore, a large quantity of expensive Fonbrin [phonetic] oil is consumed.

2) The reverse diffusion of oil results from the lubricating oil and affects the film quality of the wafers.

3) Substances produced by the CVD reaction mix in with the oil in the oil rotary pump, causing drops in performance as well as the defective operation of the pump.

2. Current Status of Low-Vacuum Oil-Free Pump

The low-vacuum oil-free pump appeared for the first time in Japan in 1982 when Unozawagumi Iron Works, Ltd. developed one for distillation purposes in the chemical industry. The company has adopted "Root's multistage type"

of pump which is the same type as that of the mechanical booster. The pump exhausts gas using two rotors which perform non-contact rotation, maintaining a clearance of 100 to 200 μm. The bearing prevents the oil in the gear chamber, driven by the rotors, from mixing by an oil seal.

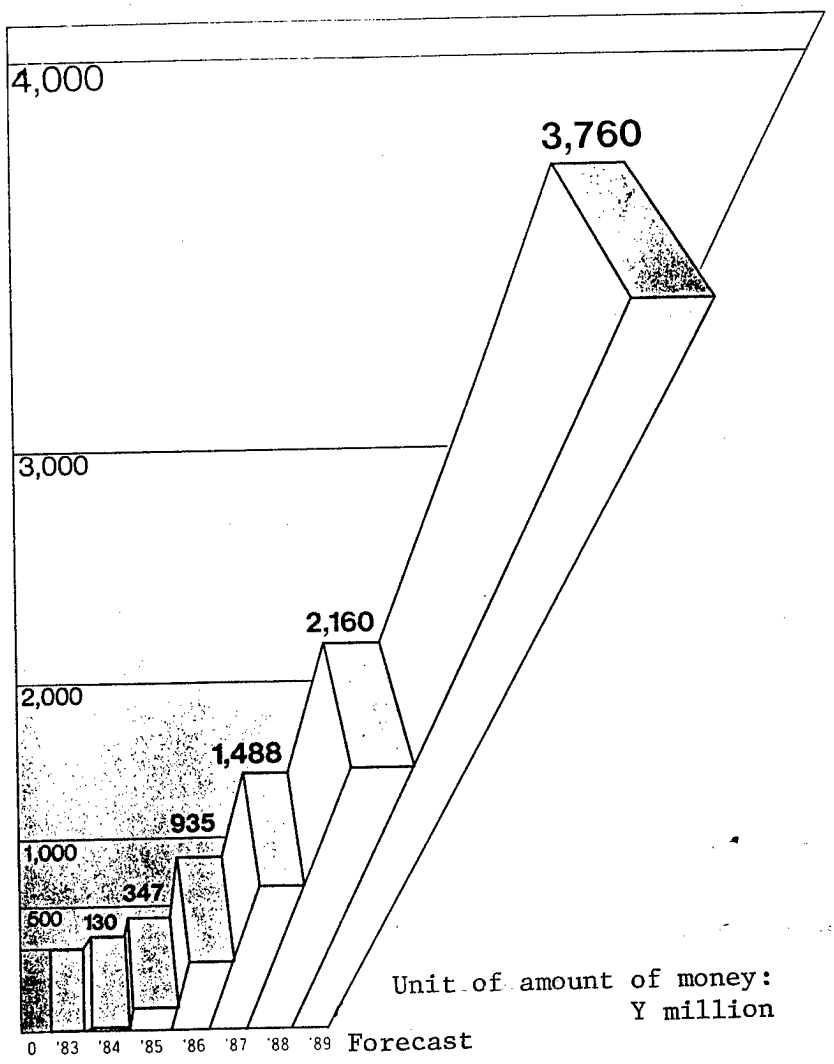

Figure 1. Market Share of Low-Vacuum Oil-Free Pump for Semiconductor Manufacturing (Estimated by Elecmate Japan, Ltd.)

Table 1. Vacuun Range in Semiconductor Manufacturing Process

Division	Degree of vacuum(Torr)	Main process	Main pump
Low vacuum	$10\text{-}10^{-3}$	LPCVD Plasma CVD RIE Ashing Plasma etching	Water-sealed pump Centrifugal pump Oil rotary pump Root's pump
High vacuum	$10^{-6}\text{-}10^{-8}$	Ion implantation Spattering SEM SIMS	Mechanical booster pump Oil diffusion pump Crio pump Spattering ion pump
Superhigh vacuum	10^{-9} or lower	SEM SOR	Turbo molecular pump

In 1985, Anlett, Ltd. entered this field with a similar pump. Currently, Hitachi, Ltd., Ebara, Ltd., Kashiyama Industry, Ltd., Nissan Edwards, Ltd., Ribolt Heraus, Ltd. (Matsusaka Trade, Ltd.), and Alkatel, Ltd. (NEC Anerva, Ltd.) are participating in this field.

Ebara, Ltd. formed an oil-free pump project team in 1985 and completed a Root's-type trial product in 1986. In 1987, this company conducted development activities in cooperation with Toshiba Corporation and completed a mass production factory for 60 units per month.

Hitachi, Ltd. first entered into this field with a screw-type pump, and later announced the turbo-type pump "SKY TORR." Hitachi, Ltd.'s pumps are mainly sold within the corporation, but "SKY TORR" is also being sold to outsiders.

Kashiyama Industry, Ltd. is selling pumps of this type, with importance attached to the screw-type pump "SDV 1500."

Nissan Edwards, Ltd. entered into this field with a claw-type pump which is characterized by a short exhaust path.

Some manufacturers are developing scroll-type oil-free pumps, and it seems that this market will be diversifying in the future.

3. Low-Vacuum Oil-Free Pump Market Expects 70 Percent Increase in 1989

It was in 1983 that the semiconductor industry started evaluating the low-vacuum oil-free pump in semiconductor manufacturing processes, and the practical use of the pump is presumed to have been started in 1984. Device manufacturers are especially conservative when parts are concerned, and this

pump was directly adopted by device manufacturers on the basis of the device manufacturers' evaluation. Since some manufacturers adopted this pump for the 256K DRAM mass production process, the pump's market has doubled each year, reaching Y130 million in 1984, Y347 million in 1985, and Y935 [million] in 1986. In 1987, since several device manufacturers adopted the pump for mass production processes, the sales Y1.488 billion. [as printed] Since the pump is also maintenance-free and running costs can be reduced, oil-free pumps are expected to be used as low-vacuum pumps in the future.

4. Ebara and Nissan Edwards Move Up

As shown in Figure 2, Unozawagumi Iron Works, Ltd., the originator, had a 40 percent share of this field. However, since Ebara, Ltd. completed a pump factory and attached importance to the sale of the pump, the iron works' share dropped to 23 percent in 1988. On the other hand, Nissan Edwards, Ltd.'s sharerose to 22 percent, presumably because its mechanism was highly evaluated. The pump, which is currently being adopted for many cases of etching, poses many problems for CVD study. Since the manufacturer developing a pump applicable to CVD occupies a large share, the market seems to have become one in which keen competition for sale and development is present.

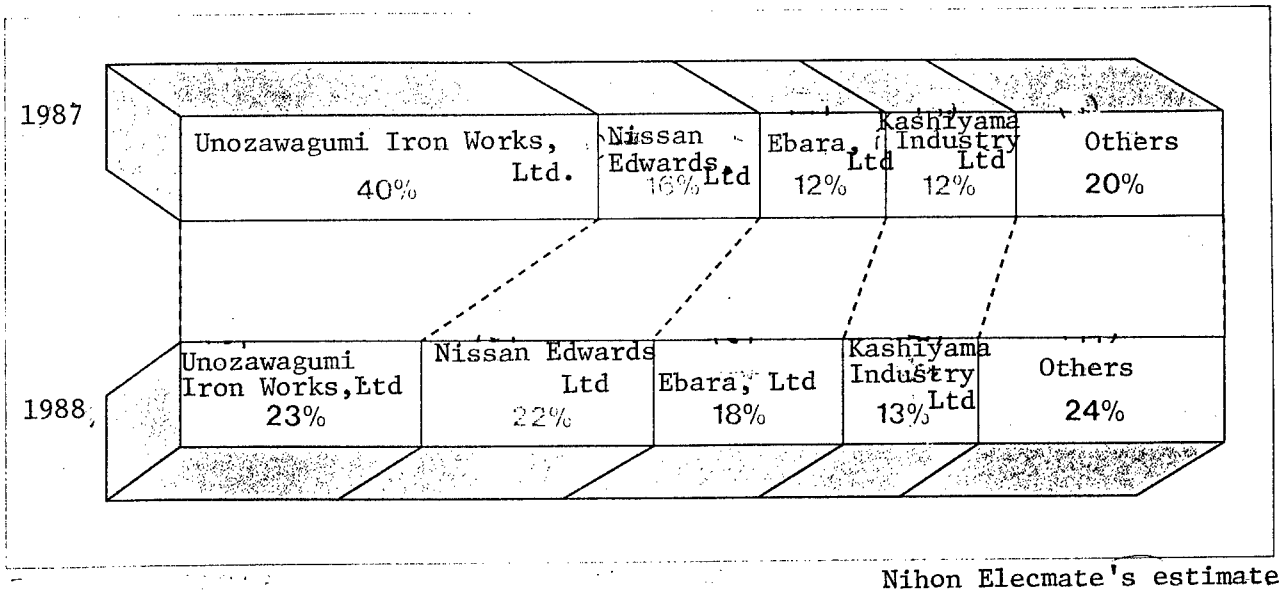

Figure 2. Market Share of Low-Vacuum Oil-Free Pumps by Individual Manufacturers (Estimated by Elecmate Japan, Ltd.)

VLSI Technology Trends for 1990s

43064044D Tokyo SEMICON NEWS in Japanese May 89 pp 82-86

[Unattributed article]

[Text] ISSCC '89, the International Solid-State Circuits Conference, which is called the Olympiad of semiconductor techniques, was held in New York City, from 15 to 17 February. The number of papers presented this year was 100 and, of these, 39 were from Japan.

First of all, in the field of memory, again this year as they did last year, three Japanese companies (Toshiba Corporation, NEC Corporation, and Mitsubishi Electric Corporation) presented a 16M DRAM manufactured on a trial basis. In addition, next-generation up-to-date techniques, such as Sony Corporation's 16M SRAM, which is the first in the world, and Hitachi, Ltd. and Toshiba Corporation's high-speed 1M SRAM, whose access time is 10 ns or less and has a 32-bit MPU, in the processor field were presented in individual fields in respect to approaching the 1990s.

Attempts to adapt the Bi-CMOS technique as a process technique to various fields, such as SRAM, microprocessors, gate arrays, and DSP (Digital Signal Processor), were also presented, and LSI seems to be pursuing higher-speed operation.

Presentations in individual product fields are reported below.

DRAM

Presentations on 16M DRAM Under Leadership of Japanese Manufacturers

First, let us look at presentations on the DRAM (dynamic RAM), which is referred to as the technology driver of the semiconductor. Regarding the DRAM, last year Matsushita Electric Industrial Co., Ltd., Toshiba Corporation, and Hitachi, Ltd. presented prototypes of the 16M DRAM, which is a next-generation product. Toshiba Corporation reported on the same subject again this year, followed by NEC Corporation and Mitsubishi Electric Corporation's presentations on the subject. This means that the 16M DRAM has been reported by a total of six major Japanese semiconductor manufacturers (see Table 1). Toshiba Corporation's presentation on the 16M DRAM this year, following last year's presentation, may be said to show the company's strong inclination to retain the top rank it currently occupies with regard to the 1M DRAM in the future in developing the 4M and 16M DRAMs.

Table 1. Comparison of Specifications of 16M DRAMs at ISSCC'89 (Toshiba's figures in parenthesis are those for '88. Hitachi and Matsushita's figures have been cited from ISSCC'88.

Item	Toshiba	NEC	Mitsubishi	Hitachi	Matsushita
Memory configuration	16Mx1/4Mx4	16Mx1/4Mx4	16Mx1/4Mx4	16Mx1	16Mx1/4Mx4
Minimum line width (μm)	0.6	0.55	0.5	0.6	--
Cell dimensions (μm^2)	4.8	4.05	4.8	4.16	3.3
Cell structure	Trench (Stack trench)	Stack	Stack	STC cell	Trench
Access time (ns)	45 (70)	55	60	60	65
Chip dimensions (mm^2)	7.87x17.4 (17.5x12)	8.2x15.9	7.7x17.5	8.2x17.3	5.4x17.38
Process technique	CMOS (CMOS)	CMOS	CMOS	CMOS	CMOS

Toshiba Corporation's 16M DRAM boasts the shortest access time--45 ns--among those announced so far. This DRAM has been attained by using N-type MOS as the memory cell and CMOS as the peripheral circuit, and further adopting the new "three-layer well structure," which combines P- and N-type impurity areas (wells) with the peripheral circuit. Since the three-layer well structure permits electric insulation between the substrate and each well and has the advantage that the voltage of the peripheral circuit can be set up independently, the operation delay that has appeared in the past when applying the voltage to suppress the consumption current to the memory cell can be prevented. Also, the reduction of cell dimensions and the suppression of wiring delays by the concentrated layout of the peripheral circuit has assisted in attaining higher-speed operation. As shown in Table 1, the chip size of Toshiba's 16M DRAM has been reduced by about 35 percent from last year's.

The most significant characteristic of NEC Corporation's 16M DRAM is its built-in "BIST circuit," which cuts the sharp increase in test costs accompanying the high integration of memory devices. This BIST circuit has built-in ROM and generates the signals necessary for testing the write and read of addresses and data, and becomes operable with clock input alone. As a result, the test time can be reduced to up to one-eighth that of the conventional method of inputting address test patterns from the outside.

Mitsubishi Electric Corporation has adopted for its 16M DRAM the design rule of 0.5 μm, the smallest of those announced so far. Also this 16M DRAM is operable with a single 3.3 V power supply. In addition, it adopts the "twist bit line structure" for the bit line, which applies the voltage for the write/read of data, aiming at reducing the noise caused by the mutual action of two bit lines by 50 percent or more as compared with that found conventionally. Furthermore, this DRAM is provided with a test facilitating circuit which utilizes a multipurpose register and a comparator and can sharply shorten the time for a pattern test. The twist bit line structure which Mitsubishi has adopted is what the company tried for in its 1M DRAM last year, and the same approach was also adopted for Hitachi, Ltd.'s 16M DRAM (last year). Hitachi, Ltd., in an attempt to overcome the noise problem caused by the capacity coupling between two adjacent bit lines, devised the bit line structure, making the bit lines intersect.

As mentioned earlier, DRAM plays the role of semi-conductor technology driver and has quadrupled high integration in 3 years. Whether or not this trend will continue is difficult to determine, but all the semiconductor manufacturers will make positive efforts to maintain the conventional high integration pace while paying attention to the problems of cell structure and light source selection in the lithography process.

SRAM

4M SRAM, the First in the World (Sony)

High-Speed 1M SRAM (Hitachi and Toshiba)

Attracting the most attention this year in the SRAM (static RAM) field were the 4M SRAM, announced by Sony Corporation, the first of its kind in the

world, and the high-speed 1M RAM announced by two Japanese companies, Hitachi, Ltd. and Toshiba Corporation, which has an access time of less than 10 ns.

First, let us look at Sony's 4M DRAM. This product adopts the design rule of 0.5 μm, which is the smallest for 16M DRAMs, and integrates 7 million transistors on a chip 7.46 x 17.41 mm^2. This SRAM has a configuration of 512K words x 8 bits, adopts two-layer polysilicon/two-layer aluminum wiring, and uses the CMOS process. The access time is 25 ns. This access time is by no means inferior to that of the 1M SRAM announced last year (by Phillips, IBM, Mitsubishi, Hitachi, and Fujitsu). In addition, the consumption current is as small as 46 mA (power supply voltage 3.3 V for operation at 40 MHz), making the SRAM mountable on portable devices.

On the other hand, the ECL-interface 256K-bit high-speed Bi-CMOS version of 1M RAM, much talked about in the SRAM field last year, has come to be passed on to high-order machines. While the 1M SRAM presented last year was entirely based on the CMOS technique, Toshiba Corporation adopted the Bi-CMOS technique this year to attain higher operation speed. On the other hand, Hitachi, Ltd., the other manufacturer presenting a 1M SRAM, has adopted the CMOS process to which the 0.5 μm process has been applied, attaining higher operation speed (see Table 2). The company's 1M SRAM has attained higher operation speeds by decreasing the two amplifiers, which were necessary in the past, to one unit by adopting a newly-devised circuit for signal detection and amplification. The access time is as low as 9 ns, recording the highest speed of a 1M SRAM using CMOS. The chip size is 5.3 x 10.3 mm^2, the smallest in the world, and the memory cells area is 21 μm^2.

The 1M SRAM presented by Toshiba Corporation adopts a 0.8 μm Bi-CMOS process and has attained 8 ns, the highest operation speed in the world for SRAM. This SRAM has a chip size of 6.5 x 16.5 mm^2 and integrates about 4.2 million CMOS transistors and about 5,000 bipolar transistors. CMOS transistors are used for the memory, with bipolar transistors for the signal input-output circuit and sense amplifier. The product adopts the bit-line ceaseless short circuit method, which constantly short-circuits the circuit by setting up one transistor element at the top part of the individual bit lines and can suppress the voltage difference between the high and low levels to 50 mV, 1/20 the conventional voltage.

Microprocessor

Data Width of 64 Bits Appears

Microprocessors whose external data widths had been expanded to 64 bits were presented by three companies--DEC, Intel Corp, and Matsushita Electric Industrial Co., Ltd.

Table 2. Comparison of Specifications of 4M SRAM and 1M SRAM

Item	Sony	Toshiba	Hitachi
Memory configuration	512K words x 8 bits	256K words x 8 bits	256K words x 8 bits
Minimum line width (μm)	0.5	0.8	0.5
Cell dimensions (μm^2)	21.24 (3.6 x 5.9)	49.84 5.6 x 8.9)	21 (3.5 x 6.0)
Access time (ns)	25	8	9
Chip size (mm^2)	7.46 x 17.41	6.5 x 16.5	5.3 x 10.3
Power consumption	46mA (in operation at 40 MHz)/3.3V power supply voltage	500mW(in operation at 50MHz)	275mW(in operation at 30MHz)
Process technique	CMOS 2-layer polysilicon/ 2-layer aluminum	Bi-CMOS	CMOS

DEC presented three papers on the product, two of which had adopted RISC for the architecture, with the other adopting CISC. The product adopts the effective performance of the RISC processor of 20 MIPS, design rule of 1.5 μm, and power consumption of 3 W or less. The CISC processor integrates 320,000 transistors and its machine cycle is 28 ns. The chip size is 12 x 12 mm^2, and the power consumption is 6 W.

Intel Corp.'s MPU adopts RISC for its architecture and has recorded a peak performance of 100 MFLOPS at a machine cycle of 50 MHz. Integer operation and floating-point addition and multiplication are made possible in one-clock parallel processing.

Matsushita Electric Industrial Co., Ltd. also adopts the RISC architecture and has attained an effective performance of 4 MFLOPS, with a peak performance of 20 MFLOPS. The design rule is 1.2 μm and the power consumption is 1.3 W.

On the other hand, regarding the 32-bit MPU, Hitachi, Ltd.'s presentation adopting a Bi-CMOS process has attracted attention. The MPU adopts a CISC processor for the architecture, and is aimed at attaining a higher operation speed by raising the clock frequency to 70 MHz, more than double that of the conventional one. What became the conclusive factor for attaining the higher operation speed was the adoption of the Bi-CMOS technique. The processing speed has been raised by 1.5 to 2 times that of the conventional one by applying Bi-CMOS to the clock driver and bus driver of the driver circuit system and, further, by making the amplifying circuit of the signal amplitude bipolar. Since the operation circuit has been designed so that the wiring length has been shortened, this MPU has attained a peak performance of 70 MIPS in one clock-one instruction processing. This MPU adopts the 1 μm process and 12 x 13 mm^2 chip size.

In addition, in the processor-related field, Mitsubishi Electric Corporation's image DSP and NEC Corporation's animation signal processor are attracting attention. Mitsubishi Electric Corporation's image DSP is a large-scale one that integrates 538,000 transistors and has attained a 50 nm or less instruction cycle. With this processor, the data width of operation has been raised from the conventional 16 bits to 24 bits and, since functions have been added for parallel processing and data operation control, the data processing ability has risen to 10 times that of the conventional one. Moreover, in the field of floating-point processors, Mitsubishi Electric presented a 24-bit floating-point DSP and, in cooperation with Osaka University, a 40 MFLOPS 32-bit floating-point DSP. The former adopts the 1.2 μm CMOS process and has attained a machine cycle of 40 ns, the highest speed in the 24-bit class. Also, since this processor is capable of using floating-point data, it requires only a small number of operations and can process a large quantity of data, with 512 x 24 bits. The chip size is 7.02 x 8.64 mm^2. The latter is of a data-driving asynchronous variable length pipeline structure and has attained 40 MFLOPS, the highest speed of the silicon-based general purpose operation element. Data in processing units of 32 bits is processed in 12 stages. The structural arrangement is such that the parallel processing of 12 data items is always permitted.

On the other hand, NEC Corporation's animation signal processor is of a 16-bit type and its instruction cycle is 25 ns. This processor adopts a variable seven-stage pipeline operation circuit and its chip size is 14.0 x 13.4 mm^2. In addition, NEC has also announced a 200 MHz DSP. This processor adopts the Bi-CMOS technique and has introduced a new method, called the "redundant binary high-speed product sum operation method," which suppresses to one position the successive carries which occur in the binary operation. The processor has also attained a speed of 1.5 times or more than the conventional high speed by a method dividing the multiplication into two parts, called the "optimized two-stage pipeline method." The design rule is 0.8 μm and the chip size is 5.87 x 5.74 mm^2.

Gate Array

Appearance of 12,000-gate ECL

Mitsubishi Electric Corporation presented an ECL (Emitter Coupled Logic circuit) gate array which integrates 12,000 gates, the highest integration in the industry. The product uses a 0.6 μm five-layer metal bipolar process and contains, as built-in memory, the conventionally installed RAM of 36K bits. Since the basic cell consists of four bipolar transistors, the wasteful use of transistors can be avoided. The chip size is 14.5 x 13.5 mm^2 and the read time of the RAM is 3.0 ns.

Furthermore, NTT presented a power supply voltage converter gate array adopting a 0.8 μm Bi-CMOS process, Hitachi, Ltd. presented a gate array installing eight blocks of 4.6K-bit RAM (and adopting a three-layer metal 0.8 μm CMOS process), and NTT and IBM presented gallium-arsenic gate arrays. IBM's gate array is the GaAs gate array for a 5K transistor and its chip size is 4.0 x 4.5 mm^2. The NTT gate array is a logic gate which uses the E-type MESFET, with a gate length of 0.4 μm and chip size of 2.8 x 2.5 mm^2.

Josephson Elements and Wafer Scale Memory

Hitachi, Ltd. presented a four-bit Josephson microcomputer exhibiting a data rewritable cache memory, the first in the world. The Josephson element represents the superhigh-speed element of low power consumption expected to be utilized for the next generation. The microcomputer integrates about 30,000 Josephson elements on a 5 mm-square silicon chip, and its information processing ability is 250 MIPS (while operating at 1.02 GHz).

Incidentally, immediately before Hitachi, Ltd. presented this Josephson element at ISSCC '89, Fujitsu, Ltd. had announced a microcomputer which was produced by mounting multipliers and an 8K-bit ROM on the Am 2901-type bit-slice processor it had announced last year.

In addition, at this year's ISSCC as well, the wafer scale memory presented by Fujitsu, Ltd. can also be cited as a conspicuous presentation (see Photograph 1 [not reproduced]. With wafer scale memory, the wafer on which memory chips are integrated is not divided into chips, but is incorporated into a device as is for use in the form of a wafer. This memory has been devised to replace the present magnetic disk, but since a completely defect-free wafer is impossible to make and a technique for avoiding defects is difficult to develop, the memory has not yet been put to practical use. Fujitsu, Ltd. succeeded in the development this time in cooperation with British venture business Anamatic, Ltd. The wafer scale memory incorporates 202 pieces of 1M DRAM and logic circuits, each of which contains 1,200 gates, and these DRAM pieces are connected to the logic circuits, respectively. British Anamatic, Ltd.'s techniques have been adopted for the wafer defect avoidance technique, which through means of a spiral configuration obtains optimum wiring among the logic circuits while avoiding the defects occurring in the wafer process, and writes into EPROM the wiring information and the defect information about the DRAM pieces. The wafer process is exactly the same as the process used for the ordinary 1M DRAM, and extra processes such as special additional wiring are not required.

Applicable Range of Bi-CMOS Process Expands

One trend of ISSCC this year has been that the expansion of the applicable range of Bi-CMOS has been attracting attention (see Table 3). Bi-CMOS literally means the mixed mounting of bipolar and MOS elements on a chip to construct a circuit which allows one element to make use of the other's strong points. Bi-CMOS has the advantage that a higher operation speed and high integration are easy to attain and the freedom of the circuit design is high, but it requires the parameters of the element characteristics to be controlled with good repeatability and at high accuracy, posing a substantial problem in manufacturing. However, since the number of presentations on the adoption of the Bi-CMOS technique this time far exceeded that last year, each semiconductor manufacturer will make full use of such characteristics as the high driving ability and current amplification rate, and will energetically try to suppress power consumption.

In that sense, this year's ISSCC can be said to have set forth the direction of diversification (differentiation from other devices) and higher operation speed of semiconductor devices for the 1990s.

Table 3. Announcement and Contents of Bi-CMOS Techniques at ISSCC'89

Company	Contents
NEC	200MHz DSP
Toshiba	1M SRAM
	512K SRAM 16K bit ECL RAM
Hitachi	Logic gate with positive feedback
	70MHz 32-bit microprocessor
NTT	460K transistor gate array
	500K transistor logic circuit
Texas Instruments	1M ECL SRAM
	Hand gap reference circuit for ECL circuit
Siemens	Current switch logic circuit
Signetics	76MHz programmable logic sequence
Stanford University	Sense circuit for digital circuit

Large-Scale Project by Agency of Industrial Science and Technology

43070700 Tokyo NATIONAL RESEARCH AND DEVELOPMENT PROGRAM in English 1988 pp 1-16

[Text] Technological development is essential for the growth of society. In Japan, living standards and industrial vitality have been improving in spite of unfavorable conditions such as a shortage of natural resources. This achievement is largely attributable to technological development.

The national Research and Development Program (popularly known as the Large-Scale Project) was started by the Agency of Industrial Science and Technology in 1966 in order to undertake large-scale, risky R&D on a commission basis under governmental leadership. It has been one of MITI's most successful undertakings in research and development.

History of the Progress

The program's first three projects focused on a super high performance electronic computer, a desulfurization system and a magnetohydrodynamic generator. The total budget in 1966 was only one billion yen. At that time, Japan's economy had just taken off but key technologies were still imported from overseas. Under such circumstances, appropriate measures to promote R&D activities in the industrial sector were badly needed. The Large-Scale Project was launched to meet this need. Its primary target has been to unite national laboratories, scholastic organizations and private industries in order to raise the standard of Japanese technology level.

In 1974, a special R&D program, the Sunshine Project, was established focusing on new energy, and in 1978 the Moonlight Project was started with energy conservation as its main concern. These two programs grew out of the Large-Scale Project, and obtained independent status during the energy crisis.

Criteria for Selecting Projects

To be chosen as a Large-Scale R&D Project, a project must involve important and urgent R&D with potential benefit for Japanese industry and society. In general, technologies chosen are those which:

are urgently required for raising the standard of Japanese technology level, improving living standards and/or ensuring a stable supply of natural resources

promise to play a significant role in the growth and creation of Japanese industries

involve problems such as higher risks and long development time

have specific targets and clear, well-thought-out prospects for accomplishment

be suitable for joint R&D among industries, national laboratories and universities

Project Outline

There are nine R&D projects now underway under the Large-Scale Project (shown in Table 1). Completed projects are briefly described in Table 2.

Table 1. Ongoing National Research and Development Projects (Large-Scale Projects)

(Unit: million yen)

Project name	R&D Period (FY)	Total R&D Expenditure	Budget for FY1988
Manganese nodule mining system	1981 – 1991	about 20,000	954
High speed computing system for scientific and technological uses	1981 – 1989	about 23,000	2,777
Automated sewing system	1982 – 1990	about 10,000	988
Advanced robot technology	1983 – 1990	about 20,000	2,479
Observation system for earth resources satellite-1	1984 – 1988	about 10,900	1,250
New water treatment system	1985 – 1990	about 11,800	2,189
Interoperable database system	1985 – 1991	about 15,000	1,140
Advanced material processing and machining system	1986 – 1993	about 15,000	1,679
Fine chemicals from marine organisms	1988 – 1996	about 15,000	20

Table 2. Completed National Research and Development Projects (Large-Scale Projects)

(Unit: million yen)

Project name	Period (FY)	Total expenditure	Outline of project
Super-high performance electronic computer	1966 – 1971	about 10,100	Large scale computer system with super-high performance
Desulfurization process	1966 – 1971	about 2,700	(1) Efficient removal of the SO_x contained in the gases exhausted from power plants or other. (2) Direct removal of sulfur from heavy oil.
New method of producing olefin	1967 – 1972	about 1,200	Economic production of olefins by direct cracking of crude oil instead of using naphtha.
Remotely controlled undersea oil drilling ring	1970 – 1975	about 4,500	Remote-control oil drilling rigs for undersea use.
Sea water desalination and by-product recovery	1969 – 1977	about 7,000	Economical large-scale production of fresh water and economical by-product recovery technology.
Electric car	1971 – 1977	about 5,700	Various types of electric car to replace ordinary vehicles in urban areas.
Comprehensive automobile control technology	1973 – 1979	about 7,400	Integrated control technology with a view to relieving traffic congestion, reducing automobile pollution and traffic accidents, etc.
Pattern information processing system	1971 – 1980	about 22,100	Computer technology for the recognition and processing of pattern information such as characters, pictures, objects and speech.
Direct steelmaking process using high temperature reducing gas	1973 – 1980	about 14,000	Direct steelmaking technology aims at a closed system which uses the heat energy from a multi-purposes high temperature gas-cooled reactor in the steelmaking process.
Olefin production from heavy oil as raw material	1975 – 1981	about 14,200	Technology for manufacturing high-value-added olefin (commonly known as ethylene, propylene, etc.) using a high sulphur-content heavy oil fraction (so-called asphalt), which is difficult to desulphurize, as the raw material.
Jet engines for aircraft	1971 – 1975 (1st phase) 1976 – 1981 (2nd phase)	about 6,900 about 12,900	Research and development of large scale turbofan engine designed for the use in commercial transports in the 1980s.
Resource recovery technology	1973 – 1975 (1st phase) 1976 – 1982 (2nd phase)	about 1,300 about 11,400	R & D on technical systems for the disposal of solid urban waste, centered on resource recycling with a view to promoting the efficient utilization of resources and facilitating the smooth application of solid urban waste treatment.
Flexible manufacturing system complex provided with laser	1977 – 1984	about 13,500	R & D on new, automatic, integrated, production systems that are flexible and provide quick through-put in the manufacture of small batches of machine components.
Subsea oil production system	1978 – 1984	about 17,200	R & D on an efficient system for subsea oil production which would be applicable to the continental shelf and slope surrounding Japan and to deep sea oil field.
Optical measurement and control system	1979 – 1985	about 15,700	R&D on an optical measurement and control system permitting massive volume of data, including picture images, to be measured and controlled in adverse environments.
C_1 chemical technology	1980 – 1986	about 10,500	R&D on a technology for the economic production of basic chemicals from C_1 compounds like carbon monoxide from alternative carbon sources such as coal, natural gas, and tar sand.

The Transfer of R&D Results to the Private Sector

All the R&D results developed under this program, both the results developed by national laboratories and those by private industries, come into the possession of AIST. As for the utilization of these results, it is our policy to grant a license to use them to anyone who wishes, provided that the applicant for the grant is qualified both technologically and financially. The licensing fee will be decided according to the general principle for the rational use of national assets.

For the effective transfer of AIST's R&D results to private industries, the Japan Industrial Technology Association, AIST's affiliated non-profit organization, was established in 1969. JITA possesses the exclusive rights, including license granting rights, for all industrial properties and

technologies of AIST. In order to promote the wide use of the results of R&D, JITA is actively providing updated information on AIST's industrial properties and techniques to all who are interested.

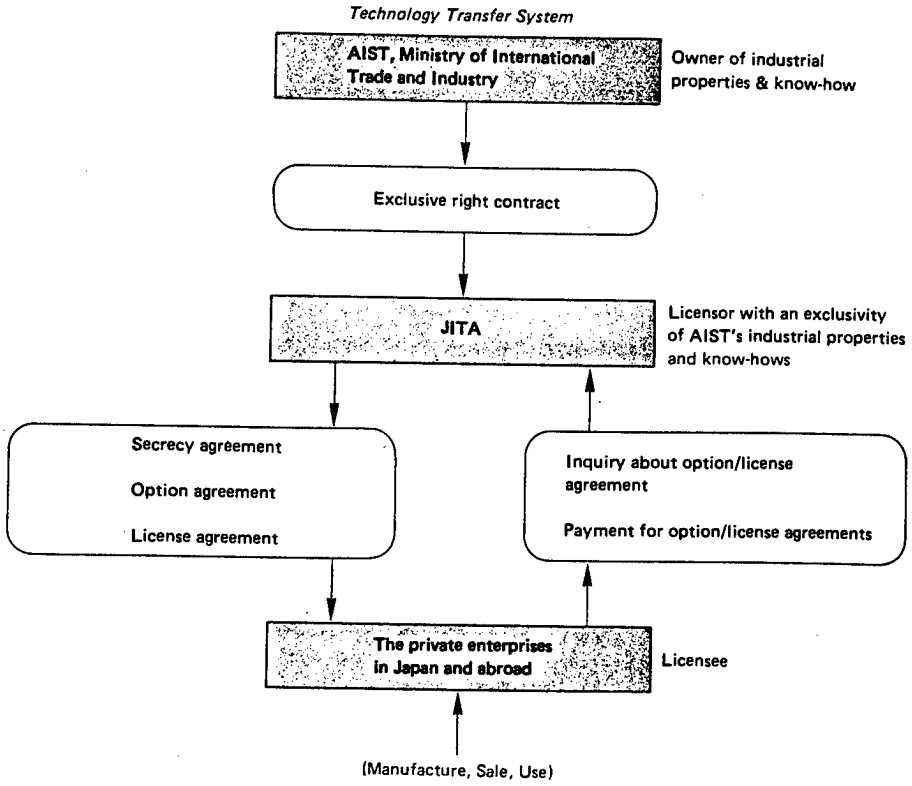

Manganese Nodule Mining System

Manganese nodules containing nickel, copper, cobalt, and manganese have been found over wide regions of the floor of the Pacific and also in several other areas of the world's oceans where water depth ranges from 4000~6000m. Though these metals are essential and indispensable resources for human life and industrial activities, the land based reserves of these metals are unequally distributed and are being gradually depleted.

Manganese nodules deposits are found worldwide on the ocean bed in international waters in large quantities. They can be thought of as attractive and stable resources, economically. From this point of view, new mining technology for manganese nodules from the deep ocean floor is required to be developed.

The mining system being developed in this project is a hydraulic mining system in which manganese nodules are collected by a towed vehicle on the ocean floor and lifted to a surface ship by the hydraulic lift system using hydraulic pump and/or air lift pump through a long pipe of several thousands meters.

This mining system consists of five systems: collector, material lifting, machinery handling, electrical control and data assembling, and the total system. At the final stage of this project, the pilot mining test is scheduled to be held in the manganese nodule province in the Pacific Ocean combining these systems.

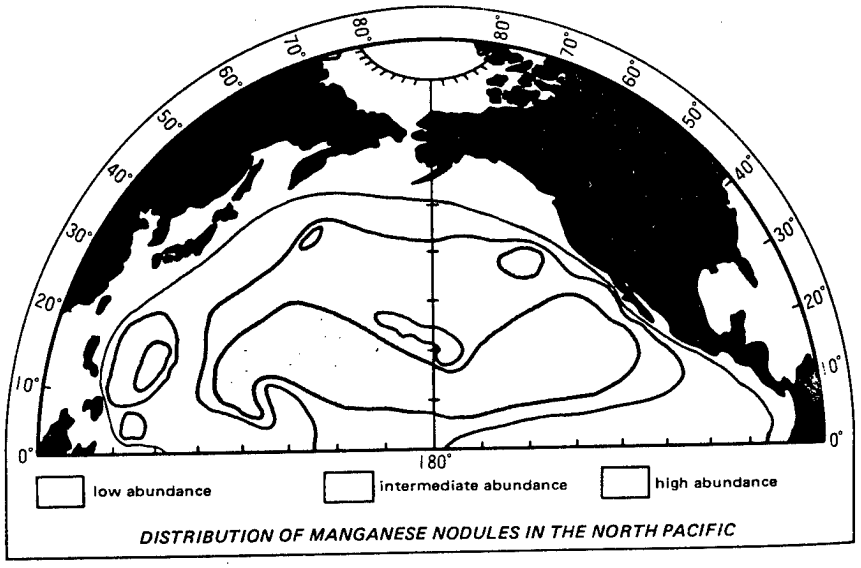

DISTRIBUTION OF MANGANESE NODULES IN THE NORTH PACIFIC

High-Speed Computing System for Scientific and Technological Uses

A high-speed computing system is clearly needed for such operations as the processing of satellite data, meteorological forecasting, aerodynamic simulation for aircraft design, and plasma simulation for nuclear fusion reactors. These operations require large-scale numerical computation in which the efficient calculation of vectors and matrices is especially necessary.

This project aims at the development of a high-speed computing system for scientific and technological applications. The system is expected to be operated at the rate of more than 10 Giga floating point operations per second, which is 100 to 1,000 times faster than the speed of conventional computers.

In order to develop this high-speed computing system, two major R&D projects are being conducted: one on high speed novel devices such as the Josephson junction device; the other on computer architecture, algorithms and languages for parallel computing. The target of this project is to fabricate and evaluate a high performance demonstration system in 1989.

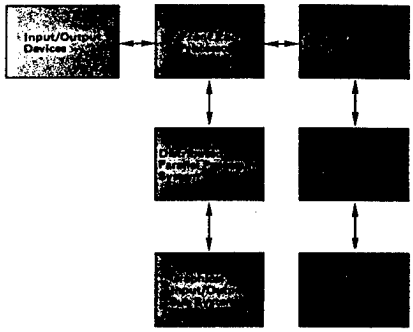

STRUCTURE OF SCIENTIFIC COMPUTING SYSTEM

	Josephson Junction Device	High-[illegible] Transistor Device	GaAs FET
Operating temperature	−269°C (Liquid helium temperature)	−196°C (Liquid nitrogen temperature)	about 20°C (Room temperature)
Targets of new devices			
Logic devices	Delay time : Below 10 ps/gate Integration : Above 3,000 gates/chip		Delay time : Below 30 ps/gate Integration : Above 3,000 gates/chip
Memory devices	Delay time : Below 10 ns Integration : Above 16 Kbits/chip		Delay time : Below 10 ns Integration : Above 16 Kbits/chip

TARGETS OF NEW DEVICES

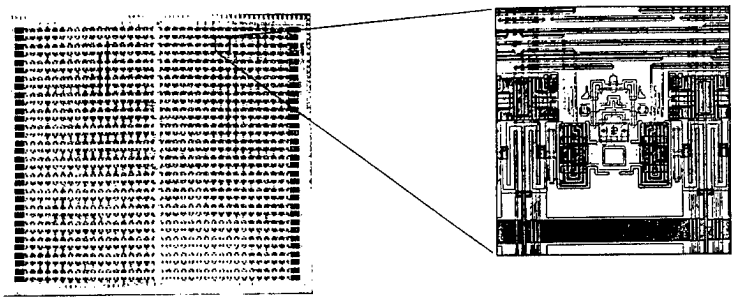

JOSEPHSON 3K-BIT GATE ARRAY

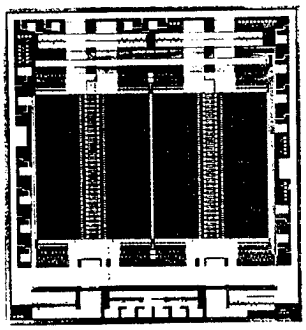

GaAs 4K-BIT STATIC RAM

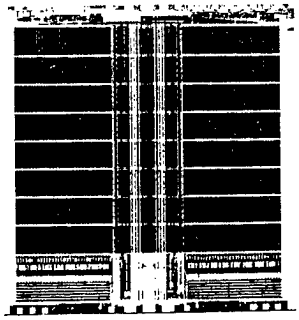

HEMT 16K-BIT STATIC RAM

Automated Sewing System

In Japan, the apparel industry has been faced with many structural problems such as diversification of consumer's needs, shorter cycles of goods, lack of skilled labor force and competition from the other developing countries. These problems have urged us to produce high added-values products, decrease the production cost and loss following the conventional anticipation production.

In order to solve such problems regarding the apparel industry, a research and development project concerning an automated sewing system that will allow to manufacture small quantities production of a variety of goods in a flexible and reasonable way has been planed and started.

The purpose of this project is to develop technologies that reduce the per-piece manufacturing time for small quantities of variety goods in small– and medium-size sewing enterprises by more than half compared with existing manufacturing time. In order to achieve this object, this proejct will carry out research and development activities on the systematic integration by combining elemental technologies of the "sewing preparation technology", "sewing and assembly technology", "fabric handling technology" and "system management and control technology".

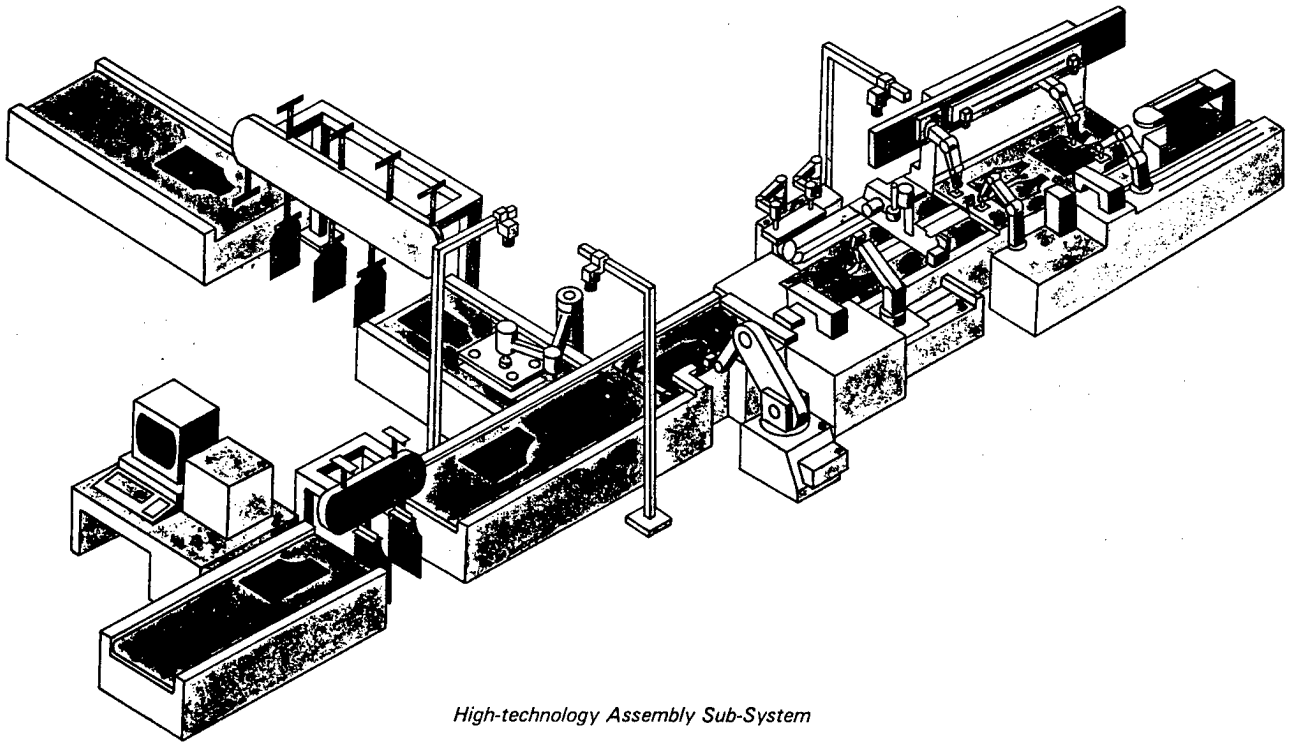

High-technology Assembly Sub-System

Advanced Robot Technology

Much of our modern life and its security is supported by activities performed under demanding conditions. These include, for example, work at nuclear power plants, underwater operations and fire-fighting and rescue operations at disaster sites. There is increasing demand for such highly skilled work, which at present can only be done by humans.

The sound development of our society, however, will depend on freeing humans from such dangerous jobs so that they may work at more pleasant and rewarding occupations.

Given the technology available today, humans can be replaced with machines only to a limited extent. New technologies will be required for the development of advanced robot systems capable of performing the operations described above.

This project aims to develop the advanced robot technology needed to free humans from work in critical environments.

In addition to R&D conducted at AIST, international cooperation on advanced robotics has been under way within the framework of this project. The cooperation program is based on an agreement made at the Williamsburg Summit Meeting in 1982. Japan was designated as a leading country together with France to promote this international program based on the consensus of the member countries.

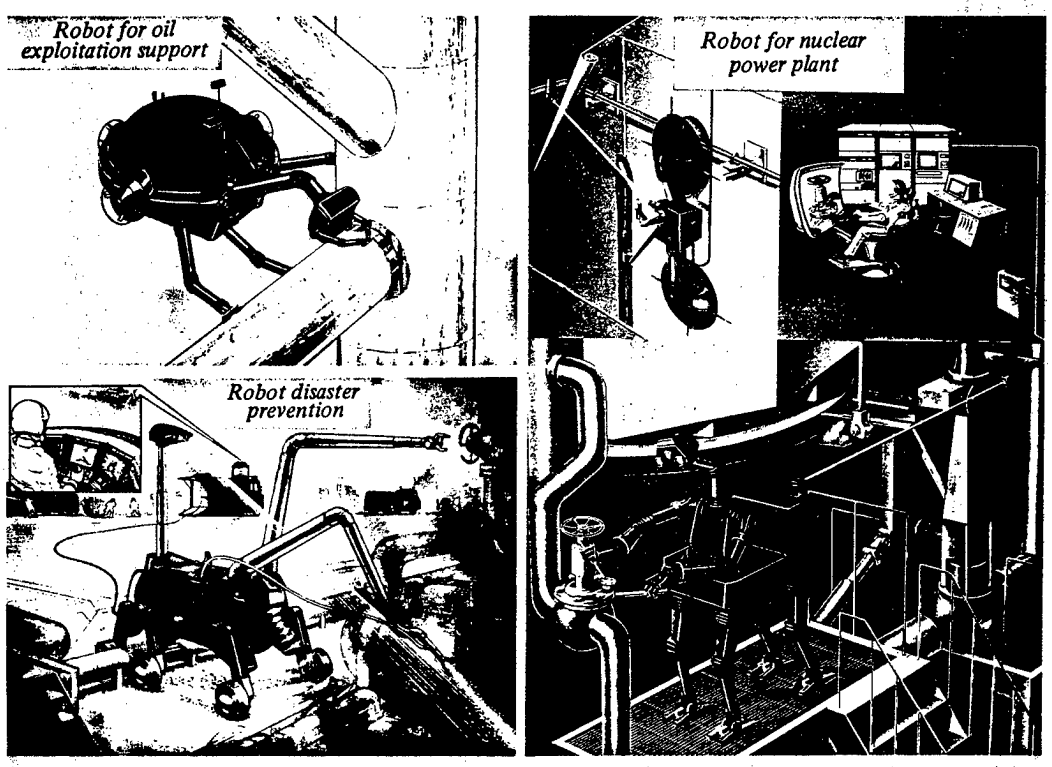

Observation System for Earth Resources Satellite-1

Geological mapping is one of fundamental technologies for energy or mineral resource exploration. Satellite remote sensing technology contributes a great deal to geological mapping by reducing the uncertainties through providing unique means for mapping geological features such as perversive but subtle structures and altered soil.

In response to the concerns of those involved in natural resource exploration, MITI, together with the Science and Technology Agency (STA), initiated research and development of the first Japanese Earth Resources Sattelite (ERS-1), MITI is responsible for developing the mission payload segment which consists of a synthetic aperture radar (SAR), optical sensor (OPS), a data recorder, and a data transmitter, and STA for developing the satellite platform and a launching rocket.

The spaceborne SAR has capability of operating all day and in all weathers, and high resolution in geological mapping. On the other hand, OPS covers a different portion of the electromagnetic spectrum which is used to identify and characterize the sources of the radiation. The spectral band is selected to provide maximum discrimination for natural resource exploration purpose. Based on the basic specifications of the SAR and OPS decided in 1986, an engineering model (EM) manufacturing of the mission playload segment is now under way. The EM evaluation test will begin in 1988.

ERS-1 is due to be launched on an H-1 rocket from Tanegashima into a sun-synchronous orbit at an altitude of 570 kilometers.

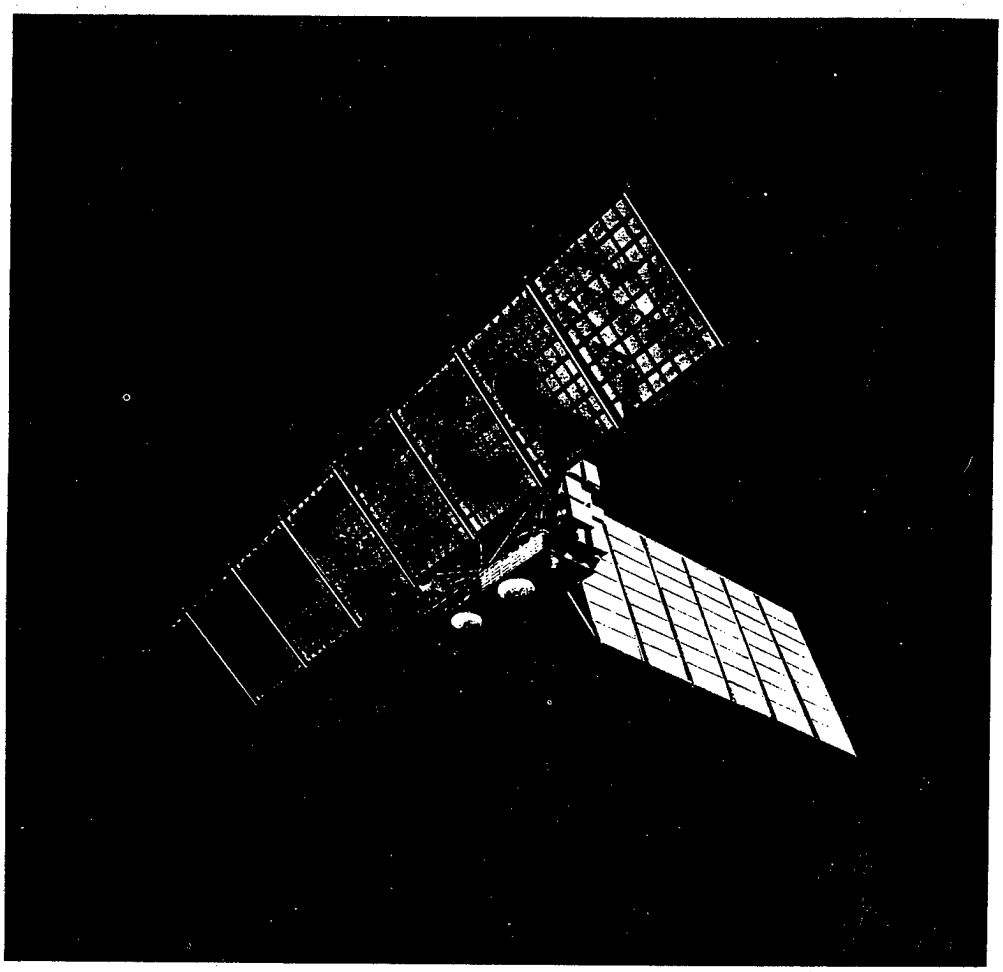

EARTH RESOURCES SATELLITE-1

New Water Treatment System "Aqua-Renaissance"

This R&D project focuses on the development of a new integrated water recycling system for the benefit of industries and municipal organizations. The technological features of the system are the search for and cultivation of high performance methane-producing bacteria and the application of membrane separation. This project was started to cope with the water shortage problem, but the methane gas production has also been recognized as another important aspect of this system. It is believed that the implementation of this innovative technology would contribute greatly to assuring the supply of industrial-use water at low cost, and would also diversify the sources of energy supply.

This system consists of three components: a bioreactor, a membrane module and a water-treatment reactor. One of the technological highlights is the development of an automated control system for methane fermentation. In order to complete the total system, the following R&D areas are being pursued: micro-organism and membrane materials; system components; the control system; and the technology to run the total system. Furthermore, this project is seen as stimulating the improvement of Japan's bio-technologies as a whole.

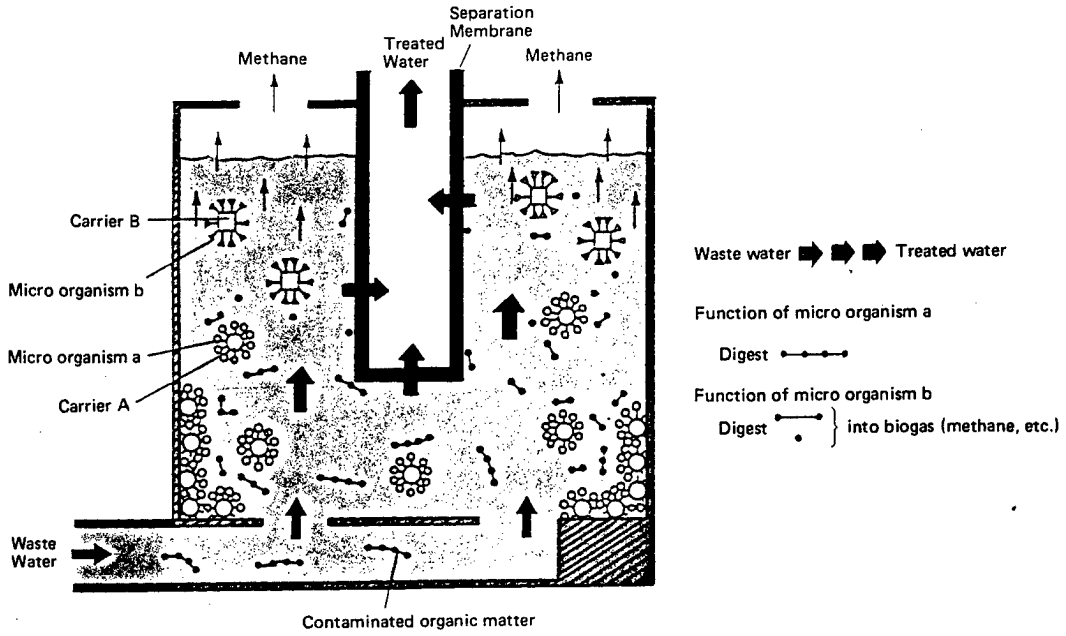

Water Treatment Mechanism
in Bioreactor-Membrane combined System

Interoperable Database System

Various social activities are becoming increasingly dependent on diversified information, particularly technical and economic information. Consequently computers and databases are becoming increasingly important. However, given the currently available technologies, it is impossible to achieve complete interoperability among different types of computers and databases. This will result in a great deal of inconvenience for computer users.

The development of interoperability, which enables the interconnection among different computer systems is regarded as the key to the foundation of an advanced information-oriented society. The development of an interconnecting protocol, which is the main feature of the project, has been conducted in compliance with the ISO (International Organization for Standardizations) as the development project for the open systems interconnection (OSI).

This project, as well as developing technologies to process characters, graphics, and images and to ensure high reliability, aims at developing technology for constructing a convenient database systems incorporating interoperable computer networks.

To accomplish the goal, the following technologies are being developed:

(1) Distributed Database Technology
(2) Multi-media Technology
(3) High Reliability Technology
(4) Interoperable Network Systems Technology.
(5) Advanced Database Technology for power plants

Example of Interoperable Database System

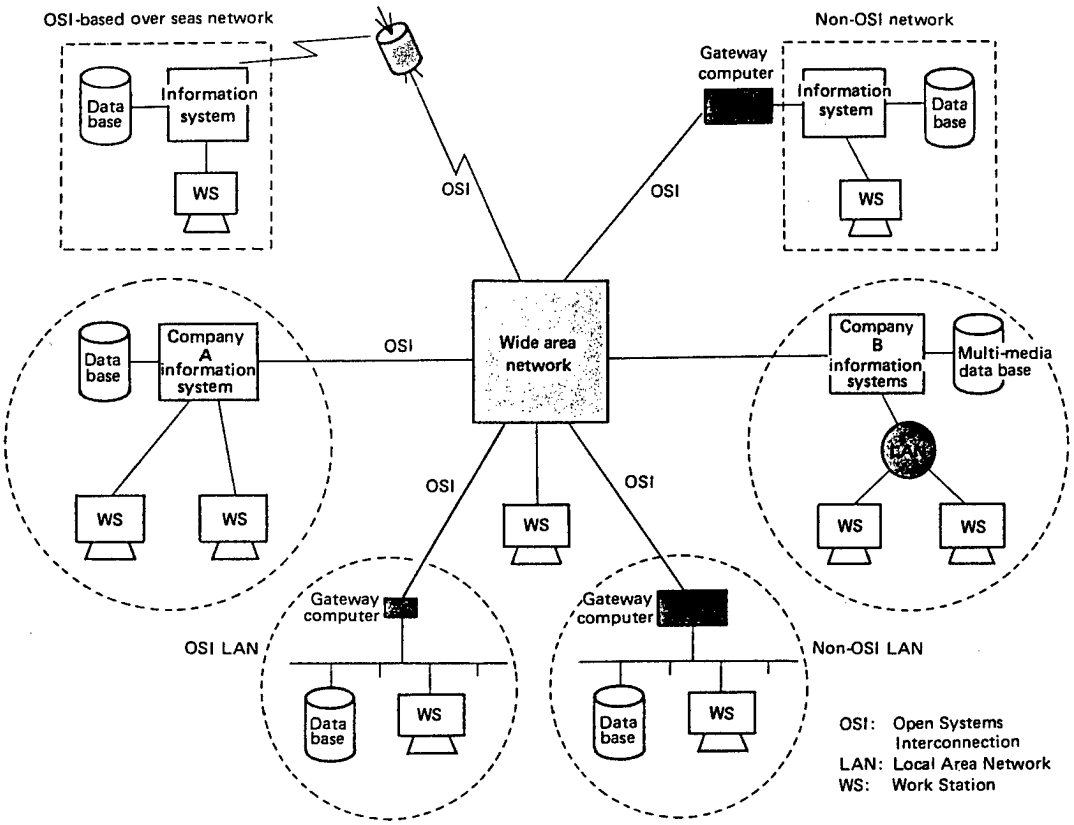

Advanced Material Processing and Machining System

Technology-oriented industries in such fields as aeronautics, space, electronics, energy and fine manufacturing have been eagerly pursuing innovative processing and machining technologies for their needs. These technologies are indispensable in processing various materials, manufacturing system parts and assembling components into a large system in order to meet the customer's exact specification requirements. However, the improvement of technological performance necessary for those growing industries has been inadequate compared with the increase of new materials and the growth of electronics technology.

On the other hand, the application of excimer laser and ion-beam, if fully developed, is seen as facilitating ultra-precise manufacturing in various industries and providing one of the seeds for future technology.

The aim of this project is to develop a high energy excimer laser system and a high density ion beam system for the purpose of surface processing. In addition to production of the hardware, application technolgies is also developed. Moreover, the project also includes the development of high performance machine tools for ultra-precision machining.

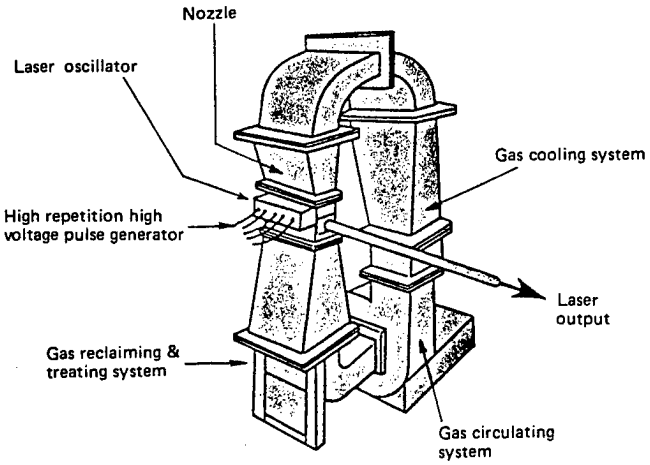

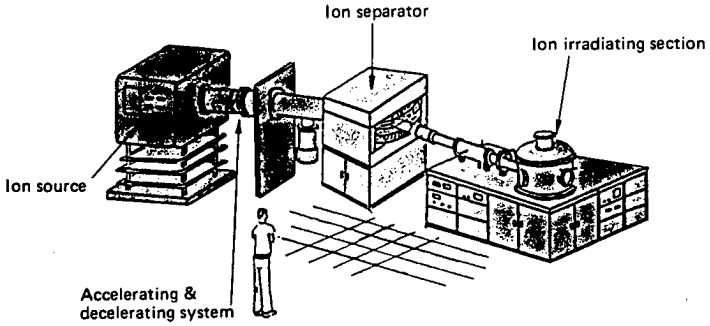

Fine Chemicals From Marine Organisms

TO BACKGROUND AND PURPOSE OF THE RESEARCH AND DEVELOPMENT

Japan has the sixth largest exclusive 200-mile economic sea area in the world. Toward the coming 21st century, the development of marine resources by the intensive utilization of advanced technology is now highly required. While Japan has been expected to be the leading nation in this field, the national project concerning ocean have so far been focused on energy and mineral resources such as petroleum, manganese nodule, and ocean thermal energy.

While biotechnology has so far been developed based on the research of the terrestrial organisms which are easier of access, the investigation of marine life system is also important to us ocean is the place where the first life system originated and marine organisms far exceed the terrestrial organisms in the total mass and diversity.

However, ocean is the vast three-dimensional water expanse which obstracts our easy access to the organisms. The sampling and maintenance of marine organisms require the development of special hardware. Because environment for marine organisms is far different from terrestrial environment in pressure, temperature, oxygen concentration, and light intensity. Moreover, the methods in the conventional biotechnology for terrestrial organisms are not directly applicable to marine ones. New technology for fermentation, gene manipulation, and cell fusion under higher salt concentration should be established.

The development of overall systems for production of a variety of chemicals with high performance based on marine biotechnology will contribute to introducing new industrial resources. New chemical products thus produced will highly contribute to elevating our living standards.

Thus the project of "Fine Chemicals from Marine Organisms" is being launched.

THE OUTLINE OF THE RESEARCH AND DEVELOPMENT

In order to establish the production technology of the useful chemical materials such as coating materials on under-water structures, pigments, dyestuffs, and moisturizing materials, the research and development programs which fall into the following two categories are carried out.

I. Research and development of production technology of useful materials, i.e. production of high performance chemicals.
II. Research and development of utilization technology of biofunction; for example, research and development of technology to remove sea-water pollutions such as oily wastes by using biotechnologically enhanced bio-functions of marine microorganisms.

Flow of research and development proces

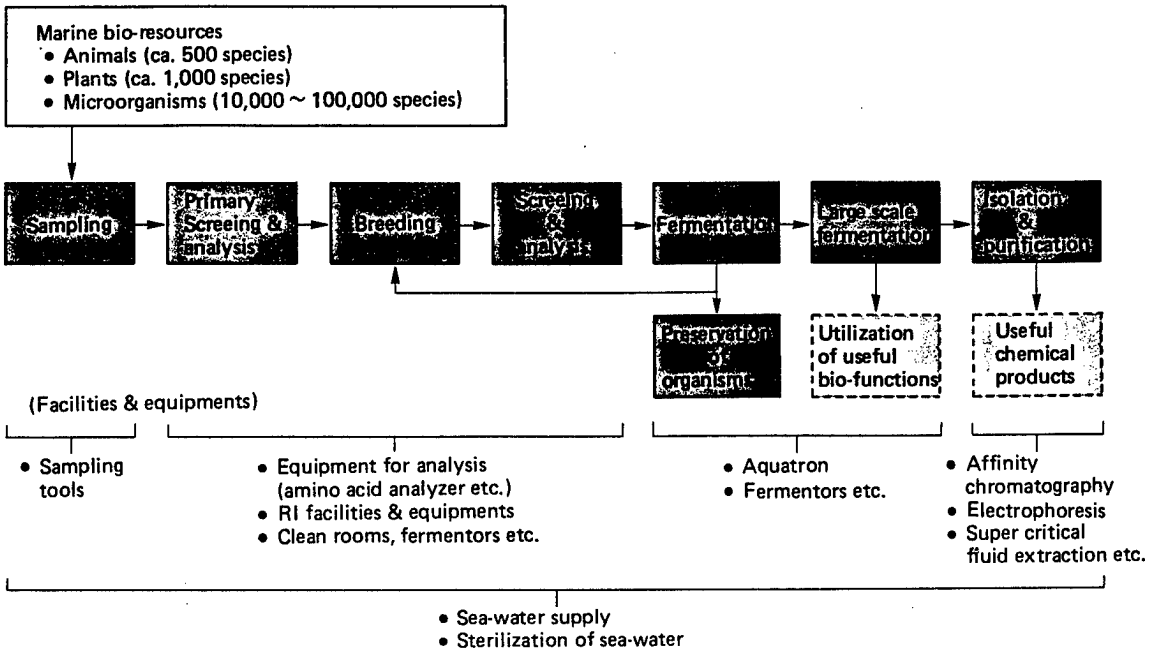

Some Examples of the Result Under the Large-Scale Project

MAGNETIC BUBBLE INFORMATION WRITING DEVICE

Patent No. : 4,101,971
Patented Date : Jul. 18, 1978
Appl. No. : 717,377
Filed : Aug. 24, 1976

Foreign Application Priority Data
Aug. 28, 1975 [JP] Japan . . . 50/103498
Nov. 4, 1975 [JP] Japan . . . 50/131446

ABSTRACT

A magnetic bubble information writing device in which a conductor loop is disposed on the magnetic bubble propagation circuit and in which magnetic bubbles are generated by sending pulse current through the conductor loop, the device having a means which after having sent the bubble generating pulse current through the conductor loop, sends pulse current for annihilating stray bubbles through the same, the stray bubble annihilating pulse current having a polarity opposite to that of the bubble generating pulse current.

AUTOMATIC CHANGE-GEAR CONTROL DEVICE FOR USE IN ELECTROMOBILE

Patent No. : 4,174,645
Patented Date : Nov. 20, 1979
Appl. No. : 743,657
Filed : Nov. 22, 1976

Foreign Application Priority Data
Nov. 29, 1975 [JP] Japan . . . 50-141836

ABSTRACT

An automatic change-gear control device for use in an electromobile which incorporates a multi-stage change gear drive system. This automatic change gear control device selects and controls a gear ratio for an optimum ratio depending on the running condition of a vehicle, and particularly provides a change-gear logic by detecting a load torque for every individual condition, in an attempt to improve the running performance of a vehicle at the time of acceleration or at the time of running on an upward slope.

TREATING PROCESS OF GARBAGE CONTAINED WASTES

Patent No. : 4,288,550
Patented Date : Sep. 8, 1981
Appl. No. : 956,724
Filed : Nov. 1, 1978

Foreign Application Priority Data
Nov. 8, 1977 [JP] Japan 52-133017

ABSTRACT

The present invention relates to a process for digesting garbage or garbage contained wastes, particularly to a microbiological treatment which facilitates the treatment with high efficiency and economics, for the recovery of methane gas, first, by effecting an alcohol fermentation treatment by alcohol fermentative yeasts which can directly convert starch into ethanol without a starch hydrolysis pretreatment in the slurry state, followed by a direct methanization by methane bacteria of the fermented product containing ethanol, without effecting sterilization treatment of garbage or garbage contained wastes.

HOT FLUID-CONDUCTING PIPE ASSEMBLY

Patent No. : 4,155,377
Patented Date : May 22, 1979
Appl. No. : 846,940
Filed : Oct. 31, 1977

Foreign Application Priority Data
Nov. 8, 1976 [JP] Japan . . 51-148988[U]

ABSTRACT

A hot fluid-conducting pipe assembly, comprising an inner metal pipe through which flows a hot fluid,

support pins regularly arranged on and outwardly projecting from the outer surface of the inner metal pipe,

refractory of said coupling members fixed to the inner metal pipe by the support pins, each coupling members having upper and lower faces concentric with the surface of the inner metal pipe,

trapezoidal side faces in the longitudinal direction of the inner metal pipe, and sectorial side faces in the circumferential direction of the inner metal pipe,

heat-insulating refractory blocks mounted between the coupling members and each having an underside portion provided with a cushioning layer formed of an elastic refractory material,

a heat-insulating layer formed of an elastic refractory material and uniformly covering the upper faces of the coupling members and of the heat-insulating blocks, and

an outer metal pipe covering the heat-insulating layer.

PROCESS FOR THE PRODUCTION OF OLEFINS

Patent No. : 4,259,177
Patented Date : Mar. 31, 1981
Appl. No. : 103,174
Filed : Dec. 13, 1979

Foreign Application Priority Data
Dec. 21, 1978 [JP] Japan 53/156893

ABSTRACT

A process for producing olefines by using a fluidized bed of coke particles provided in each of a reactor and a heater, circulating coke particles through the reactor and the heater, heating the coke particles by a combustion of fuel and, if desired, a part of the coke particles in the heater, thermally cracking heavy oil with heated coke particles as a heat carrier in the reactor, the improvement which comprises a distillation residue is converted into a high-temperature, low-calorie gas in a combustion chamber, and the coke particles is heated with the gas in the heater, further an increment of coke deposited on a surface of the coke particles is burned by blowing air into the heater.

Process for Producing Aromatic Imide Polymer Hollow Filaments.

Appl. No. : 745,144 (USA)
Field : Jun. 14, 1985

Foreign Application Priority Data
Jun. 20, 1984 [JP] Japan 59/125340

ABSTRACT

This invention relates to a process for producing aromatic polyimide hollow filaments having a selective separation in property of hydrogen from synthesis gas in addition to excellent heat and chemical resistance, and mechanical strength.

This hollow filament can be attained by a wet spinning method from a dope solution which is a phenolic solution of polyimide copolymer comprising of biphenyl tetracarboxylic acid, diphenyl ether, diamino benzoic acid, diamino biphenyl, and diamino diphenyl methane.

PROCESS FOR PRODUCING ETHANOL

Appl. No. : 844,009 (USA)
Filed : Mar. 27, 1986

Foreign Application Priority Data
Jun. 10, 1985 [JP] Japan 60/124268

ABSTRACT

This invention relates to a process for producing ethanol from methanol, carbon monoxide, and water in the presence of a catalyst composed of cobalt and tertiary phosphine.

A typical example is:

catalyst; basic cobalt carbonate/tri-n-propyl phosphine/water, solvent; benzene.

reaction conditions; 200 atm (CO), 230°C, time 3 hr.

results; consumed methanol 35%, selectivity of ethanol 88% (realizable).

- END -

10

22161
45

NTIS
ATTN: PROCESS 103
5285 PORT ROYAL RD
SPRINGFIELD, VA 22161

Foreign Broadcast Information Service (FBIS) and Joint Publications Research Service (JPRS) publications contain political, economic, military, and sociological news, commentary, and other information, as well as scientific and technical data and reports. All information has been obtained from foreign radio and television broadcasts, news agency transmissions, newspapers, books, and periodicals. Items generally are processed from the first or best available source; it should not be inferred that they have been disseminated only in the medium, in the language, or to the area indicated. Items from foreign language sources are translated; those from English-language sources are transcribed, with personal and place names rendered in accordance with FBIS transliteration style.

Headlines, editorial reports, and material enclosed in brackets [ ] are supplied by FBIS/JPRS. Processing indicators such as [Text] or [Excerpts] in the first line of each item indicate how the information was processed from the original. Unfamiliar names rendered phonetically are enclosed in parentheses. Words or names preceded by a question mark and enclosed in parentheses were not clear from the original source but have been supplied as appropriate to the context. Other unattributed parenthetical notes within the body of an item originate with the source. Times within items are as given by the source. Passages in boldface or italics are as published.

SUBSCRIPTION/PROCUREMENT INFORMATION

The FBIS DAILY REPORT contains current news and information and is published Monday through Friday in eight volumes: China, East Europe, Soviet Union, East Asia, Near East & South Asia, Sub-Saharan Africa, Latin America, and West Europe. Supplements to the DAILY REPORTs may also be available periodically and will be distributed to regular DAILY REPORT subscribers. JPRS publications, which include approximately 50 regional, worldwide, and topical reports, generally contain less time-sensitive information and are published periodically.

Current DAILY REPORTs and JPRS publications are listed in *Government Reports Announcements* issued semimonthly by the National Technical Information Service (NTIS), 5285 Port Royal Road, Springfield, Virginia 22161 and the *Monthly Catalog of U.S. Government Publications* issued by the Superintendent of Documents, U.S. Government Printing Office, Washington, D.C. 20402.

The public may subscribe to either hardcover or microfiche versions of the DAILY REPORTs and JPRS publications through NTIS at the above address or by calling (703) 487-4630. Subscription rates will be provided by NTIS upon request. Subscriptions are available outside the United States from NTIS or appointed foreign dealers. New subscribers should expect a 30-day delay in receipt of the first issue.

U.S. Government offices may obtain subscriptions to the DAILY REPORTs or JPRS publications (hardcover or microfiche) at no charge through their sponsoring organizations. For additional information or assistance, call FBIS, (202) 338-6735,or write to P.O. Box 2604, Washington, D.C. 20013. Department of Defense consumers are required to submit requests through appropriate command validation channels to DIA, RTS-2C, Washington, D.C. 20301. (Telephone: (202) 373-3771, Autovon: 243-3771.)

Back issues or single copies of the DAILY REPORTs and JPRS publications are not available. Both the DAILY REPORTs and the JPRS publications are on file for public reference at the Library of Congress and at many Federal Depository Libraries. Reference copies may also be seen at many public and university libraries throughout the United States.